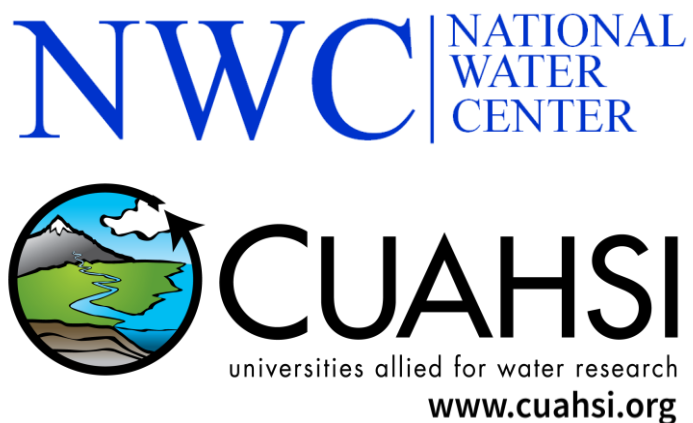


Consortium of Universities for the Advancement of Hydrologic Science, Inc.

TECHNICAL REPORT 13

OCTOBER 20, 2016



NATIONAL WATER CENTER
INNOVATORS PROGRAM
SUMMER INSTITUTE REPORT 2016

David R. Maidment
Adnan Rajib
Peirong Lin
Edward P. Clark

National Water Center Innovators Program Summer Institute Report 2016

Editors

David R. Maidment
Adnan Rajib
Peirong Lin
Edward P. Clark

Prepared in cooperation with the Consortium of Universities for the Advancement of Hydrologic Science, Inc. and the National Water Center

CUAHSI Technical Report No. 13

DOI: 10.4211/technical.20161019

October 20, 2016

Suggested citation:

Maidment, D.R., Rajib, A., Lin, P., Clark, E. P. 2016. National Water Center Innovators Program Summer Institute Report. Consortium of Universities for the Advancement of Hydrologic Science, Inc. Technical Report No. 13, 122 p.
DOI: 10.4211/technical.20161019

Contents

Preface	1
Research Summary	4
1. Radar Measurement and Flow Modeling: Methods - <i>Jim Coll, Mike Johnson and Paul Ruess</i>	7
2. Delineating Stream Flowlines and Watershed Boundaries in the Lower Rio Grande Valley Using High Resolution LiDAR Derived Digital Elevation Models - <i>Brenda Elisa Bazan, Mark Hagemann and Kyungmin Kim</i>	13
3. Relative Sensitivity of Flood Inundation Extent by Different Physical and Semi-empirical Models - <i>Shahab Afshari, Ehsan Omranian and Dongmei Feng</i>	19
4. NHDPlus-HAND Evaluation - <i>Xing Zheng, Peirong Lin, Savannah Keane, Christian Kesler and Adnan Rajib</i>	26
5. The Modified HAND Method - <i>Ryan McGehee, Lingcheng Li and Emily Poston</i>	37
6. Comparison of Flood Inundation Mapping Techniques between Different Modeling Approaches and Satellite Imagery - <i>Jiaqi Zhang, Dinuke Munasinghe and Yu-Fen Huang</i>	46
7. Object-based Segmentation to Identify Water Features from Landsat 8 and SAR Images: A Preliminary Study - <i>Yan-Ting Liao</i>	55
8. Data Science Driven Hydrological Applications - <i>Krishna Karthik Gadiraju</i>	62
9. Quantifying Uncertainty in Flood Inundation Mapping Using Streamflow Ensembles and Hydraulic Modeling Techniques - <i>Christopher Zarzar, Ridwan Siddique, Hossein Hosseiny and Michael Gomez</i>	71
10. Assimilation of Water Level Observations in River Models to Update Flood Inundation Maps - <i>Amir Javaheri and Mohammad Nabatian</i>	78
11. Real Time Postprocessor towards Improving Flood Inundation Mapping - <i>Sanjib Sharma and Bingqing Lu</i>	84
12. HAND Flood Mapping through the Tethys Platform - <i>Savannah Keane, Christian Kesler and Xing Zheng</i>	91
13. OPERA – Operational Platform for Emergency Responseand Awareness: Reimagining Disaster Alerts - <i>Mike Johnson, Paul Ruess and Jim Coll</i>	97
14. Translator TTX – Bridging the Communication Gapbetween Researchers and Emergency Responders - <i>Whitney Henson, Richard Garth and Christopher Franklin</i>	105
15. Increasing Citizen Awareness of Floodwater Risks: An Effort at Reducing Flood-related Fatalities - <i>Dawne Butler</i>	111
Appendix	117

Preface

The Consortium of Universities for the Advancement of Hydrologic Science, Inc. (CUAHSI) is an organization sponsored by the National Science Foundation in which more than 110 US universities are members, that advances hydrologic science through collective initiatives across the academic community. The Office of Water Prediction of the NOAA National Weather Service has developed a National Water Center on the Tuscaloosa campus of the University of Alabama to serve as the hub for the building of a National Water Model of the United States, and has established a National Water Center Innovators Program with CUAHSI to engage the academic community in research to enhance the National Water Model. The key activity of the Innovators Program is a 7-week Summer Institute at the National Water Center, bringing a group of graduate students together with faculty advisors and National Water Center staff to conduct group projects that involve rapid prototyping of new ideas. The **intent is to create an innovation incubator where students from many universities can exchange ideas** and advance concepts that, although they may be analyzed only for a short time and on a small study area, are illustrative of issues that will affect the functioning of the National Water Model across the continental United States.

The first Summer Institute was held in June-July 2015, and focused on the formation of a prototype National Water Model running in the Texas Advanced Computing Center of the University of Texas at Austin, which demonstrated that the discharge on 2.7 million stream reaches of the United States could be simulated and forecast in real-time using input precipitation and weather information produced by NOAA and a computational framework called WRF-Hydro developed at the National Center for Atmospheric Research. The results of this research are being summarized in a Featured Collection of articles in the Journal of the American Water Resources Association to be published later in 2016. The key innovation demonstrated at the first Summer Institute was a hybrid grid-catchment information framework for the National Water Model in which the land-atmosphere computations were carried out on square grid cells covering the continental US, and the resulting runoff was geographically transformed onto the 2.7 million catchments of the National Hydrography Dataset Plus (NHDPlus) and routed through the NHDPlus stream network. It was shown that the continental stream network could be treated in real-time as a single flow continuum, from atmosphere to oceans and from coast to coast.

This report contains summaries of research projects carried out during the second Summer Institute, held from 6 June to 20 July, 2016, which involved 34 graduate students from 21 US universities. These students were selected in an open competition, conducted by CUAHSI, in which students from any US university were eligible to apply. By June 2016, a first version of the National Water Model was in the process of being made operational on NOAA computational facilities, and the focus of the research was on translating the forecasts of discharge into flood inundation mapping and flood emergency response.

To support this activity, a year-long preparatory phase took place before the 2016 Summer Institute in which the 10 meter National Elevation Dataset of the United States was analyzed on the CyberGIS facility in the National Center for Supercomputer Applications of the University of Illinois at Urbana-Champaign and transformed into a raster called Height Above Nearest Drainage (HAND), in which each cell contains the height difference between its elevation and the elevation of the cell in the NHDPlus stream reach to which it drains. If the water depth in the stream is known, then the extent of nearby flood inundation can be determined by selecting the surrounding cells whose HAND values are less than the water depth. This activity was jointly endorsed by CUAHSI and by the Universities Consortium for Geographic Information Science (UCGIS), and was announced by the White House as part of the commitments for the White House Water Summit in March 2016. Coupled with flood forecasting from the National Water Model, the HAND approach establishes, for the first time, a foundation for locally informative, real-time flood inundation mapping continuously across the continental United States.

The support of this research by the CyberGIS facility and staff is gratefully acknowledged, in particular Yan Liu and Shaowen Wang, and of David Tarboton of Utah State University and Xing Zheng of the University of Texas at Austin who made critical contributions to this activity. A particular focus for study during the Summer Institute was flood inundation in Alabama. The contributions of Leslie Durham of the Alabama Department of Economic and Community Affairs, who provided additional detailed data from FEMA flood studies, and of Joseph Gutenson, Andy Ernest and Deborah Crocker, who provided data storage at the University of Alabama, are also gratefully acknowledged.

The National Water Model will increase the spatial density of flood forecasting by a factor of 700 compared to the existing National Weather Service River Forecast Center models. This will require densified measurement to assure the forecast results. As part of the preparatory phase of the Summer Institute, two demonstration sites for radar-based streamflow measurement were established near the National Water Center where water surface elevation and surface velocity are measured continuously. The Summer Institute students, with the collaboration of the US Geological Survey, did field work at these locations to establish streambed topography and water flow conditions, and constructed FastMech hydrodynamic models showing the spatial pattern of the flow depth and velocity for these stream reaches. The intent of this phase of the Summer Institute activity was to complement the continental scale flood inundation mapping activities associated with the HAND approach with detailed scientific study of small stream reaches using fundamental fluid mechanics. FastMech models were subsequently constructed for several other locations in various Summer Institute projects to extend that activity.

The collaboration of Peter Ward of Hydrological Services America, who loaned the radar stream measurement systems for this activity, of John Sloat of WaterCube who helped with the fieldwork, and of the US Geological Survey, in particular Jonathan Nelson and Victor Strickland, who guided the installation of this equipment, and the flow measurement and modeling, is gratefully acknowledged. The University of Alabama Geography Department and Surface Dynamics Modeling Laboratory are also acknowledged for providing field equipment (Total Station, Differential GPS and Boat Sonar) in support of this project, and computational resources for several other projects in the Summer Institute.

Real-time flood information needs to be translated into actions that improve flood emergency response. The first activity of the 2016 Summer Institute was a day-long flood emergency response exercise for Tuscaloosa County, conducted in the National Water Center's Situation Room, involving fire, police, public works staff from Tuscaloosa City and County, and local non-governmental organizations such as the Red Cross that also provide help during flood emergencies. This exercise used HAND-based flood inundation mapping for a hypothetical flood scenario based on actual conditions for a flood event that had recently occurred in Tuscaloosa County, and stepped through, stage by stage, the rise, peak and recession of the flood to assess what emergency response actions would be taken and how flood forecasting and inundation mapping could be used in decision making. A hypothetical failure scenario of the Northport Levee located on the Black Warrior River near the National Water Center was simulated using a GSSHA model created by Ahmad Tavakoly of the US Army Corps of Engineers in Vicksburg, MS. Web-based flood inundation maps created using the ESRI ArcGIS Online system were projected onto the big screens in the Situation Room at the National Water Center. These showed the juxtaposition of flood inundation mapping with address points for residences and businesses that are used when emergency response vehicles are dispatched to particular geographic locations. The success of this approach in correctly identifying an area of persistent flood risk in the Moundville area in south Tuscaloosa county was remarkable, and this illustrated the overall goal of this effort, which is to connect national flood forecasting with local flood emergency response.

Fire trucks, police vehicles and flood rescue equipment were gathered in a nearby parking lot so the students could see how rescues are carried out. The Mayor of Tuscaloosa, Walter Maddox, described how he and the city responded to a disastrous tornado in 2011 that tore through Tuscaloosa killing 53 people and destroying some of the emergency response facilities most critically needed at that time. The

cooperation of Rob Robertson, Emergency Management Coordinator for the City of Tuscaloosa, and of the more than 20 emergency response personnel engaged in the flood emergency response exercise, is gratefully acknowledged.

The key activity of the Summer Institute is the research that the students undertake in their group projects. Central to that are the relationships that they form with one another, working closely with students from other universities in cross-institutional research teams that enable exchange and connection of ideas in creative new forms. The formation and functioning of these teams was guided by two Student Coordinators, Adnan Rajib from Purdue University, and Peirong Lin from the University of Texas at Austin, both PhD students who had earlier participated in the 2015 Summer Institute. They have compiled and collated the project summaries included in this report and supervised its production. They also did valuable work prior to the start of the Summer Institute to assemble data and software ready for use in the research activity. We appreciate all the work and effort that Adnan and Peirong have contributed as Student Coordinators.

In addition, faculty from various universities served as Theme Leaders to help focus the research activities. These included Sagy Cohen and Sarah Praskiewicz from the University of Alabama, Alfonso Mejia from Penn State University, Ibrahim Demir from the University of Iowa, and Albert Van Dijk from Australian National University. In particular, Drs Cohen and Praskiewicz were resident in Tuscaloosa and worked with the students throughout the Summer Institute to provide guidance and support of the many activities involved. The support of the Theme Leaders of the 2016 Summer Institute is gratefully acknowledged. There will be another Summer Institute in 2017 at the National Water Center and planning for that event is now being initiated.

It can be appreciated that an activity of this magnitude involves a great deal of organization. Richard Hooper and Emily Clark of CUAHSI, and Pamela Harvey of the University of Alabama, were the main people who helped with the institutional arrangements and with travel, housing, and living arrangements in Tuscaloosa. Edward Clark and Fernando Salas were the key people who guided the activity and provided support from the National Water Center. The contributions of everyone who helped with the Summer Institute in ways great and small are gratefully acknowledged. We also would like to thank the University of Alabama School of Arts and Sciences for sponsoring the Capstone Event.

A key to the success of the National Water Center Innovators Program is the support it receives through the voluntary collaboration of the academic community, along with commercial and government partners. We wish to record our appreciation to the NOAA National Weather Service for this opportunity to contribute to the enhancement of water prediction for our nation.

On a personal level I wish to acknowledge that my contribution to this research was supported by NSF EarthCube Grant 1343785 and by the commercial firms ESRI and Kisters.

David R. Maidment

Technical Director, National Water Center Innovators Program Summer Institute 2016
Hussein M. Alharthy Centennial Chair in Civil Engineering
The University of Texas at Austin

Research Summary

Since becoming operational in August 2016, the state-of-the-art National Water Model (NWM) generates real-time water prediction and flood forecasting for the continental United States at 2.7 million river channels. The NWM architecture is the first nation-wide hydrologic operational endeavor at an unprecedented high spatial resolution, yet there is a need for academic community to continue to research dimensions that would improve upon and expand the capabilities of the NWM. In line with such motivation, the 2nd Summer Institute of the National Water Center (NWC) Innovators Program hosted 34 graduate student research fellows from 21 universities across the country from June 6 to July 20, 2016. During the seven-week program, the resident research fellows worked collaboratively on 12 projects, leveraging the NWM outputs. The projects were thematically categorized in four domains: flood modeling, inundation mapping, forecast errors, and emergency response. This report presents 15 papers based on the preliminary outcomes of these projects. Following discussion summarizes their key findings as a glimpse of the overall accomplishments from this collaborative mission.

Flood Modeling

Paper 1, by Coll, Johnson and Ruess, presents a field experiment to supplement shortage of hydrologic observations (e.g. velocity, streamflow) and channel properties (e.g. bathymetry) with radar measurement of streamflow. In collaboration with the United States Geological Survey (USGS), authors in Paper 1 also carried out a case study to show the utility of densified measurements in improving the precision of hydrodynamic models.

Pertaining to similar motivation, Paper 2, by Bazan, Hagemann and Kim, shows the application of high resolution Light Detection and Ranging (LiDAR) topography data in an effort to delineate more accurate drainage network in Texas Lower Rio Grande Valley. The overall approach presented in this study would help generating hyper-resolution hydraulic/topographic features with consideration of location-specific complexities, enabling better flood forecasting in hydrologically-challenging data-scarce regions.

Paper 3, by Afshari, Omranian and Feng, compares four different hydraulics/topography-based flood modeling tools, along with their relative sensitivity to complex geophysical and man-made attributes such as channel bathymetry, land use and hydraulic control structures. The outcome of this work provides insights on the trade-off between accuracy and workability of inundation mapping techniques across large scales, comparing simple, fast-computing, topography-driven approaches against detailed, slow-computing, physically-based hydrodynamic models.

Inundation Mapping

Height Above the Nearest Drainage (HAND), as a terrain-based method adapted in the NWM architecture for near real-time flood inundation mapping, has many benefits over various hydrodynamic models in terms of its speed and reasonable accuracy. Paper 4, by Zheng, Lin, Keane, Kesler and Rajib, shows the scalability of HAND method to continental-scale, addressing several questions including the influence of DEM resolution and river bathymetry on the precision of resultant inundation extents.

Paper 5, by McGehee, Li and Poston, thematically shows another variation of the HAND method based on stream order. The modification to HAND proposed in Paper 5 may enable the technique to better capture highly complex flooding situations like backwater effects from adjacent/downstream catchments.

For a selected historical flood event, Paper 6, by Zhang, Munasinghe and Huang, shows the use case of satellite imagery for evaluating the accuracy of two hydraulics/topography-based flood modeling tools.

To augment precise extraction of inundation observations from remotely sensed satellite imagery, a suite of algorithms for image segmentation and supervised machine learning are presented in Paper 7 by Liau

and Paper 8 by Gadiraju, respectively. The major contribution of Paper 7 is the use of National Hydrography Stream network (NHDPlus) and a Moisture Enhancement Index in extracting flood inundation extents from satellite imagery. The additional feature of Paper 8 is a unique perspective pointing towards the challenges of big data management in continental scale flood modeling/dissemination frameworks.

Forecast Errors

Paper 9, by Zarzar, Siddique, Hosseiny and Gomez, demonstrates probabilistic flood inundation mapping with streamflow ensembles and multiple hydraulic modeling techniques. By conducting a case study in an urbanized watershed in Pennsylvania, the authors showed the differences between deterministic versus probabilistic inundation mapping approaches (e.g. the former suggests flooding while the latter only suggests 50% chance of flooding in an oil storage tank farm). The results indicated that uncertainty quantification in inundation mapping is the key to more effective emergency response.

Paper 10, by Javaheri and Nabatian, presents preliminary results on assimilating water level measurements from the Iowa Flood Inundation System (IFIS) to update the NWM-derived depth values. Authors showed a reduced error of ~50 cm in the assimilation channel, and ~45 cm in the validation tributaries where no observation was available. As a potential post-processing module of the operational NWM, this study has implications to improve inundation mapping and short-range flood forecasting.

Paper 11, by Sharma and Lu, shows the implementation of a statistical model to produce more accurate stage height predictions from the NWM. With the statistical post-processor, the preliminary results showed generally-improved stage height and inundation extent predictions at a particular river reach, with promise for future studies on reducing uncertainty from NWM outputs.

Emergency Response

Paper 12, by Keane, Kesler and Zheng, establishes a workflow through the Tethys web-platform to visualize the HAND flood inundation maps. An easy-to-use web-based platform such as the Tethys app would help public and first responders to access and view the real-time inundation maps of their own neighborhood, which would benefit emergency preparedness.

Paper 13, by Johnson, Ruess and Coll, shows the development of a prototype Operational Platform for Emergency Response and Awareness (OPERA) system. OPERA intends to complement the current National Weather Service's flood alert system by providing a graphically interactive web portal enabling best possible warning, preparedness and response.

Paper 14, by Henson, Garth and Franklin, features another online portal that takes into account social norms and human behavior in emergency response. Paper 15, by Butler, supplements Paper 14 through the addition of an educational outreach component based on flood fatality data analysis. Joint perception of these two initiatives is helpful to address the communication problem between the "science domain" and the "social domain".

The ideas being exercised during the 2016 Summer Institute, as exemplified above, would help establish the National Water Model as the new frontier of intelligent decision support system against flood hazards. Further research is being continued by the graduate student research fellows and their academic advisors in collaboration with the NWC.

Adnan Rajib

Bilsland Dissertation Fellow in Civil Engineering, Purdue University

Peirong Lin

Doctoral Candidate in Geosciences, University of Texas at Austin

Student Coordinators, National Water Center Innovators Program Summer Institute 2016

Chapter 1

Flood Modeling

Radar Measurement and Flow Modeling: Methods

Jim Coll¹, Mike Johnson² and Paul Ruess³

¹ University of Kansas; jcoll@ku.edu

² University of California, Santa Barbara; mike.johnson@geog.ucsb.edu

³ University of Texas; piruess@utexas.edu

Academic Advisors: Xingong Li, University of Kansas, lixi@ku.edu; Keith Clarke, University of California, Santa Barbara, kcclarke@ucsb.edu; David Maidment, University of Texas at Austin, maidment@utexas.edu

Summer Institute Theme Advisors: Sarah Praskiewicz, University of Alabama, sarah.praskiewicz@ua.edu; Sagy Cohen, University of Alabama, sagy.cohen@ua.edu

Abstract: Traditional river forecasting and hydraulic modeling is limited by the type, quantity and density of measurements available. Currently, the hydrologic community is reliant on a combination of USGS gages, remotely sensed data, and field work to model the hydrologic properties of a reach. However, if hyper-resolution or continent-scale modeling is undertaken, more data is necessary than the current network can provide. The most obvious way to improve upon this shortcoming is to implement a more densified measurement network; while USGS stations are the industry standard, they are too sparsely located and often not representative of the waterways they are being used to describe. An alternative sensor, the Sommer GmbH RQ-30 radar, is more cost-effective, measures both stage and velocity, and operates autonomously. This paper outlines the rationale and objectives behind the installation of these systems, describes two study sites where these instruments have been installed, lays out different methods to gather bathymetry data, and ultimately uses these data, combined with the sensors, to model the reaches.

1. Motivation

To monitor and forecast our nation's waterways, current forecast systems rely on a network of United States Geological Survey (USGS) instruments. As of 2009, 6,880 active gaging stations existed within the United States (1), paling in comparison to the approximately 2.67 million National Hydrography Dataset Plus (NHDPlus) reaches across the contiguous United States (2). While these stations act as the backbone of hydrologic forecasting measurements, this widely distributed network cannot provide sufficient data to forecast other reaches or perform detailed modeling efforts in areas that lack the instrumentation or that are otherwise complex. The most direct way to alleviate this shortcoming is to increase the data collection density. While the ideal situation would include installing more USGS gages, the costs required for installation, maintenance, and calibration makes rapid upscaling impractical.

A potential solution to this lack of instrumentation is to supplement existing USGS stations with a modern, more affordable monitoring device such as the Sommer GmbH RQ-30 radar sensor. Compared with current USGS gaging stations, which cost between \$20,000 and \$35,000 to install and \$16,000 a year to operate, the Sommer costs approximately \$17,000 for installation and \$5,000 for maintenance (3). These differences in price and measurements encourages the use of such equipment and moves hydraulic science closer to the reality of a nationwide understanding of water. Despite these benefits, it remains

unclear how these sensors compare to the USGS stations, how they can be integrated into the existing network, or what the added velocity measurement means to modeling efforts.

2. Objectives and Scope

2.1 Objectives:

This paper highlights relative advantages by contrasting measurements taken from co-located USGS and Sommer systems. It will also explore how the addition of a velocity measurement helps constrain model solutions, and the effects of bathymetry resolution on model outputs. This is the first in a series of planned efforts to more thoroughly understand the relationships between water surface elevations derived from both physical measurements and simplifications made during the forecasting process for the National Water Model. While the ideal solution would involve a fully 3D model, the computational and data requirements for continental scale implementation of that are both limiting factors, and some channel simplification are needed if the model is to work for every reach, everywhere.

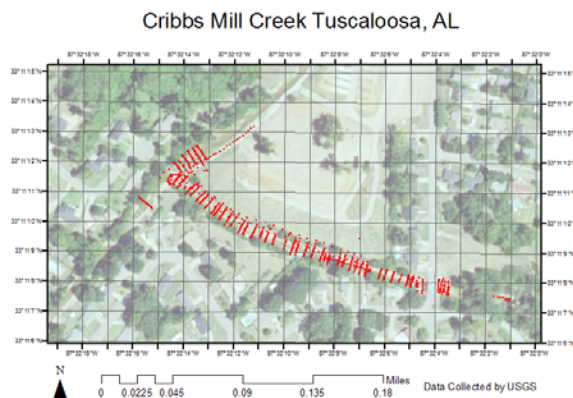


Figure 1. Cribbs Mill Creek site plan and data

2.2 Site Descriptions:

Urban stream: Cribbs Mill Creek, located directly north of Narrow Lane Road, Tuscaloosa, AL 35401, is a highly engineered, small urban stream that feeds into a weir just downstream to the west. This creek generally experiences limited flows ranging from 0.056 to 0.283 cms, although peak flow discharges can be an order of magnitude greater than that. This creek is crossed by a bridge built on top of a tunnel with concrete sides, which acts much like a concrete rectangular box culvert. The radar sensor is mounted on the downstream end of this bridge. Contextually, this creek is surrounded by homes and an RV park.

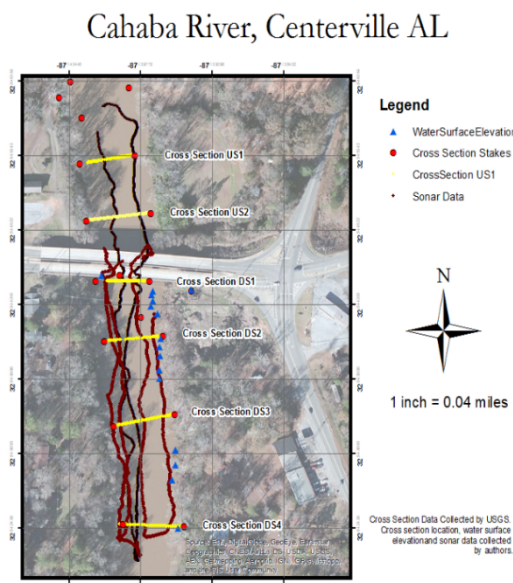


Figure 2. Cahaba River site plan and data

The risk in this creek, and the obvious purpose behind the heavily engineered banks, is the sudden inflow of water that enters the reach during storm events. The purpose for including this otherwise underwhelming stream in this research is just that; this reach may not normally be considered for a USGS gage installation, so the addition of the radar sensor provides the opportunity to explore both how well these smaller reaches can be modeled, as well as the potential to quantify the effects of urban runoff surges to better understand flood dynamics on a highly modified urban stream. The site map and bathymetry can be seen in Figure 1.

Low energy, low gradient river: The second site is located on the same bridge with the USGS gage at Centreville AL (USGS 02424000). This reach is approximately 50 meters wide and contains multiple point bar formations, dense overhanging trees, large woody debris, bedrock outcrops, smaller point bars, bridge piers, and left over construction debris all of which contribute to a complex bathymetry which complicates the modeling procedure. Low flows seen during the study period (06-

08/2016) approached 8.495 cms. There are several ways to collect the data necessary for this model, and the means is dependent upon the equipment available and the skill of the operators. As a general rule, it is best to collect data on a single day, preferably when base flow conditions dominate the river stage. This ensures that there is minimal change in water surface elevation throughout the day, making post processing much easier and results more accurate.

3. Methodology

The Flow and Sediment Transport with Morphological Evolution of Channels (FaSTMech) solver within the “International River Interface Cooperative” ([IRIC modeling software](#)) developed by the USGS was used (3). This solver was derived from the momentum equations, utilizes a finite difference method, and includes simple eddy viscosity turbulence closures which help account for backwater flow. It is also able to calculate helical sheer stress, which is where the quasi-3D properties are derived from. Additionally, it utilizes a flow/riverbed variation calculation under quasi-steady approximation, which allow it to perform calculations with extremely long time frames very quickly. The model assumes that the flow is incompressible, hydrostatic, primarily two dimensional, and not affected by strong secondary flows. To validate the model, a known (surveyed) water surface elevation accompanied each discharge measurement.

In order to run this model, in addition to the bathymetry, it also requires a known downstream boundary condition, and a discharge. Discharge measurements may come from USGS gages, the proposed Sommer sensors, or through other means. Bathymetry for Cribbs Mill Creek was collected as cross sections taken with a Real Time Kinematic Global Positioning System (RTK GPS) in five foot intervals. For the Cahaba reach bathymetry data was collected in three ways. First eight cross-sections were taken using an Acoustic Doppler Current Profiler (ADCP) by the USGS: three cross sections were measured downstream of the bridge, one directly under the bridge, and four upstream of the bridge. While these cross sections

are precise, their sparse distribution along the reach, less than 900 points for the entire reach, fails to capture some of the larger bed forms along the reach. To supplement these data, and account for the complex bathymetry, a sonar fish finder was used. The instrument used in this study was the [Humminbird Helix 999 SI](#), which can be bought new for under \$1000, and used for less than \$350, though to get the data out of the unit you will need to purchase an additional software package called the [SonarTRX](#) and the PlusPack addon for an additional \$240. This instrument was mounted



Figure 3. Left: Image of ADCP setup used; Below: Images of the mounting process and orientation of the Humminbird Fish Finder

to the side of a canoe, shown in Figure 3. In total 5 lengthwise runs were made, which added an additional ~4300 depth measurements along the reach. Afterwards, a [Sontek river surveyor M9](#), which

costs >\$45,000, was run across the entire reach, increasing the number of points to >54,000. This method of data collection also returns a full 3D profile of flow and a high resolution bathymetry model.

4. Results

Although the Sommer sensors have been lab tested and deployed successfully, it is worthwhile to perform a simple validation, shown in Figure 4, using the stations located at the Cahaba site, which indicates that the radar tends to underestimate the discharge at high flows and overestimate the discharge at low flows. It is also worth noting that the radar sensor reported negative flows during the approximate month and a half of data that was available to it. This was not unexpected, as the sensor uses a fuzzy logic algorithm to QA/QC the outputs which takes time to calibrate, though it did not flag these negative measurements as bad. Table 1 outlines several key metrics found with the model, alongside the measured counterparts.

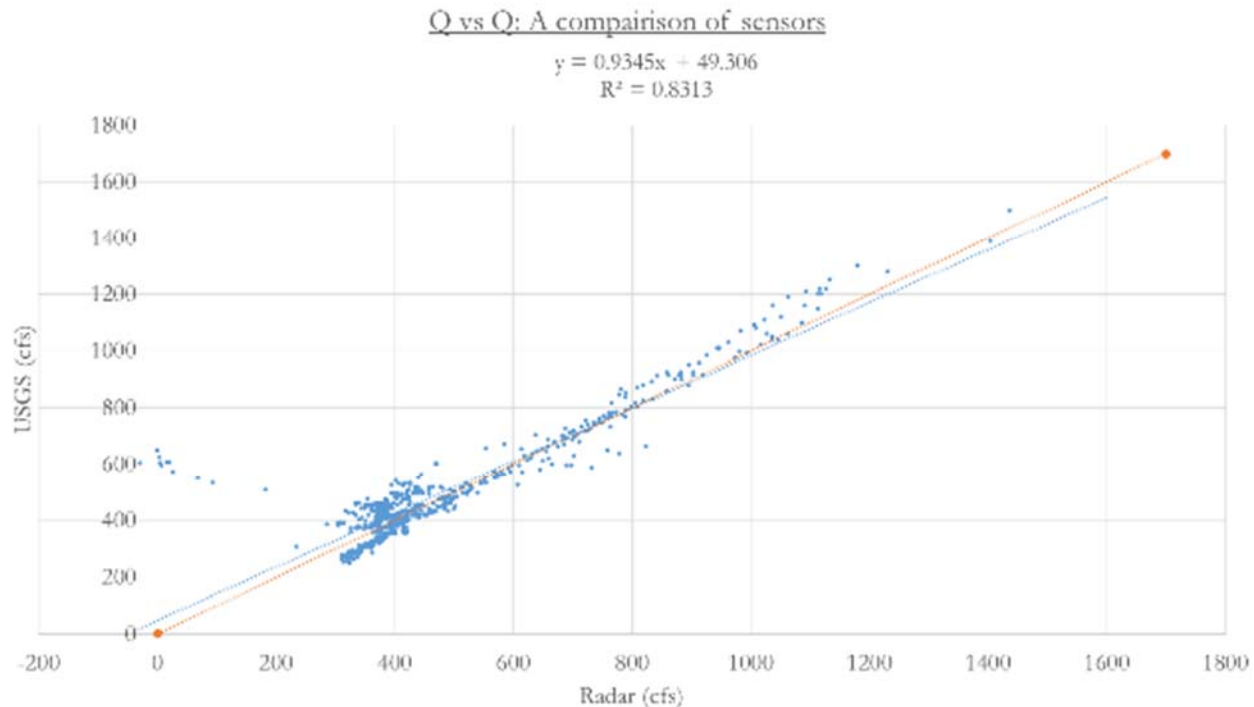


Figure 4. Validation of Q's from the USGS and Sommer stations

Table 1. Matrix of model outputs vs. sensor readings

	Drag coefficient	Modeled Q	Measured Q	Modeled V	Measured V	RMS
Cribbs mill:	0.005	9	10.02	1.91	1.87	0.1130
Cahaba (w/o sonar)	0.105	10	10.95	0.49	0.47	0.0297
Cahaba (with sonar)	0.045	24	24.63	0.64	0.64	0.0287
Cahaba (with ADCP)	0.15	9.5	9.20	0g.41	0.41	0.3000

Because additional measurements were taken at the Cahaba, three potential means of constructing channel geometry were tested, one based on the cross section measurements, one with the addition of the fish finder data, and one using the geometry derived from the ADCP, as shown in Figure 5 on the right. Based on visual comparisons, it appears that cross sections alone were not sufficient to capture the bathymetry with enough detail to produce acceptable results. The addition of the fish finder data was enough to remove the large anomalies in the cross section geometry. The ADCP measurements were able to capture micro-terrain features, and produced the closest modeled depth averaged velocities to those measured with the instrument.

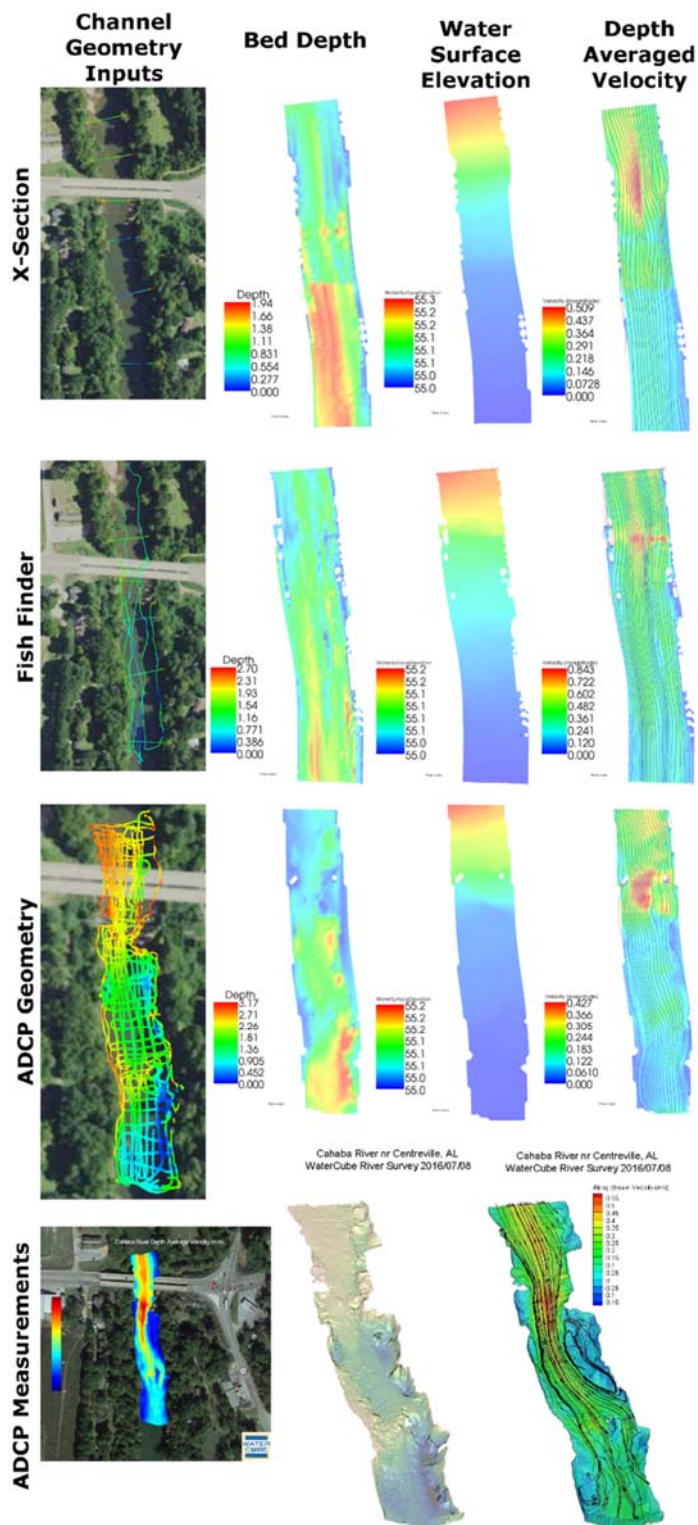


Figure 5. Model outputs from the various geometries

5. Conclusion

FaSTMECH was able to accurately back calculate the velocity at Cribbs Mill Creek to within 0.06 m/s. Of the three bathymetries tested on the Cahaba, the cross sections alone proved the furthest from measured conditions. For a comparatively low cost, the addition of the Humminbird fish finder was able to increase the accuracy of the model outputs to nearly that of the measured values. ADCP derived model outputs were even closer to reality, though as the physical measurements show, no method tested was able to accurately capture the dead water and circulation loops. While the roughness of the Cahaba was not entirely unreasonable when compared to similar Manning's roughness (4), the incorporation of the fish finder data provided much more realistic values for both the roughness coefficient and the modeled V. As a first step, this work was able to show that the addition of velocity enables more precise modeling efforts. However, site specific factors should be taken into account as the nation's water monitoring network expands to meet the needs of the National Water Model.

References:

1. McKay, L., Bondelid, T., Dewald, T., Johnston, J., Moore, R., and Rea, A., "NHDPlus Version 2: User Guide", 2012
2. Maidment, David. A Conceptual Framework for the National Flood Interoperability Experiment. Austin: N.p., 2015. Web. 7 July 2016.3. Interview with Richard McDonald from USGS in Golden, CO.
3. Nelson, Jonathan et al. "THE INTERNATIONAL RIVER INTERFACE COOPERATIVE: PUBLIC DOMAIN SOFTWARE FOR RIVER MODELING". *2Nd Joint Federal Interagency Conference*. 2010. Web. 2 Sept. 2016.
4. United States Department of Transportation, Federal Highway Administration. Guide For Selecting Manning's Roughness Coefficients For Natural Channels And Flood Plains. 2016. Print.

Delineating Stream Flowlines and Watershed Boundaries in the Lower Rio Grande Valley Using High Resolution LiDAR Derived Digital Elevation Models

Brenda Elisa Bazan ¹, Mark Hagemann ² and Kyungmin Kim ³

¹ University of Texas Rio Grande Valley; brenda.bazan01@utrgv.edu

² University of Massachusetts Amherst; mhageman@umass.edu

³ University of Texas at Austin; jenny9545@gmail.com

Academic Advisors: Jude A. Benavides, University of Texas Rio Grande Valley, jude.benavides@utrgv.edu; Mi-Hyun Park, University of Massachusetts Amherst, mhpark@engin.edu; Ben Hodges, University of Texas at Austin, hodges@mail.utexas.edu

Summer Institute Theme Advisors: Alfonso Mejia, Pennsylvania State University, amejia@engr.psu.edu; David Maidment, University of Texas at Austin, maidment@utexas.edu

Abstract: Characterized by a very flat terrain, periodic heavy rainfalls and clay soils, the Lower Rio Grande Valley (LRGV) in Texas remains an area very prone to wide-scale flooding. It is imperative that existing hydrologic models are improved and refined to further understand the potential impact of flood events, and most importantly, provide as much lead-time as possible to its more than one million residents. The National Water Model's efforts to simulate real-time and forecasted streamflow might not be enough to model this intricate and underserved area since the scale of the model cannot account for the very mild, but significant, changes in elevation in the LRGV. Taking this into consideration, high resolution Light Detection and Ranging (LiDAR) data of the LRGV was analyzed using the ROGER CyberGIS supercomputer with the objective of more accurately representing drainage networks and flood vulnerabilities in the region. Using the TauDEM toolset, LiDAR-derived digital elevation models (DEMs) were processed to produce hydrologic features such as stream networks and sub-watersheds. Existing National Hydrography Dataset (NHD) flowlines in the area were compared visually to the high-resolution DEMs and to the TauDEM-derived drainage features. The NHD network used for the NWM over LRGV was missing some of the main drainage features in the Brownsville Resaca Watershed, most of which were not consistent with the satellite images of the area. Therefore, the NHD flowlines were modified in ArcGIS to pinpoint and enhance flaws, like breaks and missing lines, in the drainage systems. This study is the first step in gathering, consolidating, analyzing and enhancing existing hydrologic data in LRGV. The results of this study should eventually reflect in terms of improved hydrologic models and flood forecasting in the LRGV.

1. Motivation

The Lower Rio Grande Valley (LRGV), located in deep South Texas, is characterized by very flat terrain, periodic heavy rainfalls, and clay soils as well as rapid urban development and a dense network of irrigation canals and drainage ditches. The LRGV is not a true valley, but is actually the ancient river delta of the Rio Grande which remains very prone to wide-scale flooding. The three major types of flooding that impact the region include: river flooding from the Rio Grande, flooding from local rainfall runoff, and the effects of storm surge during tropical storms and hurricanes.

With over 1 million inhabitants in the LRGV and another 1.5 living in Mexico across the Rio Grande, it is imperative that hydrologic models are improved and refined to further understand the possible impact of flood events and most importantly, provide as much lead-time to area residents as possible by the application of current technologies. The National Water Model forecasts streamflow over the entire country, in near real-time and with a lead-time; however, we believe the NWM efforts will not be sufficient to model this intricate and underserved area. This project proposes to look into the topography and hydrology of the LRGV in greater detail, since an approach based on larger scales may not have the spatial resolution necessary to properly assess this area.

A notable hydrologic feature of the study region is the presence of “resacas”. Resacas are old distributaries (secondary river channels) of the Rio Grande that used to convey water away from the river during periods of high flow. Their formative flow has now been interrupted, but the resacas remain. These resacas play a major role in the drainage and overland flow system in the study area watersheds; however, some of the main resacas are not included in the NHD network and the NWM.

2. Objectives and Scope

Mischaracterization of network vs. non-network features, errors in connectivity and paths, as well as omissions of important drainage features such as resacas, disregard the utility of NWM along the pre-defined NHD network without a careful review. One of the main objectives of this project was to use high-resolution elevation data (LiDAR) to assist with future modeling of flood extent and drainage in the Brownsville Resaca / Lower Laguna Madre Watershed and the Arroyo Colorado Watershed - both located within the LRGV. An area-wide LiDAR-derived digital elevation model will greatly assist with the determination of small scale stream network segments and their resulting sub-watershed delineations. A second objective of this project was to enhance and augment the NHD flowlines to more accurately reflect the actual drainage network existing in the area.

Overall, this study intends to produce reliable hydrologic drainage features for the RGV for improved flood forecasting and modeling taking into close consideration the challenges in this hydrologically complex area. Specifically, there are two essential features that needed to be re-defined, stream lines and watershed boundaries. Both of these can usually be derived from a DEM; however, as mentioned before, the terrain in the RGV is flat making the process quite troublesome and the results less reliable. In view of this challenge, other methods had to be thought of in order to create more valid stream lines and watershed boundaries. In essence, the main goal was to enhance existing streamlines and watershed boundaries derived from a high resolution DEM for an intricate, challenging area for future hydrologic modeling and flood forecasting.

3. Previous Studies

The deep South Texas area has not been studied in significant detail with respect to area-wide flooding. Some hydrologic and hydraulic (H&H) studies focusing on the role that the Arroyo Colorado plays as an important floodway (flood diversion route) in the Lower Rio Grande Flood Protection Project [1] have been completed – but they are limited to HEC-RAS hydraulic studies in the main channel of the Arroyo and North Floodway. The only other studies related to flooding have been at the hyper-resolution scale, focusing on urban waterway flood modeling. A study by Whitko [2] focuses on floodplain mapping along local resacas and drainage canals using a distributed hydrologic model. This study, a cooperative effort between the City of Brownsville, the Texas Water Development Board, Rice University and the University of Texas at Brownsville, led to a citywide Brownsville Flood Study completed in two phases (2006, 2011) [3]. Zheng et al. [4] and Bedient et al. [5] developed flood alert system technology that was to be applied in the South Texas

region, but as of the present, has not been developed – largely due to the lack of detailed hydrography, complex irrigation drainage networks that complicate overland flow analyses, and the lack of high-resolution topographic data.

4. Methodology

In order to yield more representative stream network, the available data was analyzed in three different ways. First, the NHD flowlines from the network and non-network layers are compared to a satellite image of the area. In so doing, breaks and inconsistencies on the flowlines were found and corrected by manually editing the lines. Second, comparisons were made between NHD network flowlines and the known drainage networks as depicted by local area studies. As this approach is manually intensive, we were only able to complete this for a subset of the two watershed area – namely a sub-watershed in the Brownsville region. Some of Brownsville's main flood conveyance routes were not represented as line features in the NHD network layer, and only portions were sometimes included in the non-network layer. After the comparisons were made, these features were added to the appropriate network layer since they play an essential role in Brownsville's flood water conveyance. As a third and final step, the newly determined flowlines were then compared to the streamlines derived from the LiDAR-derived DEM. LiDAR-derived digital elevation models (DEMs) were obtained from four separate surveys of Hidalgo and Cameron Counties (Figure 1). The International Boundary and Water Commission (IBWC) conducted separate LiDAR surveys in 2006 and 2011, producing 1-meter-resolution DEMs for the southern portion of the study area. The US Geological Survey (USGS) conducted surveys of the northern portion of the area in 2008 and 2011. The DEM files totaled 1375 in number and 63 GB (Table 1) in size.

Table 1. Sources and characteristics of the LiDAR DEM data

Agency	Year	No. files	Resolution (m)	projection	Total size
IBWC	2006	1190	1	Lambert Conformal	27 GB
IBWC	2011	111	1	UTM zone 14	32 GB
USGS	2008	4	1	UTM zone 14	911 MB
USGS	2011	70	2	UTM zone 14	4.7 GB
Total		1375			63 GB

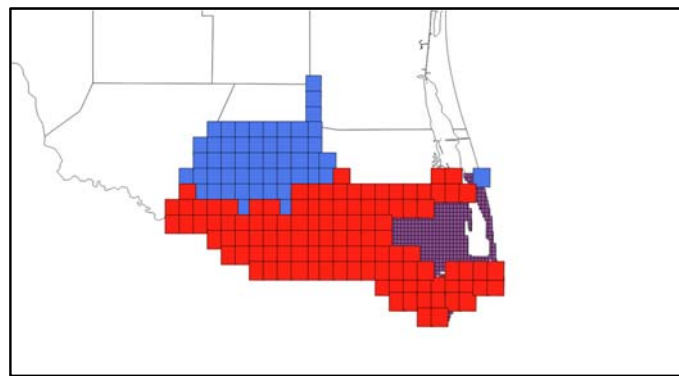


Figure 1. Coverage of individual DEM sources. Blue: 2011 USGS survey; red: 2011 IBWC survey; purple: IBWC 2006 survey.

Several automated methods to extract streamlines and watershed boundaries using high resolution DEMs already exist. Therefore, strategy to standardize a workflow needs to be set in place, which results in the best possible streamlines.

The large size of the combined dataset precluded analysis on a desktop computer, and all computations were performed on the ROGER CyberGIS high-performance computing (HPC) cluster

at the University of Illinois Urbana-Champaign. Geospatial operations were performed using the Gdal open-source library, and DEM **operations** were performed using the TauDEM package. Wherever possible, parallel computing was exploited using MPI.

Data preprocessing included re-projecting all DEM files to a common projection (UTM zone 14), combining the individual files into a single virtual raster (Figure 2), and creating lower-resolution overviews of the study area. This last step allowed the combined virtual raster to be viewed on a desktop GIS platform such as QGIS or ArcGIS. Once the data were preprocessed, a small (28000 x 18000 pixel) subset was extracted from the overall DEM for use as a pilot for TauDEM analyses. The desired TauDEM workflow was as follows. First, a “hydraulically correct” raster was computed from the raw DEM that raises local minima, forcing all pixels to drain to an outlet. Next, the d-8 slope and flow direction were computed for each pixel in the corrected raster, producing two separate rasters containing this information. These were then used to calculate a separate raster with pixel values representing each cell’s upstream drainage area. A final raster of stream locations was then computed by setting any cell with a contributing area greater than a specified threshold to have a value of 1 (representing “stream”) and all other cells to have a value of zero (“no stream”). Finally, these raster files were processed through a stream network function that produced a shapefile of stream lines and a raster of sub-watersheds.

5. Results

5.1 LiDAR DEM

Results of the LiDAR DEM analysis include the imagery itself, compiled and re-projected to facilitate viewing in a GIS desktop environment, as well as the stream networks and sub-watersheds obtained through TauDEM. These products reveal high-precision drainage features that will assist the refinement of hydrologic models and inform flood planning and management in the area. It is expected that ongoing efforts to integrate high-resolution imagery and expert knowledge will lead to a more flood-resilient Rio Grande Valley. Figure 2 below represent a composite snapshot of the combined LiDAR-based DEM for the study area. The image represents the first continuous high-resolution DEM for the study area and is already being used to reveal topographic features such as resacas (shown in higher color detail in figure 3) and their depositional nature (topographic banding due to natural levees).

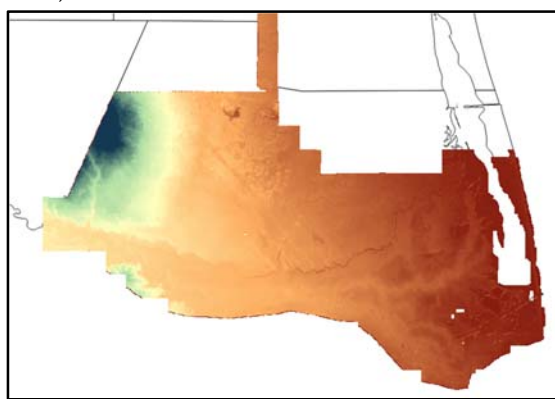


Figure 2. Combined DEM of Arroyo Colorado – Brownsville Resaca study area.

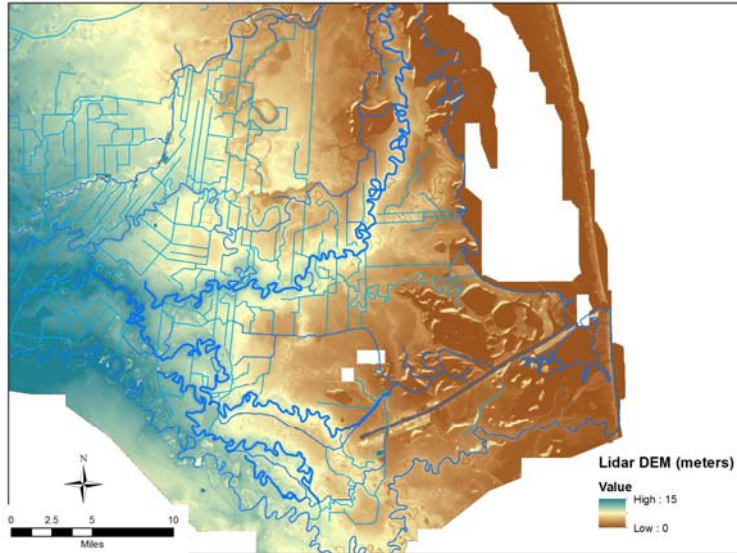


Figure 3. Close-up of Brownsville Resaca area watershed showing Resacas (wide lines) and drainage features.

While useful in that it exploits the high-resolution topographic data from the DEM, the above discussed workflow and methodology misrepresent non-topographic flow conduits such as bridges, culverts, and pipelines. Thus such features were artificially “burned in” to the DEM using the NHD vector files that had been previously enhanced. This approach combines a priori knowledge with remote-sensed data to optimally infer fine-scale hydrologic behavior. The workflow detailed above using TauDEM was repeated using the burned-in features, producing a second set of stream lines and sub-watersheds (Figure 4). Once the workflow was verified using the pilot study area, a larger section of the Brownsville region was processed in a similar fashion. While mostly successful, the products of this analysis have proven problematic in that the derived rasters include missing pixel values, and flow lines become truncated when they intersect these pixels.

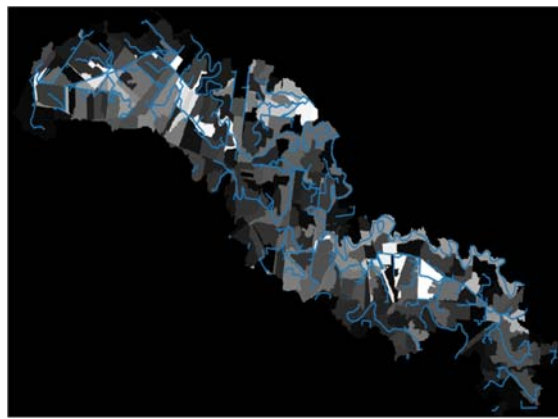


Figure 4. TauDEM analyses results from the DEM with burned in streamlines.

5.2 Streamline Delineation

Streamlines from the NHDPlus Version 2 Network and Non-Network files were manually analyzed. Breaks and missing features on the lines were found and corrected by comparing them to a satellite image. Essential features of the Brownsville drainage network were missing on the NHD Network but were included in the NHD Non-Network. These streamlines were manually selected and added to the NHD Network. (Figure 5)

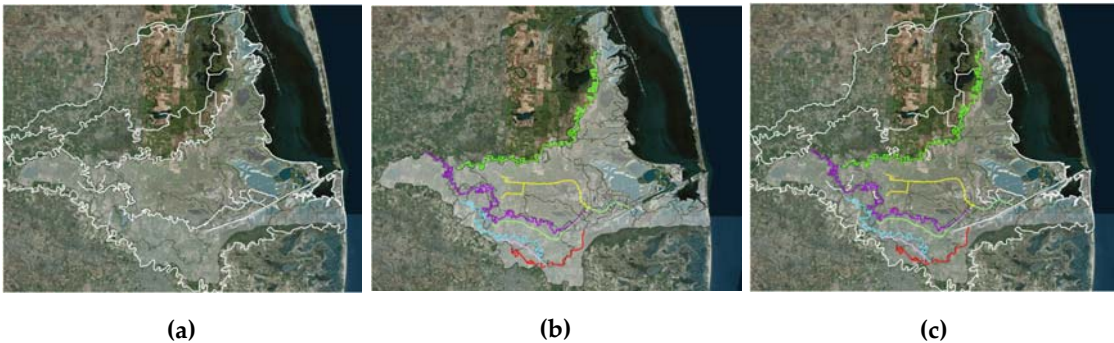


Figure 5. (a) NHD Network flowlines; (b) Brownsrvile's drainage network created by merging some Non-Network features with some Network features and manually enhanced by adding, removing and clipping streamlines; (c) NHD Network + Brownsrvile drainage network.

Streamlines were also extracted from high resolution DEMs, however the streamlines yielded from therein were not consistent with the streamlines we delineated and were sometimes faulty including nonexistent streamlines. In short, streamlines for areas as complex as Brownsville have to be delineated by a combination of methods, both automated and manual, to yield reliable results.

6. Conclusion

The Lower Rio Grande Valley is a hydrologically-complex area due to its flat terrain, complex hydrography, rapidly changing land use, and periodic heavy rainfalls in a semi-arid climate region. Although efforts to model and forecast flood events in the area have been made before, the lack of sufficiently detailed data (both topographic and hydrologic) has prevented the development of useful, area-wide and integrated hydrologic models. An extensive amount of work has gone into laying the foundation for such future work – illustrated by the development of a GIS desktop friendly, continuous LiDAR derived DEM at hyper-resolution scale and the start of a methodology to enhance the NHD / NWM network so that hydrologic modeling can commence at this scale. It is expected that this work will continue in cooperation with local, South Texas researchers throughout the year and that a specific case-study may be considered for further work at next summer's institute.

References

1. International Boundary and Water Commission, United States and Mexico, United States Section, IBWC. Hydraulic Model of the Rio Grande and Floodways Within the Lower Rio Grande Flood Control Project. June, 2003
2. Whitko, Annemarie N. "Advanced floodplain mapping of a Rio Grande Valley resaca using LIDAR and a distributed hydrologic model." (2005) Masters, Rice University. <http://hdl.handle.net/1911/17839>.
3. Ambiotec Civil Engineering Group, Inc. (2006). "Flood Protection Plan"; submitted to the City of Brownsville, TX.
4. Fang, Zheng, P. Bedient, J. Benavides, "Enhanced Radar-Based Flood Alert System and Floodplain Map Library" Journal of Hydrologic Engineering, 13(10), 926-938, 2008.
5. Bedient, P.B., A. Holder, J. Benavides, B.E. Vieux, "Radar-Based Flood Warning System Applied to Tropical Storm Allison" Journal of Hydrologic Engineering, 8(6), 308-318, 2003.

Relative Sensitivity of Flood Inundation Extent by Different Physical and Semi-empirical Models

Shahab Afshari ¹, Ehsan Omranian ² and Dongmei Feng ³

¹ City University of New York/City College; Civil Engineering and Environmental Department;
safshar00@citymail.cuny.edu

² University of Texas at San Antonio; Civil and Environmental Department; seyedehsan.omranian@utsa.edu

³ Northeastern University; Civil and Environmental Engineering Department; feng.do@husky.neu.edu

Academic Advisors: Balazs M. Fekete, City University of New York/City College; bfekeete@ccny.cuny.edu; Hatim Sharif, University of Texas at San Antonio; hatim.sharif@utsa.edu; Edward Beighley; Northeastern University; r.beighley@neu.edu

Summer Institute Theme Advisors: Sagy Cohen, University of Alabama; sagy.cohen@ua.edu

Abstract: Various hydraulic/GIS-based tools can be used for illustrating spatial extent of flooding for first-responders, policy makers and the general public. The objective of the current study is the comparison of four flood inundation modeling tools: HEC-RAS-2D, GSSHA, AutoRoute and HAND. In trade-off between accuracy and reliability of flood inundation models, simple and fast-computing semi-empirical models (AutoRoute and HAND), despite being less sensitive to detailed topography and effects of hydraulic infrastructures (levee, dams, etc.) on flood dynamics, are highly demanded than detailed and relatively accurate physical models (HEC-RAS-2D and GSSHA). This research was carried out on a 14km-long reach of Black Warrior River near the Northport levee and between Holt and Oliver dam and lock, in Tuscaloosa County, Alabama. Same geo-physical inputs (e.g. 10mx10m NED-DEM including river bathymetry and hydraulic infrastructure for physical models; low-, medium-, and high-friction values of bed-roughness associated with National Land Cover Dataset 2011; and inflow boundary conditions provided by the National Water Model for December 1st to 31st 2015) were incorporated in setting up these models. Concerning the different response of the four models for a small magnitude of flood (less than 5-year return period), flood water did not significantly overflow to the surrounding floodplains, however the inundation extents were found to vary noticeably for low- to high-friction land cover settings. Comparability analysis between inundation extents produced by HAND and AutoRoute with either HEC-RAS-2D or its union with GSSHA (~65% overlapping), showed that in average, HAND has ~16% more non-overlapping area than AutoRoute. Besides, joint-inundated regions of the four models only occupied ~35% of overall flooded extent. Further research will be carried out focusing on a different study area in order to ascertain relative comparability of these models and their sensitivity to geophysical as well as man-made attributes.

1. Motivation

A flood inundation maps are produced to show the spatial extent and depth of flooding along river channels and in the flood plain. Maps created using hydraulic and topography-based modeling tools can provide more comprehensive and dynamic outlines of various flooding extent than relying on past experiences alone. Concerning inundation models, advanced physical hydrologic-hydraulic models can be set-up for local study domain which is either labor intensive or requiring detailed

modeling initialization. On the other hand, uncomplicated semi-empirical models are going to be considered as an alternative to the complicated physicals since they are much faster and easier to be initialized in larger scales. However, there will always be the trade-off of losing the effects of landform, geologic, and geomorphologic features of the local study domain, especially while the stability of riverine flow and its response to flooding are affected by the existing hydraulic structures and water regulations. Hence, comparability among physical and semi-empirical models, accordingly their relative assessments are crucial for evaluating their strengths and weaknesses.

2. Objectives and Scope

Physical models of HEC-RAS-2D¹ and GSSHA² besides semi-empirical models of AutoRoute³ and HAND⁴ are employed in current research for producing and comparing flood inundation extent for a 14km-long reach segment of Black Warrior River, at Tuscaloosa County, Alabama. The domain is an urbanized zone being located between two hydraulic structures: Holt and Oliver lock/dam, and also protected by ~3.3km Northport levee.

Capabilities of physical and semi-empirical models in producing flood inundation maps will be evaluated according to the following approaches:

- 1) Building up the four models based on low-, medium-, and high-friction bed-roughness sets
- 2) Utilizing inflow time-series established by NWM⁵ for the December 1st-31st, 2015, while during this period flow regimes were ranging from ~250 to ~3400 m³/s (5-year flood)
- 3) Capturing the joint-inundated area of four models and contrasting it with the union of predicted flooding regions
- 4) Considering HEC-RAS-2D as true model and assess the overlapping and non-overlapping inundated regions reported by the other three models
- 5) Considering the union of inundation area produced by HEC-RAS-2D and GSSHA as true model and assess the overlapping and non-overlapping inundated regions reported by the other semi-empirical models

3. Previous Studies

Due to advances in computational speed and facilities, the application of 2D than 1D flood inundation modeling is accelerating globally. The 2D models incorporate topographic information for the channel and floodplains allowing estimations of inundation extent and river hydraulics [1-2]. Besides, recent studies argued about the impacts of horizontal resolution, vertical accuracy in topographic data, and inclusion of channel bathymetry in reducing the inundation area [3-5] along with the effects of different land covers (e.g. urban zones, vegetation, etc.) in accelerating/decelerating flood wave propagation in the flood plain [6-8].

4. Methodology

1 Hydrologic Engineering Center – River Analysis System 5.0.1 of U.S. Army Corps of Engineers

2 Gridded Surface Subsurface Hydrologic Analysis of U.S. Army Corps of Engineers approved by Federal Emergency Management Agency – National Flood Insurance

3 AutoRoute Rapid Flood Inundation Model produced by of U.S. Army Engineer Research and Development Center, Coastal and Hydraulics Laboratory

4 Height Above Nearest Drainage terrain model established by Nobre et. al., 2011

5 National Water Model – National Water Center – National Oceanic and Atmospheric Administration

The objective of this paper is to explore the difference between physical and semi-empirical 1D and 2D flood inundation models, their sensitivity to land cover and models' inherent processes. Semi-empirical models will be weighed against the physical models in terms of comparing inundation maps using following three quantities: 1) inundation area, 2) average inundation width, and 3) *F-Overlapping* inundation statistics [1, 3], that is,

$$F = 100 \times \frac{IA_{pred,obsr}}{IA_{obsr} + IA_{pred} - IA_{pred,obsr}} \text{ or } 100 \times \frac{IA_{obsr} \cap IA_{pred}}{IA_{obsr} \cup IA_{pred}} \quad (1)$$

where, IA_{obsr} is observed (true) inundation extent, while IA_{pred} denotes the predicted inundated area. $IA_{pred,obsr}$ refers to the area which is reported inundated both by observation and prediction.

In this section, four models and the associated setting will be succinctly described, and in turn, the required inputs, e.g. inflow boundary conditions, terrain model, and land cover types, will be introduced.

HEC-RAS is an advanced 1D/2D simulator of river hydraulics capable of performing flow simulation based on solving either diffusive wave or full momentum flow equations, through which various types of flow conditions can be simulated with incorporation of hydraulic infrastructures (dam, levee, weir, bridges, etc.). Especially, HEC-RAS-2D computes flood inundation boundaries from the zero-depth contour of flood depths for the selected water surface profile. Hence, it can provide the users with water depth variation across the floodplain. The RAS-Mapper module of HEC-RAS-2D adds more mapping and visualizing capability to users for manipulating and extracting required information concerning inundation extents directly from HEC-RAS platform rather than referring to GIS-based tools (e.g. ArcGIS, etc.).

GSSHA is a 2D physics-based model which uses mass-conserving equations to simulate hydrologic systems including: 1-D/2-D stream and overland flow routing, groundwater movement, precipitation, infiltration processes etc. Being spatially explicit and scalable, GSSHA is flexible to be set-up for different problems [9-10]. Compared with HEC-RAS-2D and other two semi-empirical models, time of computation in GSSHA was found significantly longer in this study.

The AutoRoute is a 1D topography-based model, developed by the Coastal and Hydraulics Laboratory (CHL) in the US Army Corps of Engineers, to determine route vulnerability caused by hydrologic factors and provide required information for the Military Hydrology Program. By using the Digital Elevation Model (DEM) data, it can calculate the flood extents, flood depth and stream cross-section profiles. The AutoRoute neglects the detail physics of channel/flood plain processes and thus it is computationally rapid than typical physical hydraulic models such as HEC-RAS-2D. Input for AutoRoute includes DEM, stream network and associated streamflow. Because of the simplicity of required input, it has an advantage over other physical hydraulic models especially when limited information, for example only DEM, is available [11].

HAND (Height above the nearest drainage) is a terrain model developed by Nobre et al. [12]. HAND normalizes the terrain topography based on the local relative heights along the drainage network. The procedure of HAND modeling includes the transformation of streamflow into flow height, comparison between the normalized terrain elevation and flow height, and then generation of flood extent maps. The transformation from streamflow to flow height is fulfilled by using a "theoretical" rating curve which is derived from Manning's Equation based on the NED terrain data. The input of HAND includes the normalized topology data (i.e. HAND raster data), streamflow along the rivers and the data defining the unit drainage boundary [12].

In this work, we use the 10 m National Elevation Dataset (NED)⁶. Stream network information is obtained from National Hydrography Dataset Version 2⁷. Streamflow data is derived from the NWM simulation. We also integrated the land use information to account for the roughness effects on the flood extents. The land use data is from National Land Cover Dataset (NLCD) 2011, and for each associated land cover type three bed-roughness (Manning's n) categories were set (consistent with roughness values pertaining to AutoRoute's nomenclature): Low-, Medium-, and high-friction.

5. Results

Three separate approaches were investigated to study the behaviour of the four models: inundation area, average inundation width, and *F-Overlapping* inundation statistics.

5.1. Trade-off between four models

Multiple inundation maps can be generated for each of physical and semi-empirical models. Figure 1 illustrates the segment of Black Warrior River where the union of inundation area (red-color group) associated with four models can be contrasted with overlapped area (green-color group) for each bed-roughness categories. The two inset figures (A and B) highlight the notion that more bed-roughness bring about extended inundations (areas having darker face-color).

Table 1 demonstrates the flooded area and average inundation width for each model corresponding to different bed-roughness settings. Semi-empirical models failed to highlight the effect of main channel capacity to hold the water even for low flood magnitudes. This was expected since the information associated with river bathymetry (~5 m deep for ~14 km reach) was not contained in 10mX10m NED-DEM as terrain models.

Apparently, HAND resulted in ~16% over-estimation of inundation extent than AutoRoute. Besides, backwater effects of Oliver Lock and Dam in immediate downstream side of study domain was not acknowledged by semi-empirical models. Meanwhile, both HEC-RAS-2D and GSSHA were set-up considering river bathymetry and hydraulic infrastructures (Levee and Dam) which caused less water intrusion to floodplains.

5.2. HEC-RAS-2D as true model; HEC-RAS-2D plus GSSHA as true models

Assessment on flooding extents generated by GSSHA, AutoRoute, and HAND were made on condition that the inundation boundary produced by HEC-RAS-2D considered as true extent. GSSHA revealed more consistency with HEC-RAS-2D than two semi-empirical models. The second approach was to consider the union of inundation area established by both physical models as true extent. Concerning either approaches, HAND demonstrated more consistency than AutoRoute with presumably true extent. Table 2 shows the outcomes for the two aforementioned circumstances.

6. Conclusion

The objective of the current study was the comparison of flood inundation extents produced by the four flood inundation analysis tools: HEC-RAS-2D, GSSHA, AutoRoute and HAND, being made for the 14km-long reach of Black Warrior River near by Northport levee and between Holt and Oliver dam/lock, in Tuscaloosa County, Alabama. Accounting for three types of bed-roughness categories

6 <https://gdg.sc.egov.usda.gov>

7 https://www.horizon-systems.com/nhdplus/NHDplusV2_home.php

(low-, medium-, and high-friction), overlaid on top of 10mX10m DEM as terrain model (including river bathymetry for HEC-RAS-2D and GSSHA) and forced by NWM streamflows (for the December 1st -31st, 2015 less than 5-year flood event), followings are the deliverables of our research:

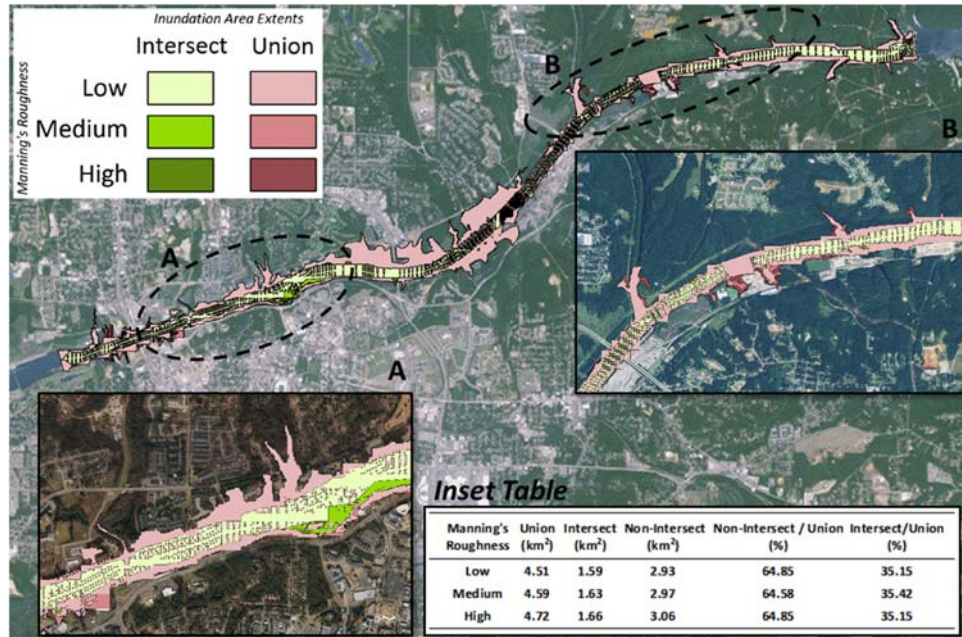


Figure 1. Flood inundation extents considering the intersected (overlapped) and union (blend) of four maps established by HEC-RAS-2D, GSSHA, AutoRoute, and HAND based upon three Manning's roughness categories (low-, medium-, and high-friction) along the floodplain.

Table 1. Inundation area average inundation width of flood maps established by physical (A and B) and non-physical (C and D) models based upon three Manning's roughness categories, n (low-, medium-, and high-friction) along the floodplain.

Index	Models	Low n	Medium n	High n	Low n	Medium n	High n
		Inundation Area (km²)			Inundation Width (m)		
A	HEC-RAS 2D	3.05	3.07	3.27	218.01	219.19	233.38
B	GSSHA	2.73	2.86	2.93	195.35	204.04	209.61
C	AutoRoute	2.13	2.16	2.23	152.03	154.28	159.04
D	HAND	3.84	3.84	3.84	274.13	274.13	274.13

Table 2. *F-Overlapping* inundation statistics (equation 1), where presuming inundation maps established by: a) HEC-RAS-2D, and b) HEC-RAS-2D plus GSSHA, as true extents, the other models' were scored according to their consistency.

Index	Models	Low n	Medium n	High n	Low n	Medium n	High n
		F-overlapping statistics (%) ^a			F-overlapping statistics (%) ^b		
B	GSSHA	66.58	66.81	65.92	-	-	-
C	AutoRoute	55.88	53.89	51.22	52.93	52.18	49.81
D	HAND	59.65	59.67	60.19	61.14	61.68	61.92

^a considering HEC-RAS-2D as the true extent;

^b considering combined inundation by HEC-RAS-2D and GSSHA as the true extent

1) simulation made by physical models in a low magnitude flood event did not result in major flood inundation extent, since the volume of water along the channel is not sufficient to overtop the banks. On the other hand, semi-empirical models lose (over- or under-estimate) about 35~45% extent

relative to true inundated areas (by the physical models) due to their drawback in not accounting for channel bathymetry and hydraulic structures; 2) bed-roughness variation did not yield major effect on flood inundation extents as the main channel inflow were not significantly large. In the future studies we will further scrutinize the four models' action and assess their relative performance in the case of larger flood events (e.g. 100-year flood) while domain is possessed by hydraulic infrastructures (dam, levee, etc.) and different land covers (urban, rural, etc.).

References

1. P. Bates and A. De Roo, "A simple raster-based model for flood inundation simulation," *Journal of Hydrology*, vol. 236, no. 1–2, p. 54–77, 2000.
2. V. Tayefi, S. Lane, R. Hardy and D. Yu, "A comparison of one- and two-dimensional approaches to modelling flood inundation over complex upland floodplains," *Hydrol. Process.*, vol. 21, pp. 3190–3202, 2007.
3. M. Horritt and P. Bates, "Evaluation of 1D and 2D numerical models for predicting river flood inundation," *Journal of Hydrology*, vol. 268, pp. 87-99, 2002.
4. D. Cobey, D. Mason, M. Horritt and P. Bates, "Two-dimensional hydraulic flood modelling using a finite-element mesh decomposed according to vegetation and topographic features derived from airborne scanning laser altimetry," *Hydrol. Process.*, vol. 17, pp. 1979-2000, 2003.
5. A. Cook and V. Merwade, "Effect of topographic data, geometric configuration and modeling approach on flood inundation mapping," *Journal of Hydrology*, vol. 377, pp. 131-142, 2009.
6. A. De Roo, O. M., G. Schmuck, E. Koster and A. Lucieer, "Assessing the effects of land use changes on floods in the Meuse and Oder Catchment," *Physics and Chemistry of the Earth, Part B: Hydrology, Oceans and Atmosphere*, vol. 26, no. 7-8, pp. 593-599, 2001.
7. T. Fewtrell, P. Bates, M. Horritt and N. Hunter, "Evaluating the effect of scale in flood inundation modeling in urban environment," *Hydrol. Process.*, vol. 22, pp. 5107-5118, 2008.
8. H. De Moel and J. Aerts, "Effects of uncertainty in land use, damage models and inundation depth on flood damage estimates," *Nat. Hazards*, vol. 58, pp. 407-425, 2011.
9. J. A. M. Jr., "Long-term Simulation in Parley's Canyon Using GSSHA, master's degree thesis," Brigham Young University (BYU), 2013.
10. W. D.M., S. B.E., D. C.W., J. Graulau-Santiago, N. Pradhan and B. A.R., "Gridded Surface Subsurface Hydrologic Analysis Modeling for Analysis of Flood Design Features at the Picayune Strand Restoration Project," World Environmental and Water Resources Congress 2015, Floods, Droughts, and Ecosystems.
11. Michael L. Follum, AutoRoute Rapid Flood Inundation Model, 2013.
12. A. Nobre, L. Cuartas, M. Hodnett, C. Rennó, G. Rodrigues, A. Silveira, M. Waterloo and S. Saleska, "Height Above the Nearest Drainage – a hydrologically relevant new terrain model," *J. Hydrol.*, 404 (1–2), 13, 2011.

Chapter 2

Inundation Mapping

NHDPlus-HAND Evaluation

Xing Zheng¹, Peirong Lin¹, Savannah Keane², Christian Kesler², Adnan Rajib³

¹ the University of Texas at Austin; zhengxing@utexas.edu, peironglinlin@gmail.com

² Brigham Young University; savk22@gmail.com, cpkesler@byu.edu

³ Purdue University ; adnanrajib@purdue.edu

Academic Advisors: David R. Maidment, the University of Texas at Austin, maidment@utexas.edu

Summer Institute Theme Advisors: David R. Maidment, the University of Texas at Austin,
maidment@utexas.edu

Abstract: The establishment of the National Water Model (NWM) has realized the high-resolution, real-time flood forecast at a continental scale. Taking the output from the National Water Model, the NHDPlus-HAND method has been developed as a framework to convert the forecast discharges to real-time inundation extents. A Height Above Nearest Drainage (HAND) raster used in the NHDPlus-HAND method has been calculated for the continental U.S. from the 10-meter National Elevation Dataset (NED). From the NHDPlus-HAND method, reach-averaged channel hydraulic properties can also be calculated for each stream reach. In this paper, the performance of the NHDPlus-HAND method is tested at a larger scale and a higher resolution. State-level inundation maps are created for Alabama during state-coverage uniform rainfall events. A new HAND raster is generated from a LiDAR-derived high-resolution DEM for Autauga County, Alabama to evaluate the influence of terrain dataset resolution on the inundation results and river hydraulic parameters derived from NHDPlus-HAND. HAND-derived channel hydraulic parameters are also compared with those computed from cross sections of local HEC-RAS models for validation. At last, channel bathymetric information interpolated by the River Channel Morphology Model (RCMM) is integrated into the original DEM and NHDPlus-HAND is rerun with the integrated DEM to estimate the underwater terrain details missing in the raw DEM.

1. Motivation

The NHDPlus-HAND method has been studied as an efficient approach of continental-scale inundation mapping and channel hydraulic property evaluation. However, several questions need to be answered before its wide implementation: (1) the scalability to a continental-scale real-time level, since the past studies are only conducted at a county scale; (2) the influence of DEM resolution to the inundation extents and channel hydraulic properties evaluated by NHDPlus-HAND, whether using a higher-resolution LiDAR-derived DEM will improve the results; (3) whether the channel hydraulic properties obtained from NHDPlus-HAND are usable in hydraulic models; (4) the solution for the absence of channel bathymetric details in the DEM dataset. These are the problems we look into in this project.

2. Methodology

NHDPlus-HAND has been successfully implemented at a county scale to map the Memorial Flood in Travis, TX and the Christmas Flood in Tuscaloosa, AL. In this study, the feasibility of NHDPlus-HAND is tested at a state scale assuming a series of uniform rainfall events in Alabama, which can be treated as the prototype of its continental-scale implementation. A constant rainfall rate range from 50mm/day to 500mm/day with an interval of 50mm/day is applied to all the NHDPlus catchments in Alabama. Since the total upstream watershed area is given for every NHDPlus reach as a field in the attribute table, the corresponding discharge of each uniform rainfall rate in each reach can be calculated by the rainfall rate times the total upstream watershed area.

Using the rating curves derived from NHDPlus-HAND, these discharges can be translated into stage heights. Then at each precipitation rate, a stage height table is created with one column of COMID and one column of stage height. The stage height table is then joined to the catchment feature class using COMID as the key. Next the catchment feature class is rasterized using the stage height as the raster value to create a water level raster across the whole state. Subtracting the HAND raster from this water level raster, we can generate a water depth raster corresponding to the flood caused by the uniform rainfall event. The above process is automated in a Python script, and has been repeated at each rainfall rate to create an inundation animation to assess the state of Alabama's vulnerability to extreme flood events at different locations.

In order to assess the influence of DEM resolution on the inundation mapping performance of the NHDPlus-HAND method, we separately generate two HAND rasters with two different resolution DEMs: one comes from the 10-meter NED, and the other is a 10-feet LiDAR-derived DEM provided by local community. Inundation maps at the same water level are created from both HAND rasters for several stage heights. The F-index is adopted to evaluate the goodness-of-overlap between inundation extents.

$$Fit (\%) = 100 * \frac{A_a \cap A_b}{A_a \cup A_b}$$

where A_a and A_b are the inundation extents predicted separately from two data sources, $A_a \cup A_b$ is the union of these two extents, and $A_a \cap A_b$ is the intersection of these two extents.

Besides the inundation extents, channel hydraulic properties evaluated using the NHDPlus-HAND method are compared at different reaches with different DEMs as the inputs. As a reference, these hydraulic properties are also compared with those calculated from the cross section dataset where local HEC-RAS models are available. Assuming there were N cross sections located on a single NHDPlus reach, at a stage height of H , the wet area of the i th cross section is calculated as $WA_{i,H}$, and the channel top width is calculated as $TW_{i,H}$. The flood volume V_H in the channel can be calculated by summing up all the prism volume between adjacent cross sections.

$$V_H = \sum_{i=1}^{N-1} \frac{(WA_{i,H} + WA_{i+1,H})}{2} L_i$$

where L_i is the river length from the i th cross section to its downstream neighbor cross section.

The reach-average channel wet area \overline{WA}_H at stage height H can be calculated as

$$\overline{WA}_H = V_H / \sum_{i=1}^{N-1} L_i$$

Similarly, the channel surface area SA_H at stage height H can be calculated as

$$SA_H = \sum_{i=1}^{N-1} \frac{(TW_{i,H} + TW_{i+1,H})}{2} L_i$$

The reach-average channel top width \overline{TW}_H at stage height H can be calculated as

$$\overline{TW}_H = SA_H / \sum_{i=1}^{N-1} L_i$$

From \overline{WA}_H and \overline{TW}_H , the reach-average wetted perimeter \overline{WP}_H , hydraulic radius \overline{HR}_H at stage height H can also be obtained.

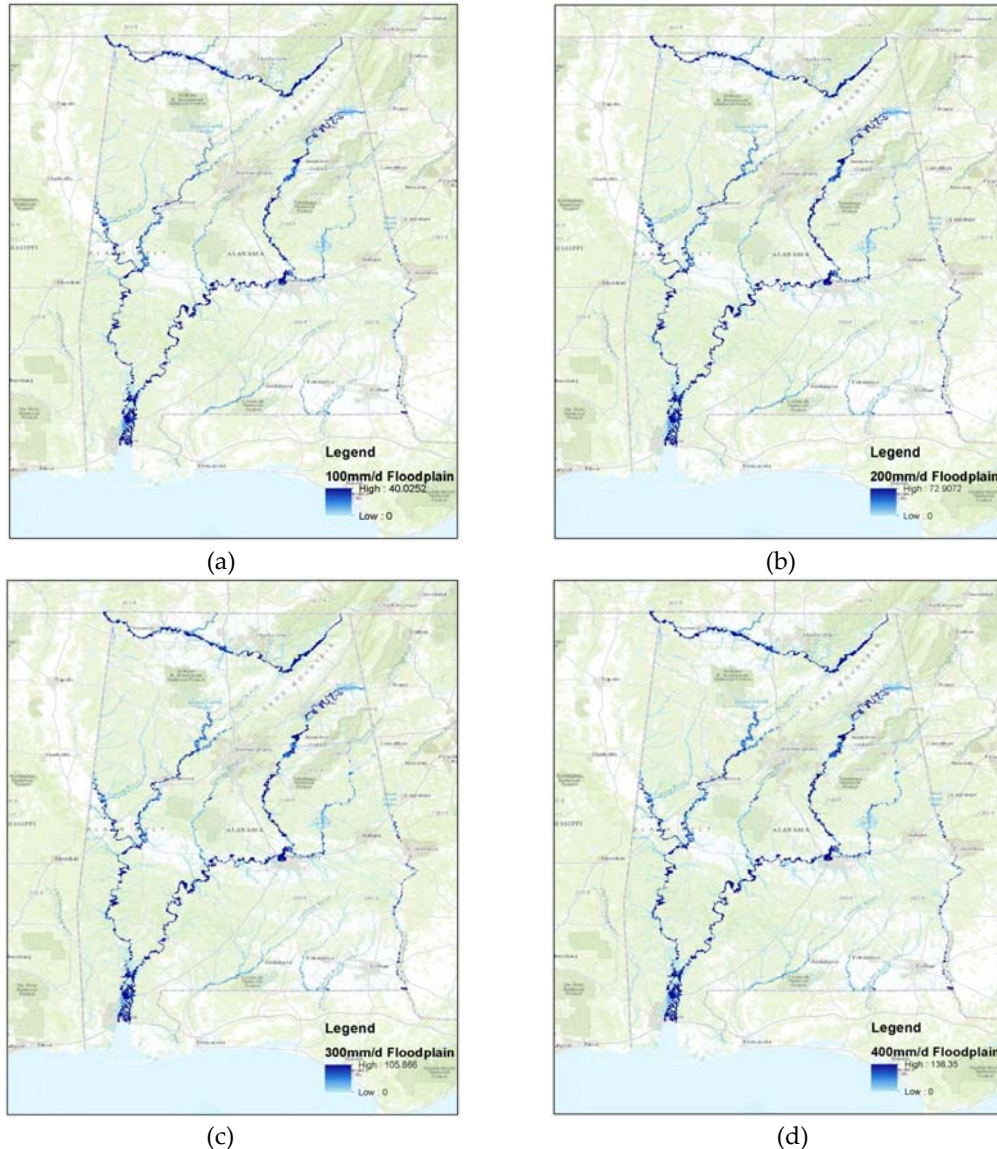
Even in the LiDAR-derived high-resolution terrain dataset, the channel bathymetric details cannot be fully recorded due to the poor performance of LiDAR underneath the water. Therefore, feasible alternatives should be examined. One of the alternatives is the River Channel Morphology Model (RCMM). RCMM takes several channel morphologic and hydraulic characteristic parameters to create a three-dimensional channel-bed mesh grid, which is made up of cross sections and profile lines. The bathymetry information stored in this mesh grid can then be integrated into the raw DEM

to provide a more comprehensive view of the river terrain. At last, the NHDPlus-HAND method is applied to evaluate the effectiveness of RCMM by comparing the river hydraulic properties derived from the raw DEM and those derived from the bathymetry-integrated DEM.

3. Results

3.1. Statewide NHDPlus-HAND Implementation

Figure 1 shows the state of Alabama inundation maps created using the NHDPlus-HAND method during a series of uniform rainfall events.





(e)

Figure 1. Alabama NHDPlus-HAND inundation maps during uniform rainfall events (a) precipitation rate = 100mm/day; (b) precipitation rate = 200mm/day; (c) precipitation rate = 300mm/day; (d) precipitation rate = 400mm/day; (e) precipitation rate = 500mm/day

3.2. NHDPlus-HAND Implementation with Different Resolution DEMs

A 10-foot LiDAR-derived DEM for Autauga County, Alabama is shown in Figure 2(a). Taking this DEM and the NHDPlus flowline features (Feature 2(b)) as the inputs, we run the NHDPlus-HAND method to generate a new HAND raster for Autauga County as shown in Figure 3(b). Another HAND raster of the same coverage is clipped as Figure 3(a) from the continental-coverage 10-meter HAND raster generated with the NED and the NHDPlus river network on ROGER.

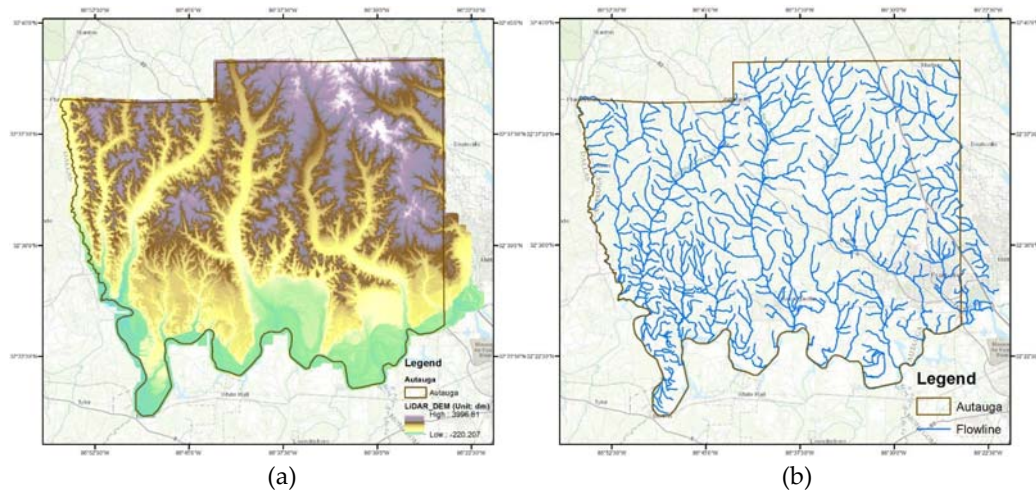


Figure 2. Autauga County, AL overview (a) 10ft*10ft LiDAR-derived DEM coverage; (b) NHDPlus river network in Autauga, AL

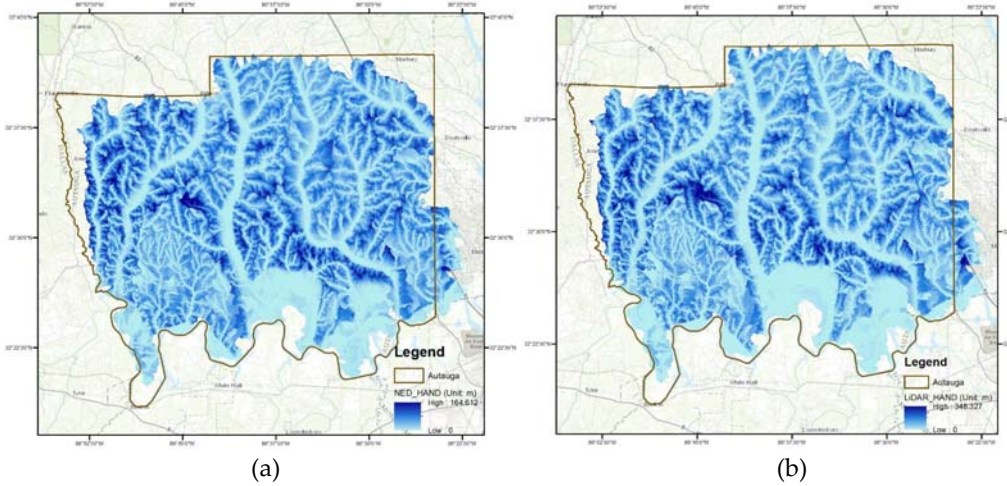


Figure 3. HAND rasters created for Autauga, AL with NHDPlus-HAND (a) from 10m*10m NED; (b) from 10ft*10ft LiDAR-derived DEM

Several analysis processes are conducted to compare these two HAND rasters. First, the raster calculator function is used to subtract the NED HAND value from the LiDAR HAND value. The difference raster is shown in Figure 4. A clear difference pattern (LiDAR-HAND value is greater/smaller than NED-HAND value) cannot be found in this image that occurs throughout the full coverage between these two HAND rasters. The mean value of the HAND value difference is 0.63m, and the standard deviation is 6.33m. From this figure, we can even see that the difference between these two HAND rasters in the channel section is actually relatively small, compared with the difference at other locations.

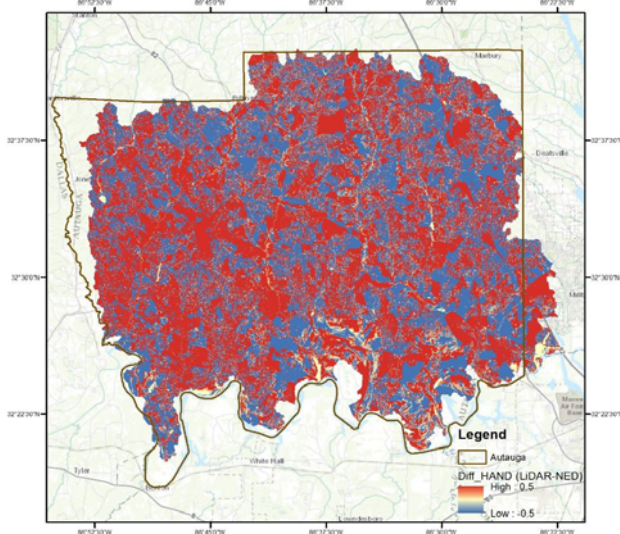


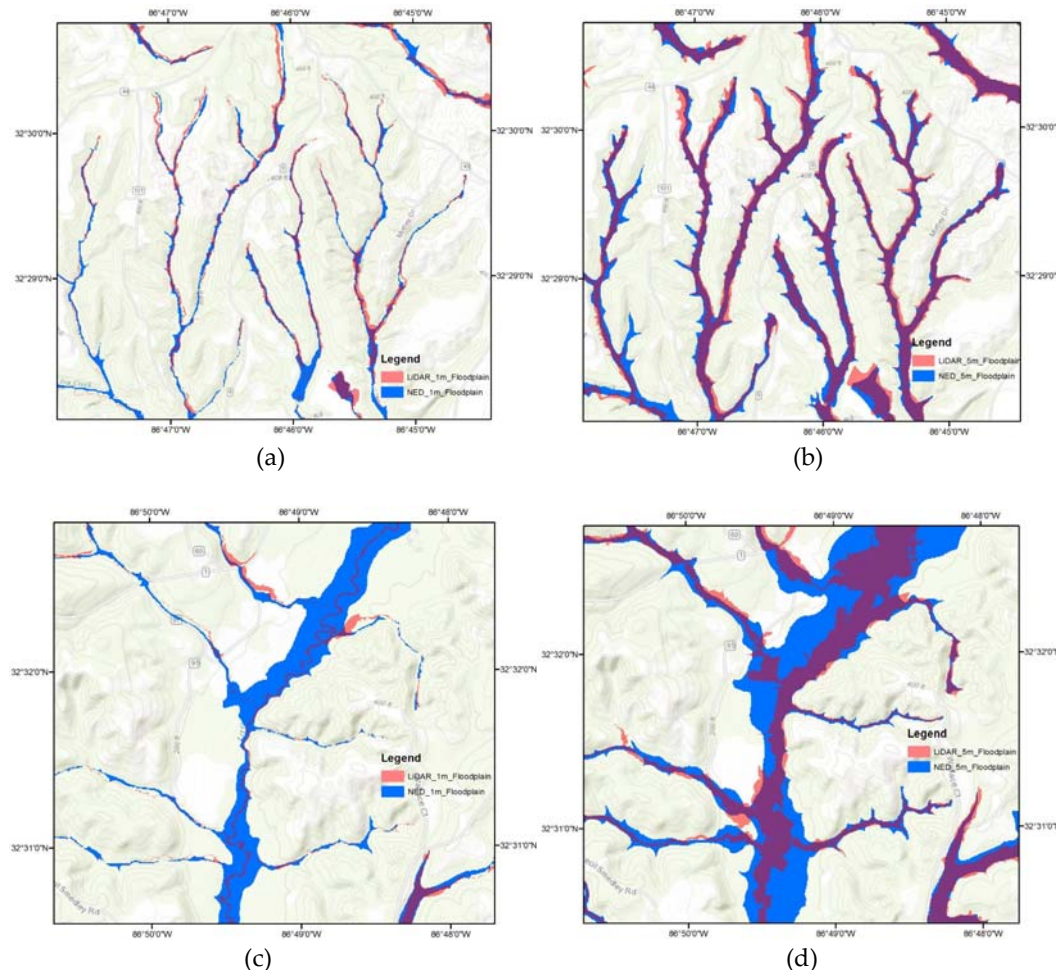
Figure 4. The HAND value difference between LiDAR-HAND and NED-HAND

Table 1 summarizes the comparison between the inundation extents generated from two HAND rasters. Figure 5 is a group of inundation map snapshots at some typical places. From Table 1 and Figure 5 we can see that: (1) For all stage heights, the inundation extent predicted by the NED-HAND raster is larger than the extent predicted by the LiDAR-HAND. This difference can be interpreted as the more detailed channel terrain information stored in the higher-resolution LiDAR-derived DEM, which leads to a thinner centerline used in NHDPlus-HAND and consequently, a better-bounded channel zone. However, the area difference between inundation

extents from two sources does not necessarily increase as the stage height rises. (2) Due to the DEM resolution difference, the raster grid alignments are different, causing a slight displacement between the river centerlines generated from two DEMs. This displacement can be one reason for the lower F index. (3) The improvement that a higher DEM resolution brings to the inundation extent is more significant on main rivers (5c, 5d, 5e, 5f) than small tributaries (5a, 5b), while such an improvement gradually diminishes as the stage height rises.

Table 1. NED-HAND & LiDAR-HAND Inundation Information Summary

Stage Height (m)	NED-HAND Inundation Area (km2)	LiDAR-HAND Inundation Area (km2)	Intersection Area(km2)	Union Area(km2)	F Ind ex
1	101.07	96.10	51.88	145.28	0.36
2	162.81	157.22	106.27	213.77	0.50
3	213.80	208.68	157.22	265.26	0.59
5	302.46	299.59	247.91	354.14	0.70



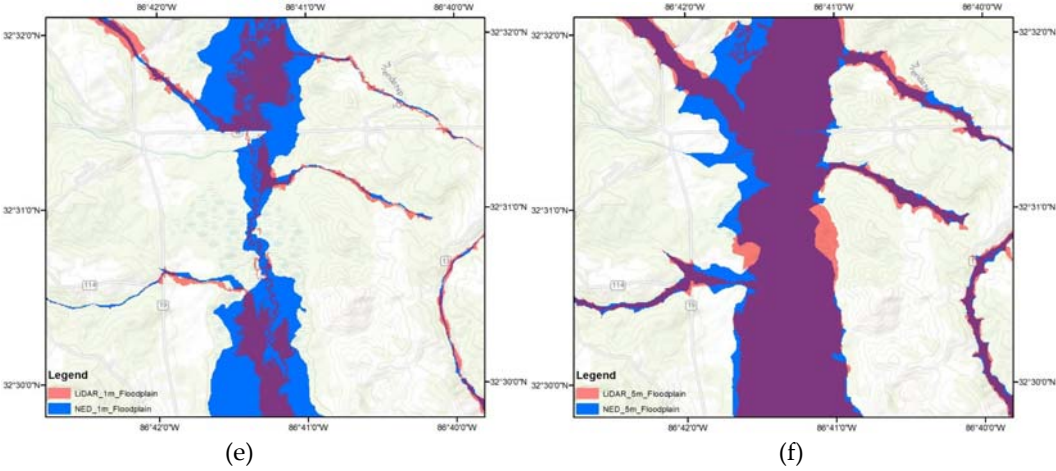
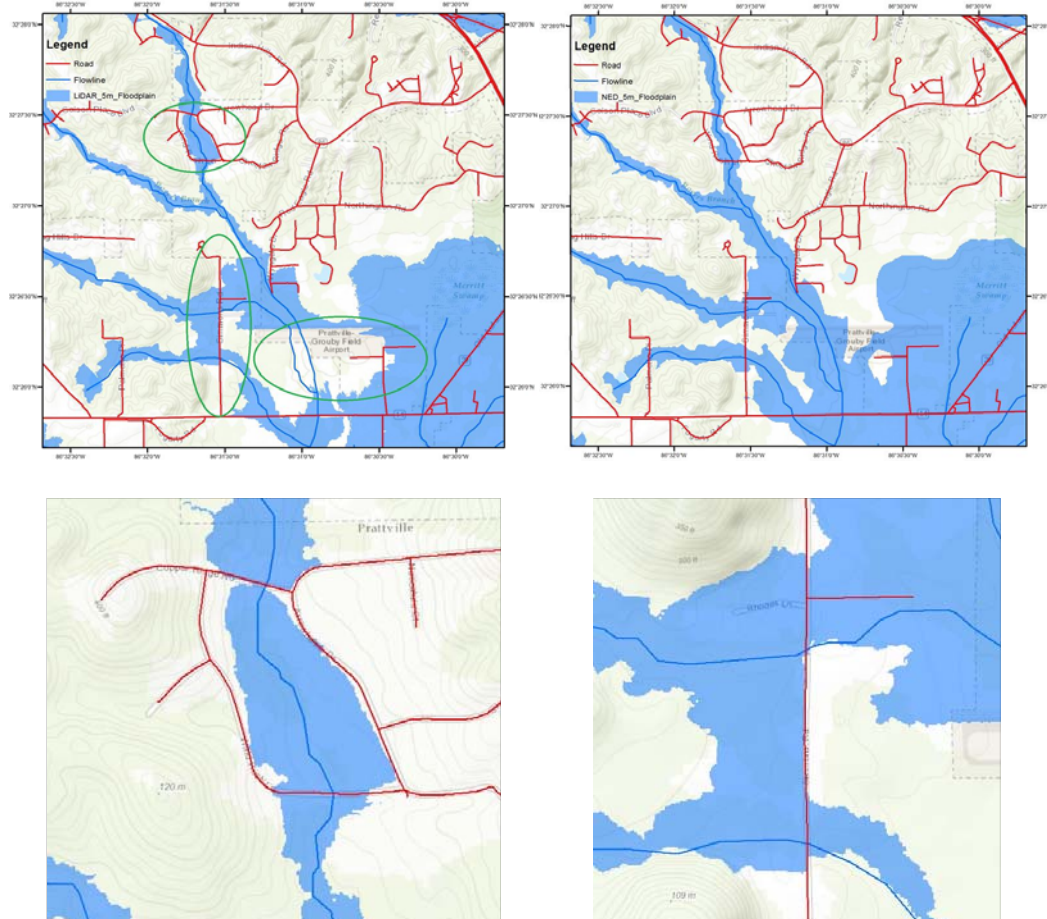


Figure 5. NED-HAND & LiDAR-HAND Inundation Extent Comparison

A distinct disadvantage of LiDAR-HAND, compared to NED-HAND, is the river-crossing artificial structures detected in high-resolution LiDAR-derived DEMs such as roads, bridges, dams, and airports. These relatively high structures act as obstacles lying in the channel, which prevent water from passing through their location, and force water ponding on their upstream side. Consequently, these artificial structures result in an overestimation of inundation extent in the structure's upstream areas, and an underestimation of inundation extent within the structure's location and its downstream areas.



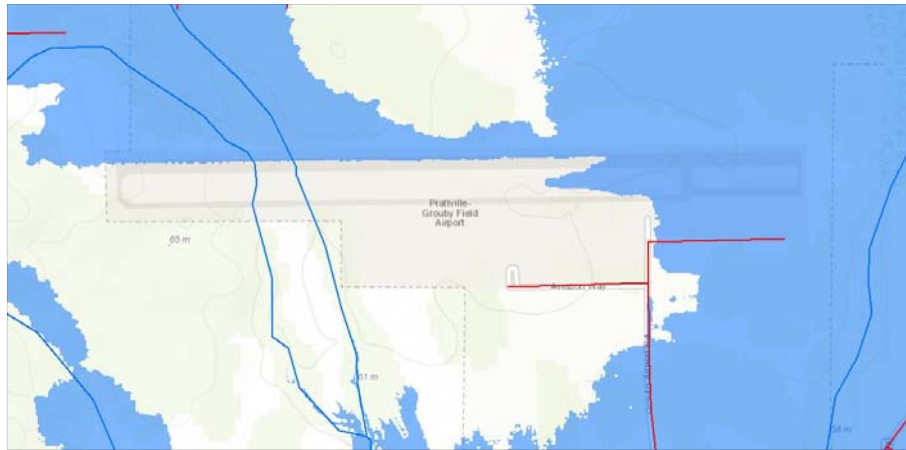
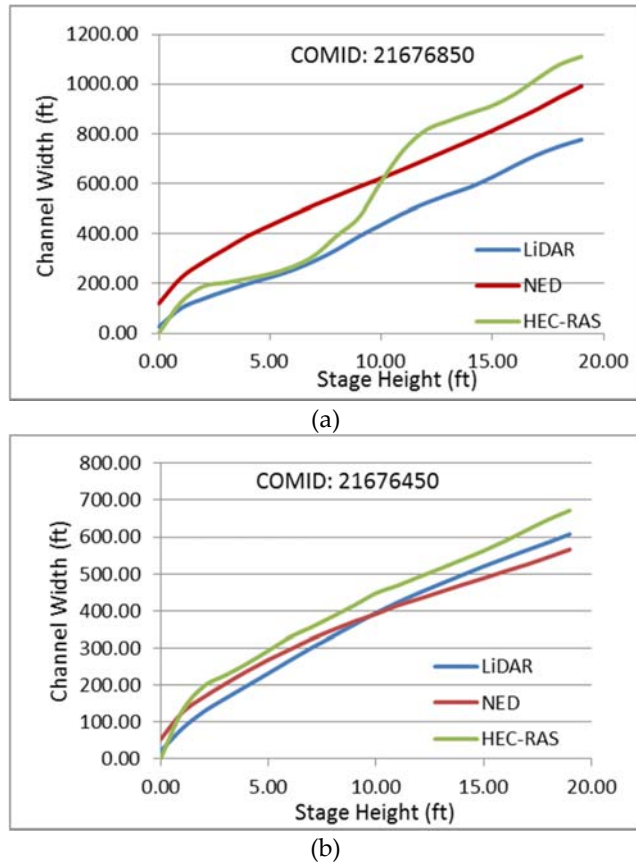


Figure 6. LiDAR-HAND issue at artificial structures (a) LiDAR-HAND inundation extent; (b) NED-HAND inundation extent; (c)(d) Inundation extent distortion caused by roads; (e) Inundation extent distortion caused by an airport

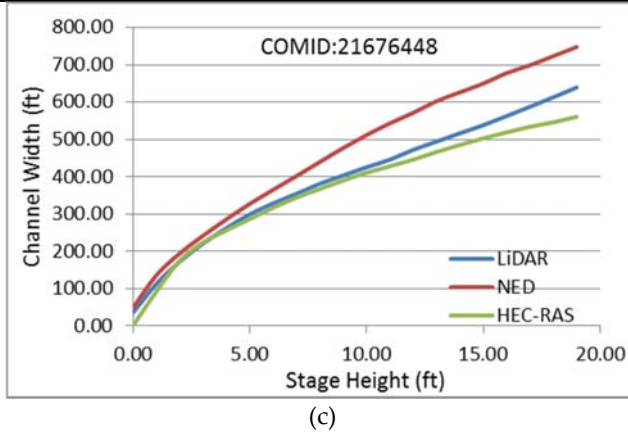
3.3. NED-HAND, LiDAR-HAND and HEC-RAS Reach-averaged Channel Hydraulic Property Comparison

Taking the HAND rasters generated in Section 3.2, reach-averaged hydraulic properties are calculated for all the NHD reaches in Autauga County following the NHDPlus-HAND workflow. Cross section data on three NHDPlus reaches (COMID=21676448, 21676450, 21676850) are collected from local HEC-RAS models to calculate HEC-RAS reach-average hydraulic properties. The result is shown in Figure 7 and Table 2.



(a)

(b)



(c)

Figure 7. NED-HAND, LiDAR-HAND, HEC-RAS reach-average channel width comparison

Table 2. NED-HAND, LiDAR-HAND, HEC-RAS reach-average channel width comparison

COMID	Avg. Channel Width Difference (LiDAR-HECRAS) (Unit: ft)	Avg. Channel Width Difference (NED-HECRAS) (Unit: ft)	Avg. Difference Percentage (LiDAR-HECRAS)	Avg. Difference Percentage (NED-HECRAS)
21676448	26.22	95.88	0.06	0.24
21676450	52.00	52.93	0.16	0.12
21676850	159.73	125.95	0.23	0.35

From Figure 7 and Table 2 we can see that both NED-HAND and LiDAR-HAND provide reasonable reach-average hydraulic property evaluation, compared to those obtained from local HEC-RAS models. However, both of them are subject to the overestimation problem due to a lack of channel bathymetric details in the DEM. Although compared to NED-HAND, the hydraulic property derived from LiDAR-HAND is slightly closer to that derived from local HEC-RAS model, however, due to the limited sample size analyzed in this study, a general conclusion cannot be drawn here that simply states a higher-resolution LiDAR-derived DEM necessarily improves the accuracy of the reach-average hydraulic property estimation using the NHDPlus-HAND method. Further study with a larger sample size is needed.

3.4. Bathymetry-Integrated NHDPlus-HAND (BIH)

In order to handle the channel bathymetry details, RCMM is applied to create a bathymetry-integrated DEM from the raw DEM with some channel morphologic and hydraulic parameters. Two case studies have been conducted on Brazos River, TX and Strouds Creek, NC. The coverage of the raw 10ft*10ft LiDAR-derived DEM on Brazos River is shown in Figure 8. Figure 9 shows the comparison between the cross section profiles of the same location, which are drawn from two DEMs – one is the raw DEM and the other is the bathymetry-integrated DEM generated by RCMM. As shown in Figure 9, RCMM is able to interpolate an about 20-feet-deep bathymetric terrain underneath the water surface for a main river like Brazos, which cannot be detected by LiDAR. A shift of channel location is also found in Figure 9. This shift is due to the mechanism of RCMM, which uses splines to build a smooth mesh. One of the variables to build the spline is the flowline curvature, which describes the meandering of the river. RCMM then generates an asymmetric channel mesh that corresponds to the river's meandering characteristic. Figure 10 shows the difference between the raw DEM and the bathymetry-integrated DEM.

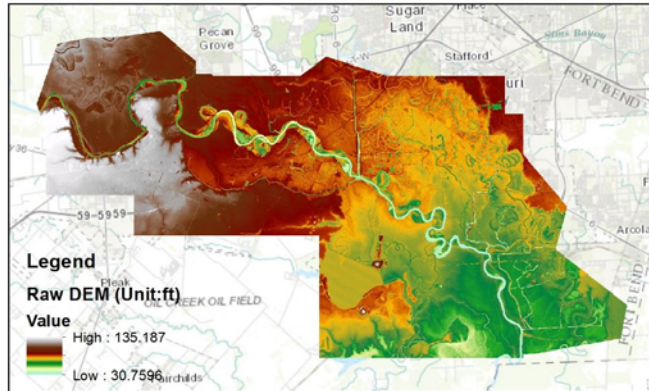


Figure 8. Raw LiDAR-derived DEM on Brazos River, TX (resolution: 10ft*10ft)

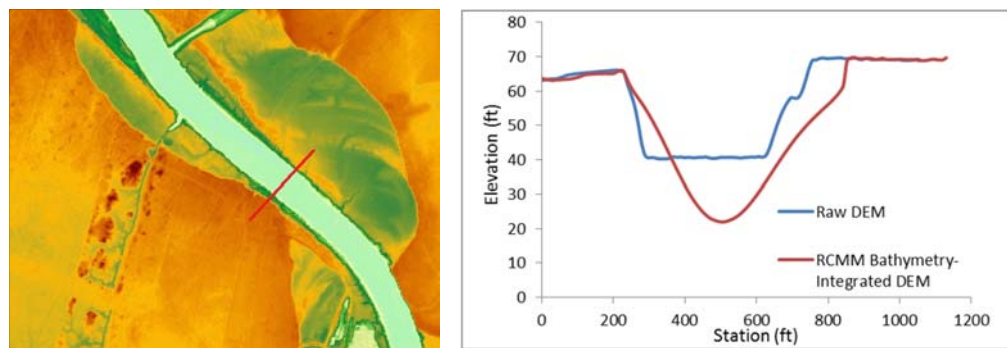


Figure 9. Cross section profile comparison between raw DEM and bathymetry-integrated DEM (a) cross section location; (b) cross section profile

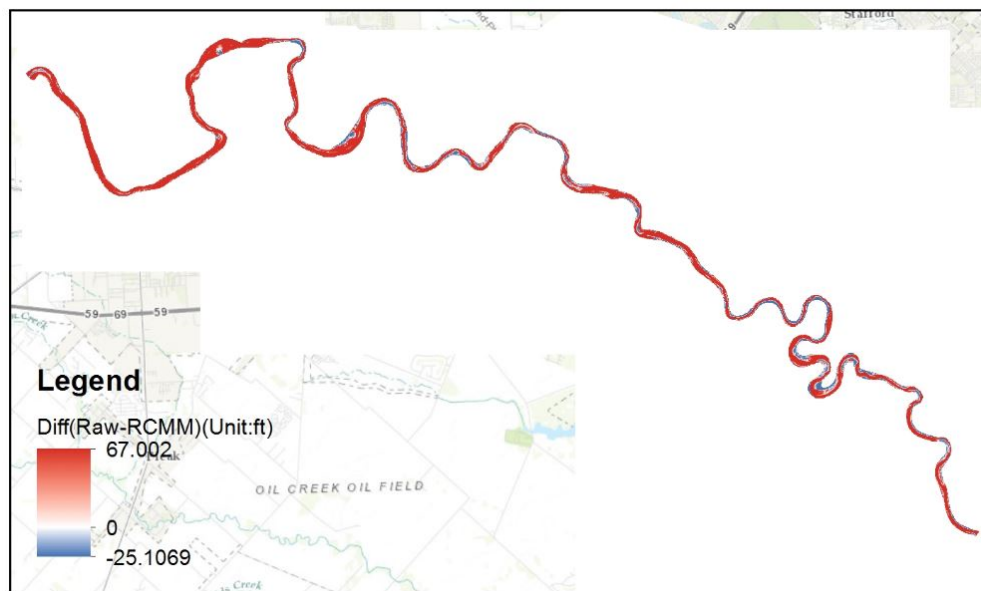


Figure 10. Elevation difference between raw DEM and bathymetry-integrated DEM

NHDPlus-HAND is applied with the bathymetry-integrated DEM to generate the inundation extents and channel hydraulic properties. From the new water depth-channel width relationship generated from the bathymetry-integrated DEM, a water depth is interpolated that corresponds to the bottom width generated from the raw LiDAR-DEM. This depth can be treated as the stage height

shift we should adjust for the rating curve generated by NHDPlus-HAND. The result of the Brazos case study can be found in Table 3.

Table 3 Stage height shift for rating curves derived from LiDAR-HAND

COMID	Stage Height Shift (ft)
3123738	11.3
3123746	8.5
3123760	5.5
3123774	8.5
3123776	6.1
3123780	3.9
3123782	11.9
3123784	8.4
3123786	6.6
3123790	0.8
3123792	21
3123794	13.5
3123806	4
3123808	1.8
3123810	6.6
3124648	-8.2
3124682	3.4
mean	6.68
st. d.	6.21

4. Conclusion

In this project, we (1) demonstrate the feasibility of implementing NHDPlus-HAND at a larger scale, where the case study coverage increases from a county to a state, and river reach number increases from several thousands to a hundred thousand; (2) investigate the influence of DEM resolution on the NHDPlus-HAND inundation extent; (3) identify the pros and cons when the high-resolution LiDAR-derived DEM is used in NHDPlus-HAND; (4) validate the reach-averaged channel hydraulic properties obtained from NHDPlus-HAND; (5) explore possible alternatives to incorporate river bathymetry information into the current NHDPlus-HAND method, which proves to be quite promising.

Reference

1. Liu, Y., et al. "A CyberGIS Approach to Generating High-resolution Height Above Nearest Drainage (HAND) Raster for National Flood Mapping CyberGIS." Center Technical Report
2. Nobre, Antonio Donato, et al. "HAND contour: a new proxy predictor of inundation extent." *Hydrological Processes* (2015)
3. TauDEM. <http://hydrology.usu.edu/taudem>. Accessed on June 12, 2016.
4. Merwade, V., & Maidment, D. R. (2005). River Channel Morphology Model: A Tool for Analyzing and Extrapolating River Channel Bathymetry. University of Texas at Austin, Center for Research in Water Resources, JJ Pickle Research Campus.

The Modified HAND Method

Ryan McGehee ¹, Lingcheng Li ² and Emily Poston ²

¹ Auburn University; rpm0010@auburn.edu

² University of Texas at Austin; lingchengli@utexas.edu, emilyposton@utexas.edu

Academic Advisors: Puneet Srivastava, Ph.D., P.E., D.WRC, Department of Biosystems Engineering, Auburn University, srivapu@auburn.edu; Zong-Liang Yang, Ph.D., Jackson School of Geosciences, University of Texas at Austin, liang@jsg.utexas.edu; Paola Passalacqua, Ph.D., Department of Civil, Architectural and Environmental Engineering, University of Texas at Austin, paola@austin.utexas.edu

Summer Institute Theme Advisor: Albert van Dijk, Ph.D., Fenner School of Environment and Society, Australian National University, albert.vandijk@anu.edu.au

Abstract: The National Water Model (NWM) is a hydrologic and hydraulic model that forecasts streamflow over the entire continental United States. Upon becoming fully operational one of the most anticipated products from the model will be real-time flood inundation mapping. This is a difficult task given the computational demand of hydraulic models. It is imperative to use a simpler method for this task that may otherwise be impossible given economic and computing constraints. Some have suggested that the Height Above the Nearest Drainage (HAND) method be used for this task, but some improvements in this method are possible. We propose that a modified HAND method—based on stream order—be used to complement the weaknesses of the original method. These enhancements include enabling non-uniform inundation within a catchment, accounting for backwater effects in catchments with precipitation and flooding downstream of the catchment, and bypassing hard flow paths that are shorted during large flooding events. We expect that other benefits that are not so obvious to become more apparent as the method is further analyzed. We have generated the modified HAND rasters for all stream orders in Alabama and its 9 related HUC4 basins (8 stream orders in total). We demonstrate that the modified HAND method retains the strength of the original method in cases where the original HAND is more appropriate (e.g. uniform inundation conditions), but better represents cases in which the original HAND has performed poorly. There are two computational demands of these methods: setup and operation. The modified HAND method requires slightly more setup computation but certainly less than a 50% increase in computation (for initial raster creation at each stream order). The operational computation is comparable to the original method and can even be less due to the potential to group catchments and perform somewhat of a lumped parameter analysis. The main point here is that the modified HAND provides far more flexibility for potential water balance computation, whereas HAND is at least more difficult to implement water accounting if it is even possible. We recommend that the modified HAND be implemented in any and all cases where HAND is currently employed for better results and potentially smaller computational demand.

1. Motivation

The National Water Model (NWM) uses hydrologic and hydraulic modeling to yield streamflow for every NHDPlus v.2 catchment for the entire continental United States. Upon becoming fully operational the output from the NWM can be used for emergency management, municipal and regional planning, water resource management, water quality modeling, drought management, etc. However, even when fully operational, there will still be limitations of the NWM, many of which arise from a constrained computing environment. Hydraulic modeling in particular quickly becomes computationally expensive. The challenge presented is to achieve expedient modeling results at a resolution and comparative accuracy of typical hydrologic and hydraulic models that can be used to coordinate local, regional, and national planning and relief efforts for various water

sectors in the United States. Obviously, these models must perform well under normal conditions, but many times it is actually the extreme conditions that we care more to know about. Flooding and drought in particular are examples of extremes that are constant threats to the economy and infrastructure but more importantly to life. In its current state the NWM does not have the capability to model flooding nor is it likely that it should be included in the near future given the highly simplified channel routing component, which is based on simple Muskingham calculations and assumed trapezoidal channels. There is a discussion about potentially integrating 2D hydraulic modeling for the routing portion of the NWM. This will require significantly more computation on an already strained system. Our motivation for this work is founded on the belief that there must be a simpler way to achieve accurate flood modeling without having to move to a higher dimension of hydraulic modeling.

2. Objectives and Deliverables

This project is primarily a flood mapping endeavor, which utilizes cyber GIS infrastructure, with implications that could lead to improved flood modeling. Therefore, all the objectives of this study relate to one or more of the three areas including: flood mapping, flood modeling, and cyber GIS. We have focused our efforts on the first of these three, which is flood mapping. Conclusions regarding future work and likely outcomes for each of these study areas will be provided in the conclusion. We realize many of our objectives have not been solved on the first iteration of this new method, especially due to time constraint. Still, we include them because they are the metrics by which we will continue to evaluate our work using the modified HAND method. Our primary objectives include the following:

1. mapping real-time flood inundation for spatially significant areas
2. modeling multiple basin flood interactions (which create backwater flood scenarios)
3. modeling overbank spills (which attenuate flood waves)
4. modeling temporary storage losses (which affect the extent and duration of floods)

Our first objective may seem obvious, but various obstacles have made this a difficult task using conventional hydraulic models. This almost demands that a simple method such as the HAND method be used in order to map the entire continental United States. We believe that if we can demonstrate the concept of light computation flood mapping that it would prove the scalability of the method for larger areas. Each of the last three objectives will be discussed more in the conclusion. Some deliverables for this study (both completed and planned) include:

- modified HAND workflow and methodology (completed)
- HAND and modified HAND rasters by stream order for study area (completed)
- HAND and modified HAND library of inundation rasters (in progress)
- inundation mapping workflow and methodology (under development)

There is also a significant potential to improve water accounting in the flood mapping and modeling schemes within the NWM. We consider this to be the ultimate goal of flood mapping and modeling, and it is well within the scope of our study, but it is not likely to be achieved in the first implementation of either HAND or the modified HAND.

3. Methodology

The Height Above the Nearest Drainage or HAND model is a terrain model that normalizes DEMs according to the local relative heights found along the drainage network [1]. Using the raw DEM as the input, several fundamental hydrological terrain analyses are performed such as pit removal to

ensure a coherent DEM, flow direction calculation to identify the flow paths and flow accumulation calculation to define and delineate the drainage network. With this hydrological terrain information, HAND then generates a nearest drainage map, or in other words, calculates each cell's relative vertical distance to the closest stream cell it drains into. Although the model was originally developed for soil water dynamics and the determination of local draining potential, HAND has been proved applicable to flood inundation mapping and analysis as well. In a study by Nobre et al. [2], the HAND terrain model was used to determine the inundated potential of grid cells in a study zone by utilizing the same logic as [1]. The study proved that the relative drop in vertical elevation as determined by HAND is an effective predictor of flood potential. Using a contour concept, the study developed an approach for mapping inundation extent of flooding events that does not depend on flood observations but instead, drainage-normalized topography and flow paths. See the workflow of the HAND method and the proposed modified HAND method below (Figure 1).

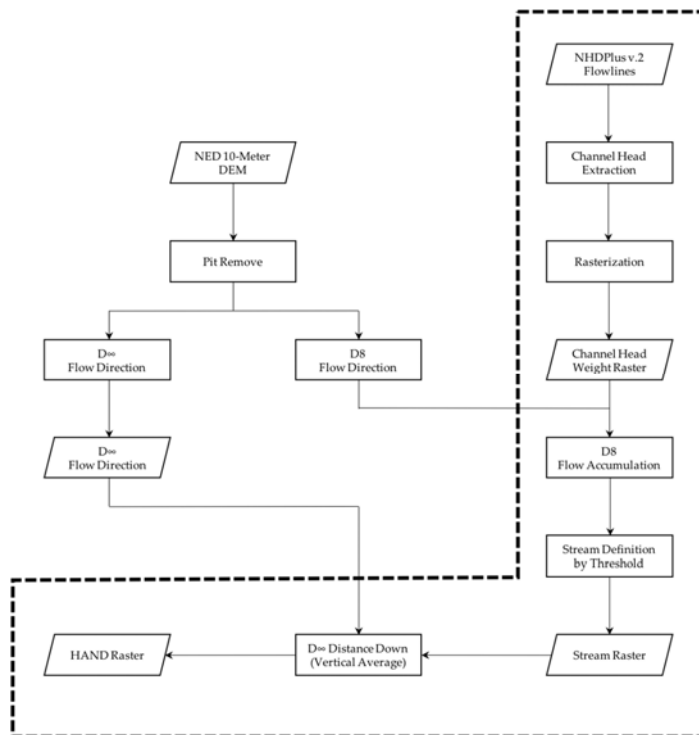


Figure 1. Workflow of the modified HAND method where items enclosed in the dashed area must be repeated for each stream order of the entire drainage network being mapped. Objects are identified with parallelograms and processes by rectangles. Adapted from [3].

The modified HAND method differs from the HAND method in that it takes stream order into account when determining the nearest drainage. HAND is generated using all NHDPlus v.2 or later flowlines (as pictured above). The modified HAND is a combination of HAND rasters based on each stream order from 1st order to the highest order within the drainage area of interest plus the DEM, which is used in coastal flood inundation mapping. HAND is identical to HAND1. HAND2 uses the same workflow as HAND, but the flowlines have had all 1st order streams removed from the analysis. This means that HAND2 is calculated for all flowlines from 2nd order and higher. HAND3 is for 3rd order and higher and so on until the stream order has reached the maximum. That concludes the modified HAND method, which is really quite simple. It should not be confused with the inundation mapping method which is to follow this method. The implementation of the modified HAND method for real-time flood inundation mapping needs more work, although we already have seen many cases where it improves inundation mapping over the HAND method. We are looking into a number of possible implementations and will compare the results of these in the

future. This is certainly an area that has a high impact factor on flood mapping and modeling, and we invite others to research in this area too. In general, we find it possible to implement the modified HAND for inundation mapping and for that to be better than the original HAND method. Other groups from the Summer Institute are reporting similar findings regarding the limitations of HAND and the better performance of modified HAND. An optimized implementation will yield even further gains of the modified HAND method due to its computational and structural flexibility.

4. Results

The modified HAND method was successfully created for the State of Alabama and all of its 9 related HUC4 watersheds. There were a total of 8 stream orders in Alabama, which brings the total number of rasters required for this drainage area to 9 including the DEM. See Figure 2 for more general input output information.

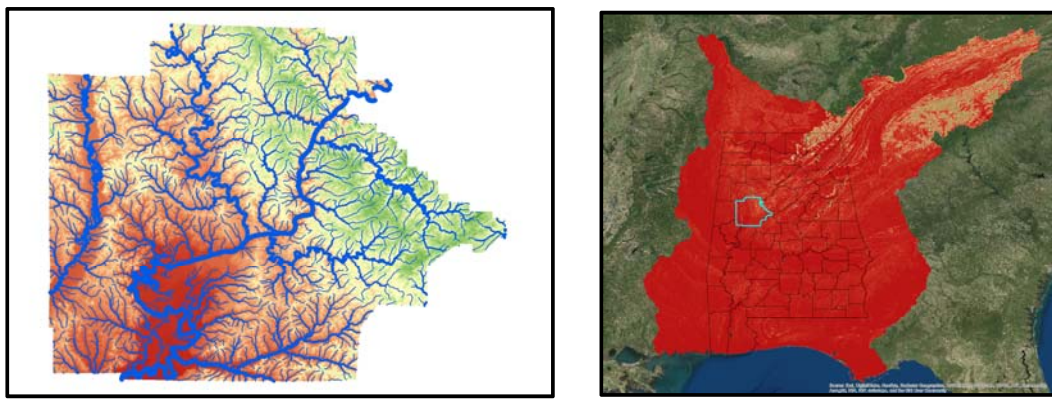
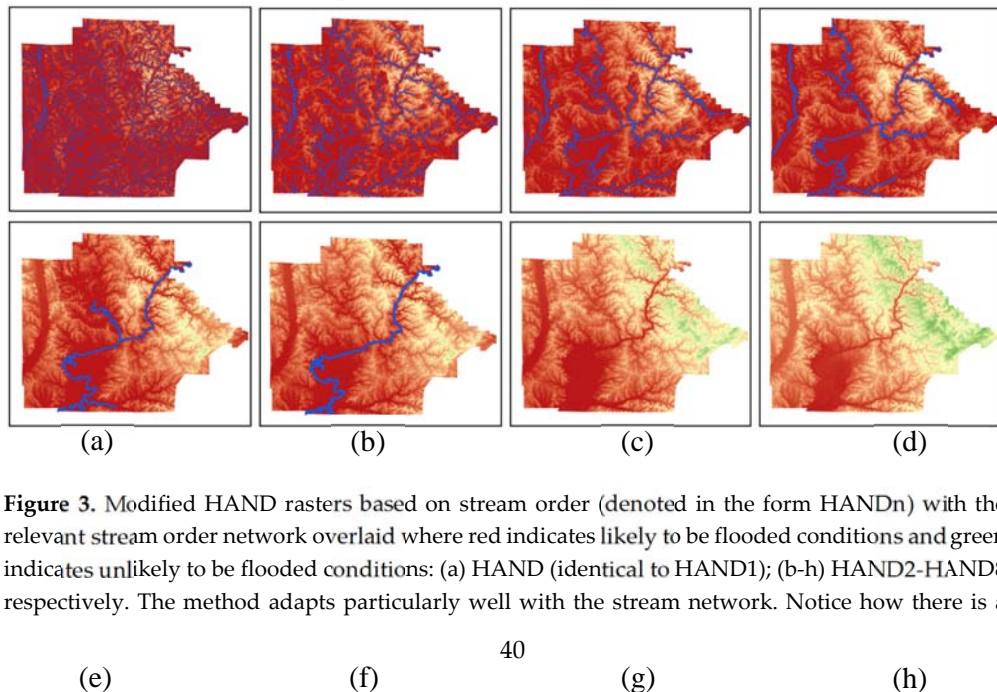


Figure 2. Input and output visualization for the modified HAND method: (a) Tuscaloosa DEM and NHDPlus v.2 flowlines with widths according to stream order (for visualization); (b) Output HAND raster for the study area.

4.1. The Modified HAND Method Output

Figure 3 displays the results of the modified HAND method for Tuscaloosa County, AL with n^{th} stream ordered flowlines according to the n^{th} HAND raster.



significant change from HAND4 to HAND5 ((d) to (e)) because the number of drainage lines at that scale for Tuscaloosa County changes rapidly. Also note that despite lacking a seventh or eighth order stream within Tuscaloosa County, there is still a small risk of flooding from these stream orders. The event would need to be very large in order for this to happen, but the modified HAND preserves these realistic physical relationships very well, when it is difficult for us to even conceive that this county could receive flooding from those downstream catchments. Finally, note that larger order HAND rasters (based on larger drainage areas) present a ‘scaling’ picture of flood risk, and that areas at risk for flooding become more sensitive to elevation as the scale of the drainage increases.

Upon the completion of the modified HAND method it is easy to begin inundation comparisons using the original HAND method and various n^{th} order HAND rasters.

4.2. Modified HAND Flood Inundation

To compare HAND inundation to modified HAND inundation is to compare a vector to a matrix. HAND of course is like a vector in which there are a set of values that can be changed along a single dimension, whereas the modified HAND can be changed over two. In order to illustrate this we have included two figures: Figure 4 and Figure 5. Figure 4 demonstrates how the modified HAND can be changed over the stream order dimension for a given inundation depth (5 meters in this case). Figure 5 demonstrates how both HAND and the modified HAND can be changed over the inundation depth dimension. These are critical images for understanding the potential of the modified HAND method for superior flood inundation modeling despite using the same or less calculation than that of HAND. Neither of these figures has an implementation method based on water balance or empirical relationships to improve flood inundation mapping, but when they do, the modified HAND stands to gain much more than HAND alone can possibly achieve.



Figure 4. The modified HAND method displaying (from lighter to darker colors) HAND to HAND6 5-meter inundation (there is no flood inundation for HAND7 or HAND8 at this depth). Notice that darker colors shift toward larger streams.

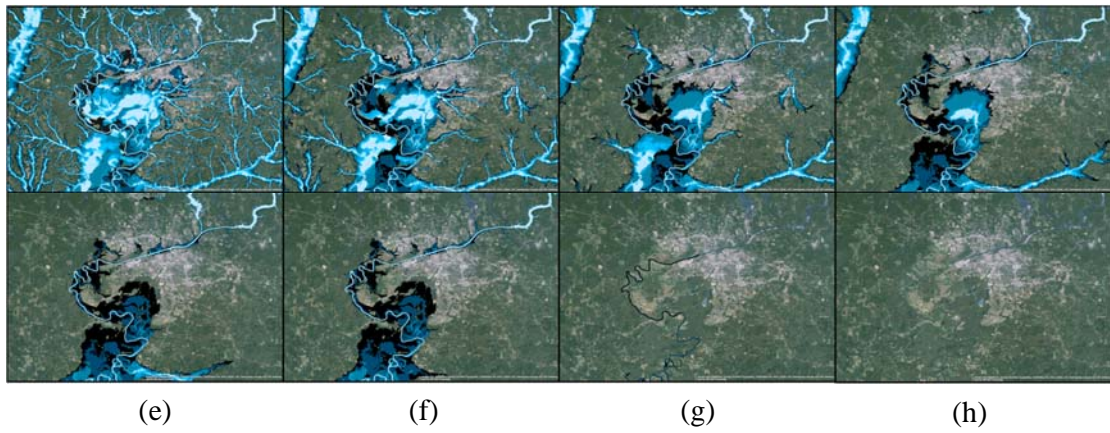


Figure 5. HAND and modified HAND displaying (from lighter to darker colors) small inundation (0.5-meter) to larger inundation (10-meter): (a) HAND or HAND1 inundation; (b-h) HAND2-HAND8 inundation. Note how little control over the inundation HAND or HAND1 has compared to the remaining suite of modified HAND rasters. The modified HAND not only controls the shift toward larger streams, but it can also control (to varying degrees) the shift to lower elevation streams, which is subtly but importantly different from Figure 4 and the original HAND method.

5. Discussion of the HAND and Modified HAND Methods

We have demonstrated that the methodology of the modified HAND is sound, and have delivered it here. This methodology, used to generate rasters for a large area to validate the new method, was also included here. These rasters were then used to demonstrate the difference in flood mapping between the original HAND and the modified HAND method. It is now appropriate to begin a discussion of the limitations of the HAND method, when it applies, when it does not, and how to implement that in flood mapping especially for the post-processing of NWM outputs.

While studying this method, we have identified a few primary weaknesses accompanied with figures when appropriate and convenient for a clearer understanding. All weaknesses we have identified for the HAND method belong to one of four sources listed below.

The Original HAND Method:

- allows only uniform inundation within a catchment
- lacks handling of networked catchment inundation
- must have well-defined drainage and flow path
- built upon a rigid computation structure

5.1. Uniform and Non-Uniform Inundation

The first of these issues is one that occurs frequently in floods. HAND always assumes that the inundation water slope is equal to that of the bed slope. In some cases, this will be true, especially those in which either a) precipitation is small compared to the size of the channel or b) precipitation is completely upstream of the catchment being modeled. If it is not one of these cases, the assumption is jeopardized. Modified HAND has the potential to outperform HAND in cases where precipitation is large within a catchment because it will be the contributing areas within the catchment that dominate the flooding (as the channel approaches the outlet, the routing of upstream catchment areas and contributing downstream catchment areas will produce flooding more similar to Figure 6b).

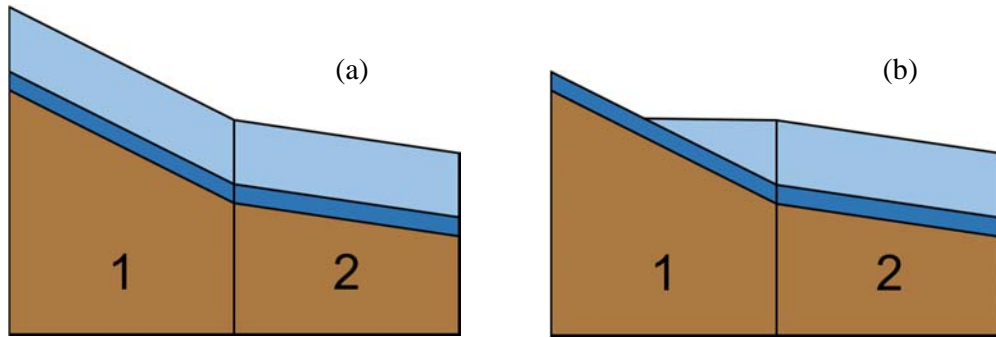


Figure 6. A comparison of HAND and modified HAND inundation models for two catchments—a first order catchment and a second order catchment where light blue is flood inundation on normal flow conditions and the elevation model: (a) Uniform inundation for each catchment as modeled by HAND; (b) Uniform inundation in the lower catchment—identical to HAND—and non-uniform inundation in the upper catchment. The extent of the non-uniform inundation is dictated by a combination of inundation depth and stream order. Slopes and shapes exaggerated for effect.

5.2. Networked Catchment Inundation

There are at least two great examples where HAND falls short in mapping and modeling floods when it comes to a network of catchments. The first case that is easy to visualize evolves when there is precipitation only in downstream catchments (simulated in Figure 7 for HAND and the modified HAND). In these cases, the modified HAND will always outperform HAND. The difference can be relatively small in lower order catchments and extremely large in higher order catchments, but it will always be better.

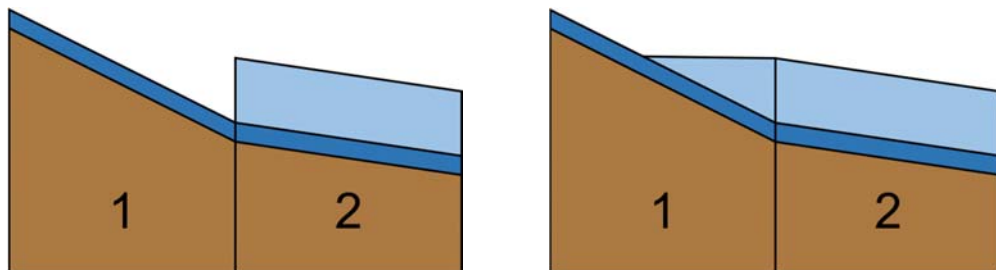


Figure 7. A comparison of HAND and modified HAND inundation when there is only downstream precipitation: (a) HAND fails to produce inundation in catchments with no excess runoff; (b) Modified HAND can map floods across catchment boundaries—even upstream backwater effects from downstream precipitation. Slopes and shapes exaggerated for effect.

The second network case that is too difficult to illustrate efficiently, is a case when perhaps only one second order catchment in a third order catchment network is receiving flow from upstream. In this case the modified HAND method allows for that second order catchment to be mapped using HAND, while the remaining second and first order catchments are mapped using HAND2 or HAND3 (whichever is more appropriate to that specific network). There is potential here to perform a water balance that HAND is less capable of modeling. In this case, overlapping inundation in that catchment from HAND and modified HAND can be redistributed into all the remaining catchments of the third order. This makes it possible to account for the effect of that one contributing catchment on the network of streams. This is not an easy task, and runs the risk of complicating the method depending upon how often this case occurs. Nonetheless, it is a viable option for the modified HAND method whereas HAND has no option for complicated cases like these.

5.3. Well-Defined Drainages

An often overlooked area involves inundation mapping in coastal areas. It is difficult to map coastal flooding. There are tidal effects, storm surge, flood waves from river networks, estuaries and bays with sometimes complex routing networks, and not to mention the high water table usually prevalent in these areas. Our initial modified HAND method did not have an answer for these areas, though we knew that the uniform inundation produced by HAND would be even more spectacularly shortcoming in these areas due to daily oscillations of sea-level. Thus, the idea of a HAND that could expand to the sea was birthed. We call it (very appropriately) Height Above Sea Level or HASL for short. It is the exact same as the DEM, but we use it in the same manner that we use higher order HAND rasters, which is for level-pool inundation. At the moment, this method assumes uniform sea-level (probably a good assumption for many conditions though certainly not all), but as we learn of sea-level oscillations and fluctuations from storm systems, we plan to update this with a non-uniform sea-level. Again, the addition of water accounting can significantly improve this sector of hydrology, especially since flooding in these areas carries a significant risk of shorting or bypassing well-defined flow paths.

5.4. Computation Structure

Lastly, HAND turns out to be quite an inflexible method when it comes to computing structure. This is inherent with the HAND method and not much can be done to change this. In plain terms, the HAND method must always be calculated for every catchment in order to obtain mapping for every catchment, and one must hope that the flood conditions are those within the capability of HAND to capture. The modified HAND has the ability to ‘scale’ computationally with the scale of the event or drainage of interest. One flow rate from the NWM (converted to depth using rating curves or another comparable method) can generate flood mapping for an entire n^{th} catchment order. For example, Tuscaloosa has a single 6th order stream running through the county but hundreds and almost on the order of thousands of 1st order catchments in the county. HAND must calculate each and every catchment and cannot afford to lump the catchments of interest into a single entity, for the result would beyond poor, especially in 1st order catchments. The modified HAND allows for the flexibility to compute flood mapping on the scale most appropriate to the catchment order and is inherently more accurate due to the non-uniform inundation mapping that is so critical to this method’s success.

5.5. Future Work

The bulk of the work still lies ahead. There is still some significant work that must be completed in getting the flow rate from the NWM to a useable depth for the inundation maps produced by HAND or modified HAND. We have pursued two options currently: one which uses SPRNT to develop rating curves for each stream, which seems like the ideal choice, but it takes a long time to compute, even on supercomputing resources. The other possibility involves bathymetry data and the National Elevation Dataset (NED) DEM which can be used to obtain stream cross-sections and profiles for determining depth at given points, likely to be just above catchment outlets. There are still a number of issues that must be worked out in this second method. Once we have a reliable depth, we can generate reliable flood inundation from HAND or modified HAND. It is important to remember that HAND is a great method in some cases, but the goal of the modified HAND is to greatly expand on those cases and to enhance the ones that are already fairly good.

Subsequent to flood inundation mapping, it is possible to determine new channel parameters, which is not currently achieved in the NWM. In addition to this, losses from evaporation and infiltration will impact flood extent and duration. It is foreseeable that a post-processed flood map could be used to define new channel routing components for the following time step in the NWM. Then this channel could be continually reduced by outflow and losses until conditions return to normal. This would fulfill a great need of the NWM in the aspect of flood modeling. We look forward to potential

collaborations with those who have ideas to implement these methods or other promising light-computation, post-processing to the NWM outputs for an improved NWM.

6. Conclusion

Our observation of the HAND method was that it tended to produce too much flooding in lower stream order, higher elevation catchments and too little in higher stream order, lower elevation catchments. The limited aspect of HAND appears in lower stream order, lower elevation catchments because of an inherent limitation preventing an accounting for nearby high stream order catchments which spill over into neighboring smaller catchments. This is a frequent occurrence in flooding in which HAND will produce no flooding in cases where the flood wave is arriving from upstream (in a neighboring catchment) and no precipitation is occurring in the catchment of interest. Even when there is precipitation, there will be a discrepancy between the amount forecasted by the NWM and HAND inundation.

In short, it is difficult to imagine a scenario where the modified HAND would perform worse than the original HAND due to its flexibility to use when appropriate. The modified HAND does require more upfront computation for its generation, but it also offers the capability for operationally superior computation expense and results. Our preliminary evaluation suggests that the modified HAND be used in every case where the HAND method is currently employed for a much more flexible method and better physical representation of flood inundation. We look forward to refining the inundation mapping implementation of the modified HAND, specifically into that of which stream order raster to use for various weather, hydrologic and hydraulic cases.

References

1. Nobre, A. D., et al. "Height Above the Nearest Drainage—a hydrologically relevant new terrain model." *Journal of Hydrology* 404.1 (2011): 13-29.
2. Nobre, Antonio Donato, et al. "HAND contour: a new proxy predictor of inundation extent." *Hydrological Processes* (2015).
3. Yan Y. Liu, et al. "A CyberGIS Approach to Generating High-resolution Height Above Nearest Drainage (HAND) Raster for National Flood Mapping." CyberGIS Center Technical Report (2016).

Comparison of Flood Inundation Mapping Techniques between Different Modeling Approaches and Satellite Imagery

Jiaqi Zhang ¹, Dinuke Munasinghe ² and Yu-Fen Huang ³

¹ University of Texas, Arlington; jiaqi.zhang@mavs.uta.edu

² University of Alabama; dnanayakkaramunasinghe@crimson.ua.edu

³ University of Hawaii at Manoa; yfhuang@hawaii.edu

Academic Advisors: Nick Fang, University of Texas, Arlington, nickfang@uta.edu; Sagy Cohen, University of Alabama, sagy.cohen@ua.edu; Yin-Phan Tsang, University of Hawaii at Manoa, tsangy@hawaii.edu

Summer Institute Theme Advisors: Sagy Cohen, University of Alabama, sagy.cohen@ua.edu; Sarah Praskievicz, University of Alabama, sarah.praskievicz@ua.edu

Abstract: Flood inundation extent serves as a crucial information source for both hydrologists and decision makers. Accurate and timely inundation mapping can potentially improve flood risk management and reduce flood damage. In this study, the authors applied two modeling approaches to estimate flood inundation area for a large flooding event that occurred in May 2016 in the Brazos River: The Height Above the Nearest Drainage combined with National Hydrograph Dataset (NHD-HAND) and the International River Interface Cooperative - Flow and Sediment Transport with Morphological Evolution of Channels (iRIC-FaSTMECH). NHD-HAND features a terrain model that simplifies the dynamic flood inundation mapping process, which is suitable for large-scale application. iRIC-FaSTMECH is a hydraulic model that simulates flood extent under quasi-steady approximation. In terms of data source, HAND and iRIC utilized the National Water Model (NWM) streamflow output data and the United States Geological Survey (USGS) stream gage data, respectively. The flood inundation extent generated from these two modeling approaches were validated against the Landsat Satellite Imagery data. Four remote sensing classification techniques were used to provide alternative observations: supervised, unsupervised, normalized difference water index and delta-cue water change detection. According to the quantitative analysis that compared inundated and non-inundated areas with different remote sensing classifications, the advanced fitness index of iRIC simulation ranges from 57.5% to 69.9% while that of HAND ranges from 49.4% to 55.5%. We found that even though HAND better captures some details than iRIC in the inundation extent, it has problems in certain areas where subcatchments are not behaving independently, especially for extreme flooding events such as on May 2016 (Water level reaching 16.8 meters at Brazos River near Hempstead). The iRIC model performs better in this case, however, we cannot simply conclude iRIC is a better-suited approach than HAND considering the uncertainties in remote sensing observations and iRIC parameters. Further research will include more comprehensive assessments based on a larger variety of flood events. This study found that the fair performance of HAND method positively justified its utility on large-scale riverine inundation mapping. Better performance of HAND could be achieved by considering the interactive behavior of subcatchments during extreme flood events.

1. Motivation

Floods are one of the leading causes of the death from natural disasters in the United States. Floods can damage and devastate homes and farms, displace families, damage crops, disrupt agriculture and business. Therefore, flood inundation extent serves as a crucial information source for both

hydrologists and decision makers. Accurate and timely inundation mapping can potentially improve flood risk management and reduce flood damage. Hydrologic and Hydraulic (HH) modeling forced by meteorological data provides a solution for such challenge. However, lack in reliable observation for validating purposes prohibits the utility of HH models in flood inundation mapping. The advent of satellite-based remote sensing technology has given rise to its application in a vast variety of fields, including hydrology and hydraulics. Therefore, this study is motivated to combine the advantages in HH modeling and remote sensing for improving the timeliness and precision of flood inundation mapping.

2. Objectives and Scope

Using a large flood event that occurred on the Brazos River as a case study, this study aims to achieve the objectives as outlined below:

- 1) To simulate flood inundation maps using the *Nearest Drainage combined with National Hydrograph Dataset (NHD-HAND)* and *International River Interface Cooperative (iRIC)*, respectively.
- 2) To generate observed flood inundation maps from Landsat 8 data using four classification techniques, i.e. supervised, unsupervised, normalized difference water index and delta-cue water change detection.
- 3) To compare the resulted inundation maps to gain perspectives on the advantages and disadvantages of individual mapping tool.

3. Previous Studies

The Height Above the Nearest Drainage (HAND) concept was first introduced by a research group in Brazil (Rennó et al, 2008). The HAND model normalizes topography based on relative heights found along the nearest drainage network (Nobre et al, 2011). Liu et al calculated the HAND raster at national scale combined with the National Hydrograph Dataset (NHD), which eventually resulted in the NHD-HAND model (Liu et al, 2016).

The International River Interface Cooperative (iRIC), a 2D hydrodynamic model, employs a cylindrical coordinate system, and is accessible for the calculation with long timeframes because of its steady or quasi-steady approximation (Nelson and McDonald 1996; Nelson et al. 2003). The iRIC model framework was upgraded from the Multi-Dimensional-Surface Water System Modeling System (MD-SWMS). It implements the Computational Fluid Dynamics General Notation System, originally developed at NASA for stable and computationally-fast modeling of complex 2D+ fluid dynamics (McDonald et al. 2005). There are some plug-in modules in iRIC, including flow simulation, sediment transport, landform evolution, and habitat modeling. In this study, the Flow and Sediment Transport with Morphological Evolution of Channels (FaSTMECH) module was selected because of its simulation efficiency, ease to use, and low requirement for gage data. Moreover, FaSTMECH shows the maximum inundation area from the peak discharge.

Using remote sensing techniques, floodplain boundaries have been delineated with the Landsat campaigns almost since its inception in 1972 (Rango et al., 1975; Hollyday, 1976; Sollers et al., 1978; France and Hedges, 1986; Jensen et al., 1986; Watson, 1991; Blasco et al., 1992; Lougeay et al. 1994; see Smith, 1997). They have been used in many studies to map inundated areas over regions characterized by very different conditions in climate, morphology and land use.

4. Methodology

In this study, the research team focused on a flood event along Brazos River in Texas in May, 2016. The USGS gage at Brazos River near Hempstead (ID: 08111500) recorded a peak discharge of 4445.7

m^3/s at 2 p.m. on May 27th. The total rainfall was 255.8 mm within 30 hours according to the same USGS gage.

4.1 Models

4.1.1 NHD-HAND

The Nation Water Model provides the discharge of each NHDPlus flowline as input for HAND. These flow hydrographs are further translated into stage height using rating curves (stage-discharge relationship), which are generated from channel properties in the HAND model. Next, the HAND raster further determines the inundated area, which has lower elevation than water surface elevation. **Figure 1** shows the schematic flowchart of the procedure for creating inundation maps.

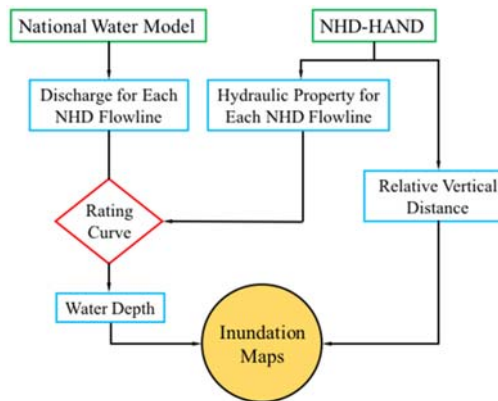


Figure 1. Flowchart of generating inundation maps from HAND

We also compared the observed streamflow from USGS gage in Brazos River at Hempstead, TX with the NWM simulation output. From **Figure 2**, the simulated hydrograph from NWM almost perfectly matches the observed hydrograph and rating curves from HAND and the USGS gage also show good agreement in the low to moderate flow range. Therefore, such comparison, to certain extent, excludes the uncertainty from the model input, hence narrowing down the source of uncertainty to observation and HAND itself.

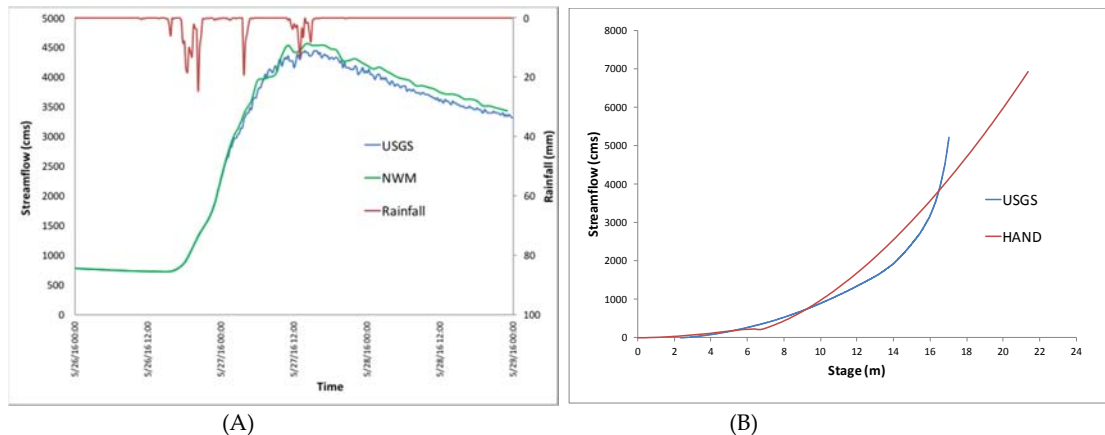


Figure 2. Comparison between USGS gage with (A) NWM discharge output and (B) Rating curve generated by HAND

4.1.2 iRIC-FaSTMECH

The iRIC model herein utilized USGS gage data as the only downstream boundary condition. Two tests were conducted using (1) various grid sizes and (2) various roughness values. Changing grid size from $5 \text{ m} \times 5 \text{ m}$ into $10 \text{ m} \times 10 \text{ m}$, the inundation area shows little change but more details can be obtained with smaller grid size. For the test on toughness, land was classified into three types: main channel, wooded area, and pasture or cultivated areas with Manning's numbers being

0.03, 0.05 and 0.035 respectively. The results show that more details can be captured by considering various land types than by applying uniform roughness across the modeling domain. However, in order to compare with HAND in this study, we keep the uniform roughness with the Manning's coefficient being 0.05. The final settings are shown in **Table 1**.

Table 1. iRIC model settings

Setting Menu	Description
Initial Condition	
Initial Water Surface Elevation	1D step-back water
1D Discharge (m^3/s)	4445.7
1D Stage (m)	49.7 m
1D Drag Coefficient	0.3
Grid Size	5 m × 5 m
Iteration	
Discharge (m^3/s)	1500
Stage (m)	4300
Drag Coefficient	49.7
Lateral Eddy Viscosity	0.014
Re-wetting	0.5 to 0.05
	On

4.2 Satellite Image Analysis

The remotely sensed imagery used in this study included the Landsat 8-Operational Land Imager (OLI) multispectral images (<http://earthexplorer.usgs.gov>) of pre-flood (25 March 2016) and during flood (28 May 2016) times. Erdas Imagine®- 2015 Image processing software (Hexagon Geospatial, Norcross, GA, USA) was used for image pre-processing and subsequent data manipulation. Geometrically and Radiometrically rectified images were generated from: (1) Unsupervised Classification based on the K-means classification algorithm, (2) Supervised Classification based on the maximum likelihood classifier, (3) Delta-cue change detection on Pre/During flooding scenarios and (4) The use of the Normalized Difference Water Index (McFeeters, 1996; see Zha et al., 2003), a spectral water index for the delineation of the spatial extent of floods. Spatial interpolation and filling techniques were applied to pixelate clouded regions with water. Accuracy Assessments were performed on the classified imagery prior to being post-processed through a 3×3 high pass kernel to accentuate the water features for improved visualization.

4.3 Advanced Fitness Index

As a common areal statistic, the fitness index is the ratio of fitted inundated area to the jointed inundated area. This index is widely used to indicate the agreement/discrepancy between satellite observation and the model simulations (Bates and De Roo 2000). However, the fitness index only accounts for inundated area, but not non-inundated area. In this study, the advanced fitness index was calculated to quantify both the inundated and the non-inundated areas as shown below:

$$\text{Advanced Fitness (\%)} = \frac{IA_{obs} \cap IA_{model} + NIA_{obs} \cap NIA_{model}}{A_{obs} \cup A_{model}} \times 100 \quad (1)$$

where IA_{obs} / NIA_{obs} is inundated/non-inundated area from the satellite imagery; IA_{model}/NIA_{model} is inundated/non-inundated area from the model, and A_{obs}/A_{model} is the entire calculated area from the satellite imagery/model.

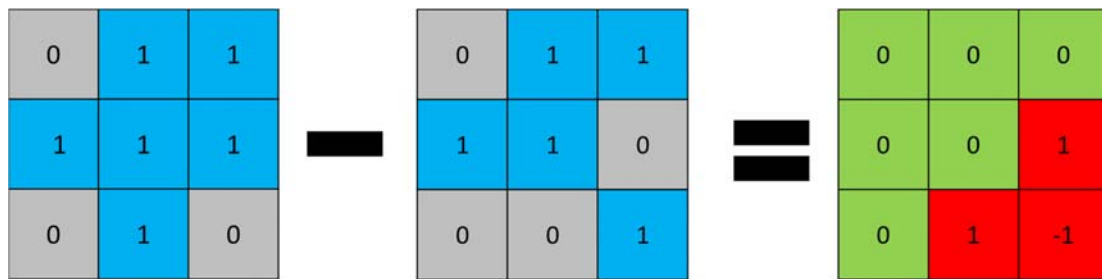


Figure 3 Concept illustration for calculating intersection between inundated and non-inundated areas

In Figure 3, the two matrices on left side of the equal sign represent simulation and observation where value one and value zero signify inundated and non-inundation areas, respectively. As a result, subtraction yields the intersection between inundated and non-inundated areas indicated by the value zero.

5. Results

Figure 4 below shows inundation maps generated from iRIC, HAND and four remote sensing classification techniques. These preliminary results show some discrepancies between the modeled and observed inundated area. Based on the advanced fitness indices, the inundation map derived from iRIC fitted satellite imagery better than HAND, as HAND missed two inundation areas in the simulation domain. However, as highlighted by the red circles, HAND better captured the details in some inundated area than iRIC. **Figure 5** compares the advanced fitness indices between the two simulations and the four observations (from four classification methods). It can be found that iRIC performed better than HAND and NDWI had inferior agreement with the simulations to the other three classification techniques.

Figure 6 shows the two missed areas (in yellow circles) by the HAND simulation. In **Figure 6A**, the red line is subcatchment boundary; the blue lines stand for flowline; the green color stands for inundation area; the yellow circle is the missing part; and the white number is COMID for each flowline. **Figure 6B** shows a selected cross-section, where the blue line is the modeled water depth; the red dotted line stands for subcatchment boundary and the black line is the HAND elevation. The HAND calculation is subcatchment-based, which means that inundation extent values on different sides of the subcatchment boundary are calculated based on two different water depths. Consequently, in the HAND simulated results, the left side of the subcatchment got flooded while the right side did not. However, in this case the two catchments should have been considered as a whole. In other words, inundation calculation herein should have considered the interaction between the subcatchments.

Figure 7 shows flow velocity vectors and inundation calculated from iRIC with two white circles highlighting the two inundated areas missed by the HAND simulation. The velocity vectors indicate that the main stem got overflowed at two circled areas, which explains how the two models performed differently for this particular event.

Figure 8 shows the inundation maps generated by the original HAND and a modified HAND. NHD-HAND calculates the inundated area based on individual NHD catchment with corresponding water depth modeled in the NHD flowline. as illustrated in **Figure 8A**, when one considers three subcatchments (highlighted in light blue) as one catchment and applies the water depth of the nearest main stem, the two originally missed parts can be filled as shown in **Figure 8C**.

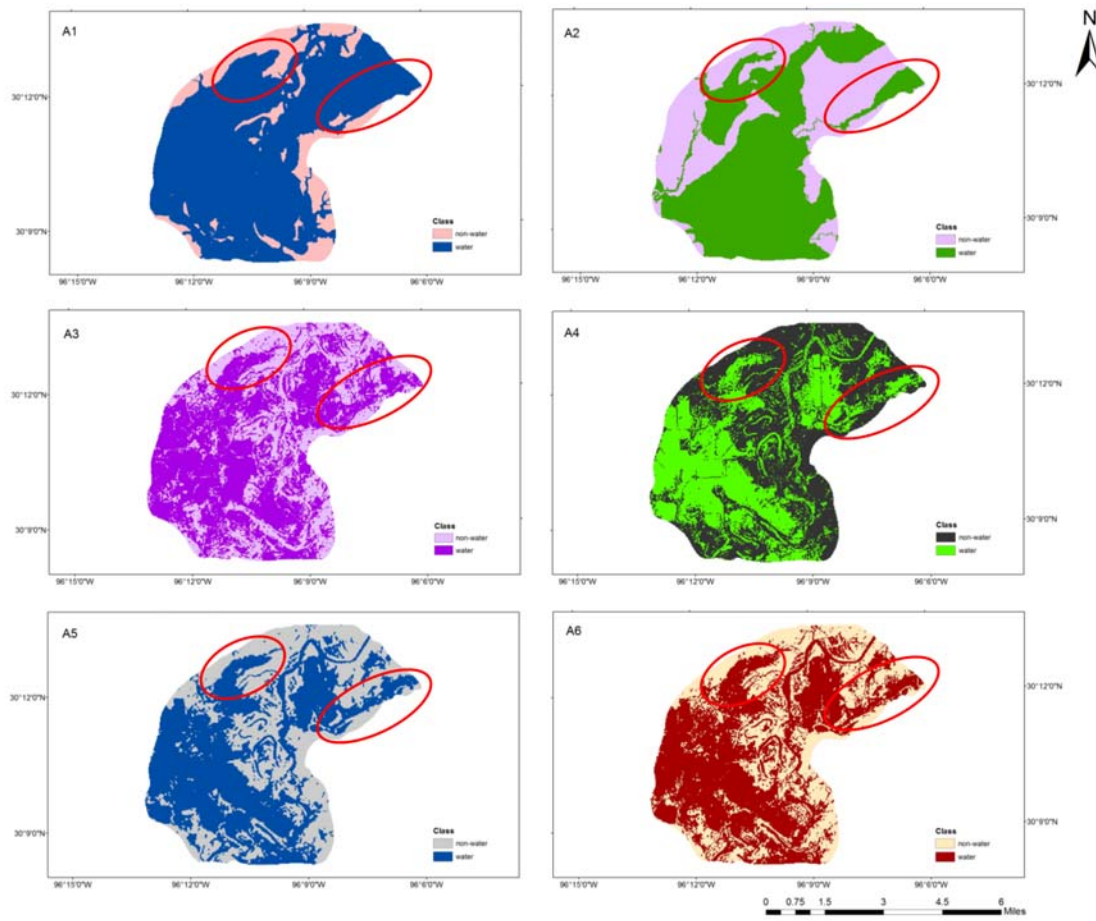


Figure 4. Inundation maps of different models and remote sensing techniques: (A1) iRIC, (A2) HAND, (A3) Delta-Cue, (A4) NDWI, (A5) Unsupervised and (A6) Supervised. (Red circles show the difference in simulating performances by HAND and iRIC)

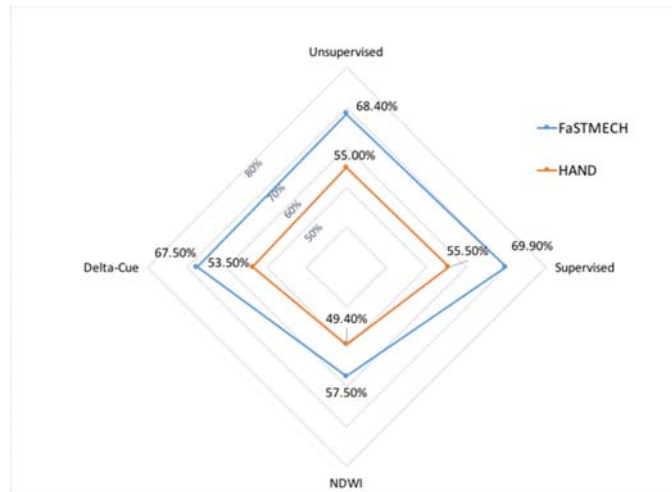


Figure 5. The radar chart of the advanced fitness index within iRIC, HAND and different classification method in satellite imagery. (UN stands for unsupervised classification, SUPER is supervised classification, NDWI is Normalized Difference Water Index, and DELTA is delta-cue.)

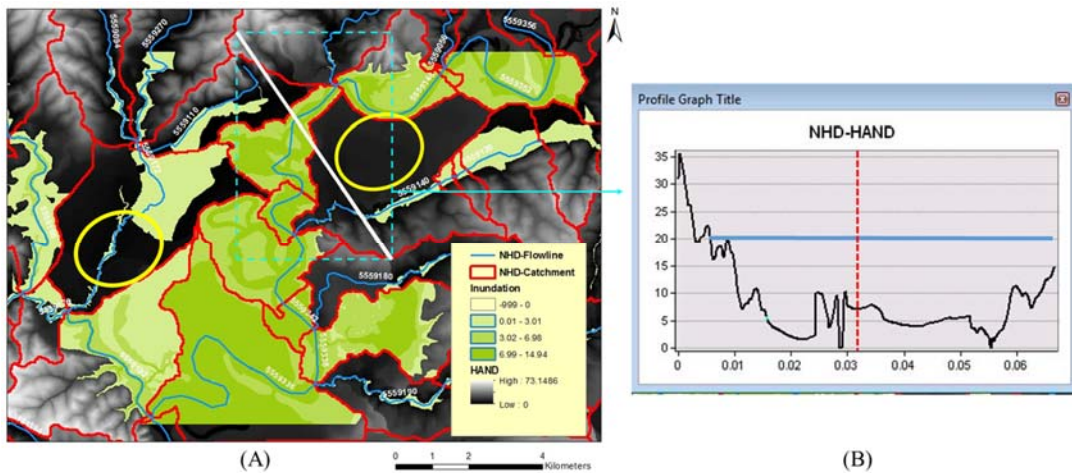


Figure 6. Two inundated areas missed by HAND (A) and HAND profile for selected cross-section (B).

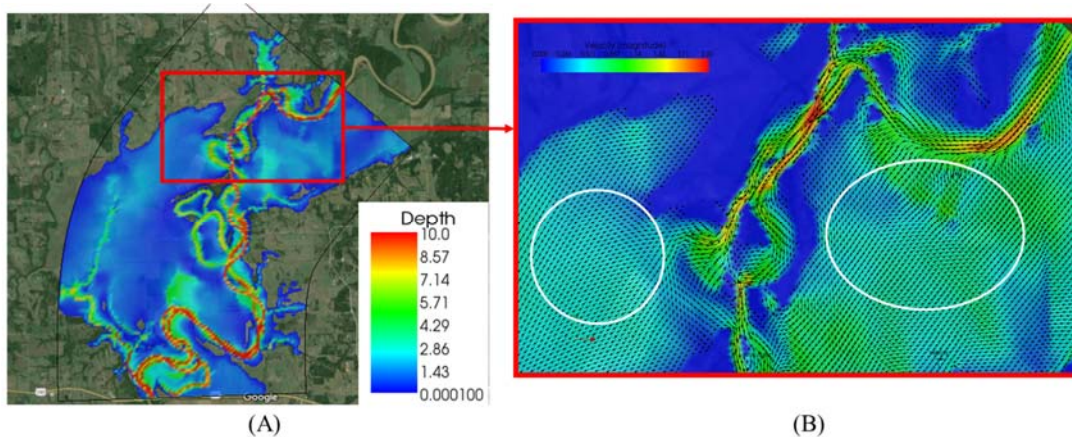


Figure 7. Simulated inundation water depth from iRIC (A) and velocity vectors in the selected area (B).

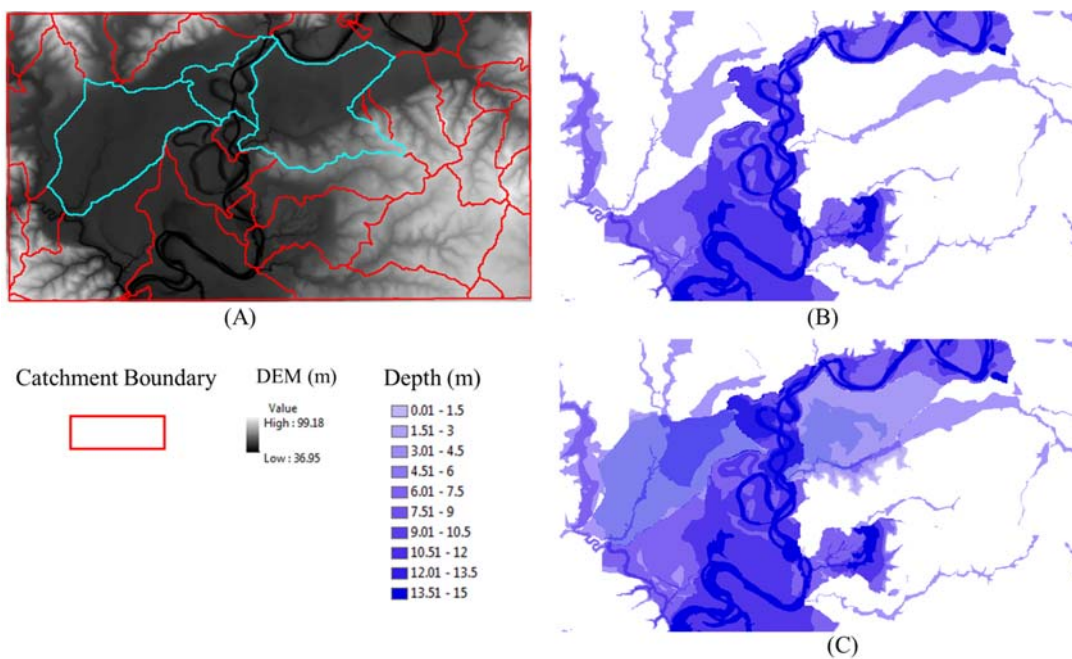


Figure 8. DEM (A), inundation maps generated by original HAND (B) and modified HAND (C).

6. Conclusion

Both HAND and iRIC generated fair (> 50% of Advanced Fitness Index) fit with the satellite imagery. iRIC performed better (~ 70% in fitness index) in this extreme flood event, where water level reached 16.8 m at Brazos River near Hempstead Gage. However, HAND better captured details than iRIC in some inundated areas. There were two inundation parts missed by HAND modeling, because subcatchments were behaving interactively during this event. The modified HAND provided a remedy to such issue by simply apply water depths of the nearest river stem to the adjacent subcatchments. Solely based on the studied flood event, one cannot simply conclude iRIC is a superior approach than HAND considering the uncertainties in remote sensing observations and iRIC parameters. Further research will include more comprehensive assessments based on a larger variety of flood events. The findings from this study also indicate that, for extreme events, simplification on the intricacy of flow dynamics have relatively minor influence on prediction, which in the authors' opinion positively justifies the utility of HAND on large-scale riverine inundation mapping.

Although the results based on 10 m digital elevation model (DEM) are promising, there are several directions through which performance variation of the two models can be tested. With the availability of high quality DEMs acquired through Light Detection and Ranging (LiDAR), the representation of floodplain processes may get better. However, most areas in United States lack LiDAR availability due to the higher cost of data acquisition. It is also a well-accepted fact that LiDAR DEMs still do not include information on channel cross-sections. Better representation of channel shape, in addition to LiDAR-based floodplain topography can significantly improve simulations from both HAND and iRIC. Because our study domain does not have surveyed channel cross-section data, a semi-empirical approach proposed by Merwade and Maidment (2004) will be used in our future endeavors.

Supervised classification of remote sensing yields the best observation results because unlike other classification algorithms sample pixels representative of flood water were manually selected and training sites were created. Subsequently, flood water pixels of the entire image were classified based on this accumulation of spectral signatures. This method yields a definite advantage over the other methods simply because user experience and knowledge allows for the clustering of flood water pixels, which is a mixture of water, soil, sediment and vegetation. In comparison, as spectral signatures of flood water could be different depending on the mixture, they have a very high likelihood of being classified into different landuse classes which is highly probable in other classification algorithms. It is envisioned to use image fusion techniques and the Modified Normalized difference Water Index (MNDWI) as future research in order to obtain comparable results. Image fusion on OLI imagery allows the user to improve spatial resolution based on the fusion of the higher resolution panchromatic band with other band composites while the MNDWI is expected to enhance open water features while efficiently suppressing and even removing built-up land noise as well as vegetation and soil noise to accentuate water features more than the NDWI (Hu, 2006).

References

1. Bates, P.D. and De Roo, A. P. J., (2000). A simple raster-based model for flood inundation simulation. *Journal of hydrology*, 236(1), 54-77.
2. Liu Y.Y., Maidment D.R., Tarboton D.G., et al. (2016). A CyberGIS approach to generating high-resolution Height Above Nearest Drainage (HAND) raster for national flood mapping. CyberGIS Center Technical Report: CYBERGIS-TR-2016-005-i
3. McDonald, R.R., and Nelson, J.M. (1996). Field Measurements of flow ion Lateral Separation Eddies in the Colorado River in Grand Canyon: Report to Grand Canyon Monitoring and Research Center, Flagstaff, Arizona.

4. McDonald, R.R., Nelson, J.M., and Bennett, J.P. (2005). Multi-dimensional surface-water modeling system user's guide: U.S. Geological Survey Techniques and Methods, book 6, chap. B2.
5. McDonald, R.R., Nelson, J.M., Kinzel, P.J., Conaway, J. (2005). Modeling surface-water flow and sediment mobility with the Multi-Dimensional Surface Water Modeling System (MD_SWMS): U.S. Geological Survey Fact Sheet 2005-3078.
6. Merwade, V., Maidment, D. R., (2004). Geospatial Description of River Channels in Three Dimensions. The University of Texas at Austin. Center for Research in Water Resources online report 04-8. Available at: <http://www.crwr.utexas.edu/reports/2004/rpt04-8.shtml>
7. Nelson, J.M., and McDonald, R.R. (1996) Mechanics and Modeling of Flow and Bed Evolution in Lateral Separation Eddies: Report to Grand Canyon Monitoring and Research Center, Flagstaff, Arizona.
8. Nobre, A. D., Cuartas, L. A., Hodnett, M., Rennó, C. D., Rodrigues, G., Silveira, A., ... & Saleska, S. (2011). Height above the nearest drainage—a hydrologically relevant new terrain model. *Journal of Hydrology*, 404(1), 13-29.
9. Rennó, C. D., Nobre, A. D., Cuartas, L. A., Soares, J. V., Hodnett, M. G., Tomasella, J., & Waterloo, M. J. (2008). HAND, a new terrain descriptor using SRTM-DEM: Mapping terra-firme rainforest environments in Amazonia. *Remote Sensing of Environment*, 112(9), 3469-3481.
10. Smith, L. C. (1997). Satellite remote sensing of river inundation area, stage, and discharge: A review. *Hydrological processes*, 11(10), 1427-1439.
11. Zha, Y., Gao, J., & Ni, S. (2003). Use of normalized difference built-up index in automatically mapping urban areas from TM imagery. *International Journal of Remote Sensing*, 24(3), 583-594.

Object-based Segmentation to Identify Water Features from Landsat 8 and SAR Images: A Preliminary Study

Yan-Ting Liau ¹

¹ University of Texas at Dallas; vxl159130@utdallas.edu

Academic Advisor: May Yuan, University of Texas at Dallas, mxy141230@utdallas.edu

Summer Institute Theme Advisor: Sagy Cohen, University of Alabama, sagy.cohen@ua.edu

Abstract: Floods are one of devastating natural hazards in the United States. Effective flood inundation mapping can provide timely information to facilitate decision making of first responders. One of the fundamentals in flood inundation mapping is to identify rivers. This study proposes a data integration framework to identify rivers in two steps. The first step identifies river features that persist across multiple images. Major improvement was made to the moisture enhancement index (MEI) by combining two existing moisture indices and eliminating urban reflection. This study calculates MEI using data from Landsat 8 imagery and shows that using threshold-based segmentation can effectively extract sustained water features from the MEI layers and Synthetic-Aperture Radar (SAR) imagery. The second step applies a snake algorithm to reshape the morphological characteristics of existing river shapefiles and water features. The framework was examined in the suburban of San Antonio and a meandering of the Brazos River. The results showed improved accuracy in identifying shapes and locations of big rivers and lakes. Additionally, MEI provides the clue to identify small rivers in both study areas. However, the proposed method improves the identification of existing rivers, and further improvements are necessary to recognize floods extents.

1. Motivation

Flood inundation mapping can provide initial information for first responders in search and rescue. In particular, the first goal is how to effectively map the extent of floods with high accuracy. Most studies on flood inundation mapping considered one image source or two. Specifically, pixel-based water detection is widely used for flood inundation mapping using optical satellite-based imagery (e.g. [1] [2]), whereas object-based water segmentation is commonly when SAR imagery is used for flood mapping (e.g. [3] [4]). Thus, the common deficiency is unable to deal with change detections across multi-source and multi-temporal data. In this study, the author focuses on examining possible solutions over time and across various sources as the first step for existing challenges.

2. Objectives and Scope

Object-based image analysis has showed to provide higher accuracy of classification or feature extraction than pixel-based image analysis (e.g. [5]). The improvement is due to reducing noises through statistical summaries of characteristics within spatially similar objects, such as modes, means and variances. Object-based image analysis may improve flood inundation mapping by generalizing spectral characteristics and polarization of active sensors in water bodies. Nevertheless, object-based image analysis has several drawbacks, such as longer processing time, limitedly testing over different areas, and difficulties in handling diverse boundaries across multiple images. The main goal of this study is to improve object-based

image analysis for efficient flood inundation mapping with high accuracy. To achieve this goal, a data integration framework is proposed to identify water objects from Landsat 8 and SAR images.

3. Previous Studies

The choice of methods for water detection relies heavily on imagery characteristics. Optical satellite images, one of the most commonly used imagery data, have been processed by thresholding and pixel-based classification to identify water features. Examples include Sun et al. (2010) [1] and Kuenzer et al. (2015) [2]. They both adapted the decision tree classifier and developed the dynamic threshold across images for water detection. Their results cannot deal with issues related to vegetation blockage of water bodies. Additionally, imagery data from active sensors, such as SAR, use object segmentation at a higher spatial resolution and avoid speckle noises. Nevertheless, most existing object-based algorithms only have been tested within limited study areas (e.g. [3] [4]). For the goal to support the first responders, both existing methods will be limited without developing a new methodology to detect persistent water features over large areas and different data sources.

4. Methodology

This study proposes a data integration framework with a threshold-based segmentation to extract features and segment water objects for efficient flood inundation mapping in two steps. In the first step, unchanged objects across images are extracted from optical satellite images (Landsat 8) and SAR images. Specifically, existing pan-sharpening techniques [6] are examined based on the image similarity between original images (30 meters) and new images (15 meters), while the moisture enhancement index is developed based on the visual examinations on water features over multiple land cover types. In the second step, these extracted features and existing river shapefile are integrated into the morphological snake algorithm [7] for better performances of water detections. The final results are evaluated by visual quality. The reason of not using quantity method is that most supervised accuracy assessment methods require ground truths, while most unsupervised methods are evaluated globally (i.e. not considering any specific land cover).

4.1. Study Area

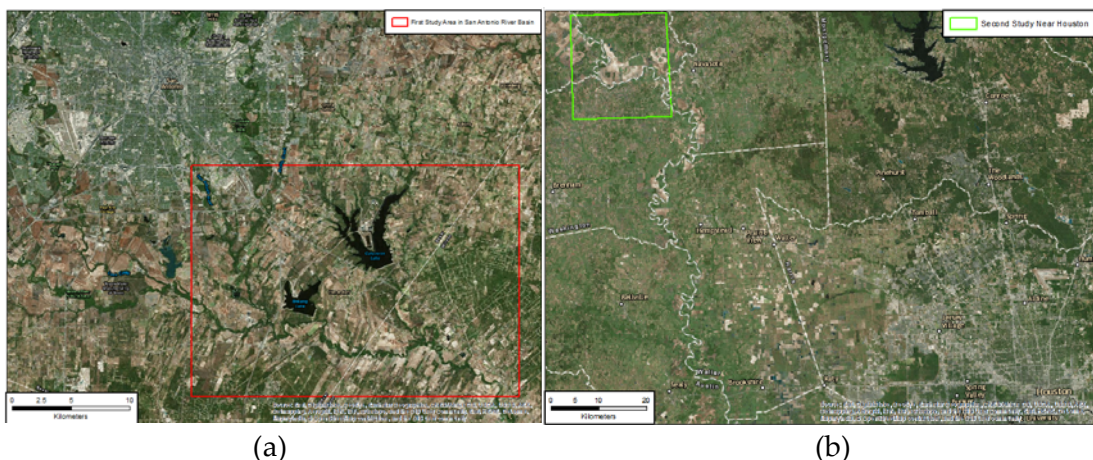


Figure 1 Study Areas: (a) the Suburban of San Antonio, (b) a Meandering of the Brazos River. Note the green and red boxes indicate boundaries of the study areas and point out the distance from the main cities.

The framework is examined in the two small study areas, representing two diverse scenes. One is located in the suburban of San Antonio City, and another is located in a meandering of the Brazos River far away

from Houston City (Figure 1). In the first study area, the challenge is to eliminate complex urban features, whereas in the second study area, the challenge is how to handle irrigation areas. Due to limited time to handle cloud influences, the cloud-free images are selected from 2015 to the middle of 2016. The suburban of San Antonio includes 9 cloud-free images (01/25/2015, 02/26/2015, 03/14/2015, 05/01/2015, 07/20/2015, 11/09/2015, 01/12/2016, 01/28/2016, 05/03/2016), whereas the meandering of Brazos River includes 7 cloud-free images (01/18/2015, 03/23/2015, 07/29/2015, 11/18/2015, 12/04/2015, 02/06/2016 and 03/25/2016).

4.2. Pan-sharpening techniques

Pan-sharpening techniques as the pre-processing step refer to enhancing the spatial resolution of multispectral images by a panchromatic image with higher spatial resolution (often taken by the same sensor and at the same time, same as multispectral images). This study tested seven techniques, including Brovey, Ehlers, HPF, Principal Component, multiplicative and wavelet in ERDAS IMAGINE and Gram Schmidt in ENVI Classic 5.3 [6] to see which pan-sharpening techniques can preserve more information, compared to the original image. Whereas Spectral Angle Mapper is used to evaluate spectral similarity [8], RMSE is used to evaluate spatial differences [8]. Then, the Pearson correlation coefficient is further used to evaluate the general similarity.

4.3. Moisture Enhancement Index (MEI)

Previous studies have reviewed twenty moisture indices [9]- [16]. Nevertheless, the confusion between water and other land cover categories is expected, due to weak differences between any two bands. For example, vegetation can be extracted from the high difference between the red band and the near-infrared band (NIR, wavelength between 0.85 - 0.88 micrometers), but the water reflection is low in all percent reflectance [10].

This study combines the three elements to handle the week differences by the summation of equation (1) and equation (2). In the first step, the water category is enhanced by combining two moisture indices (i.e. the Normalized Difference Water Index (NDWI) and the Modified Normalized Difference Water Index (MNDWI)) (equation (1)). The vegetation objects can be eliminated because vegetation has high reflectance in NIR and Short-wave Infrared 1 (SWIR1, wavelength between 1.57 - 1.65 micrometers) bands compared to the low values in the green band (G, wavelength between 0.53 - 0.59 micrometers), but water reflects few differences (equation (1)). Second, the urban reflection (i.e. soil) is eliminated by applying the difference between band 1 (coastal aerosol) and the green band, because water and urban object reflectance in the band 1 is low, and the urban reflection in the green band is higher than the water reflection (equation (2)). Then, the results are evaluated by the water segmentations visually.

4.4. Data Integration

Based on the pre-processing improvements of Landsat 8 images, two types of data integrations in the morphological snake algorithm are examined [7]. This algorithm is advantage by applying contours to delineate long and irregular shapes of water features [7], and is commonly used to segment water bodies and flood extents on SAR images. However, this algorithm requires makers, which indicate locations of detected object, so existing river shapefiles and sustained features, which provide up-to-date water information, were applied. This study used the existing implementation in [17], and to reduce noises, the gaussian filter has been also implemented [17].

5. Results

5.1. Pan-sharpening Techniques

Overall, since Panchromatic band and other multi-spectral bands were taken by the same sensor at the same time, their Pearson correlation coefficients (esp. band 1 to band 7) in two study area were high (greater than 0.7). The angle SAM index, which evaluated the spectral similarity, showed higher differences between the original image and the fusion image in the Meandering of the Brazos River. The RMSE value, which evaluated the spatial differences between the original image and the fusion image, showed that no method consistently has better performances than others across two study areas and bands. The evaluations showed fairly consistent results that different land cover types affect the spectral performances, and all methods performed equally well. In this study, Gram Schmidt (GS) method is selected based on the literature for its good performances on water detections [14].

5.2. Moisture Index and feature extractions for improving segmentation

Visually, MEI as well as other moisture indices all helped segment the Brazos River. Furthermore, using MEI showed certain improvements on segmenting small rivers in the Landsat 8 images, even if the confusion with other land cover categories still exists. Two typically difficult cases in Figure 2 present the better segmentation performances of MEI, compared to NDWI and MNDWI. The improvements not only generate correct shapes (Fig 2 (d) (e) (f)) but also more importantly differentiate rivers from nearby landscapes. Although MEI cannot deal with small rivers in a suburban setting well, the result still provides a smaller constraint to indicate rivers (Fig 2 (a) (b) (c) the pick circles). On account of the limited ability of MEI using Landsat 8 images, further data integration should be necessary to derive water information.

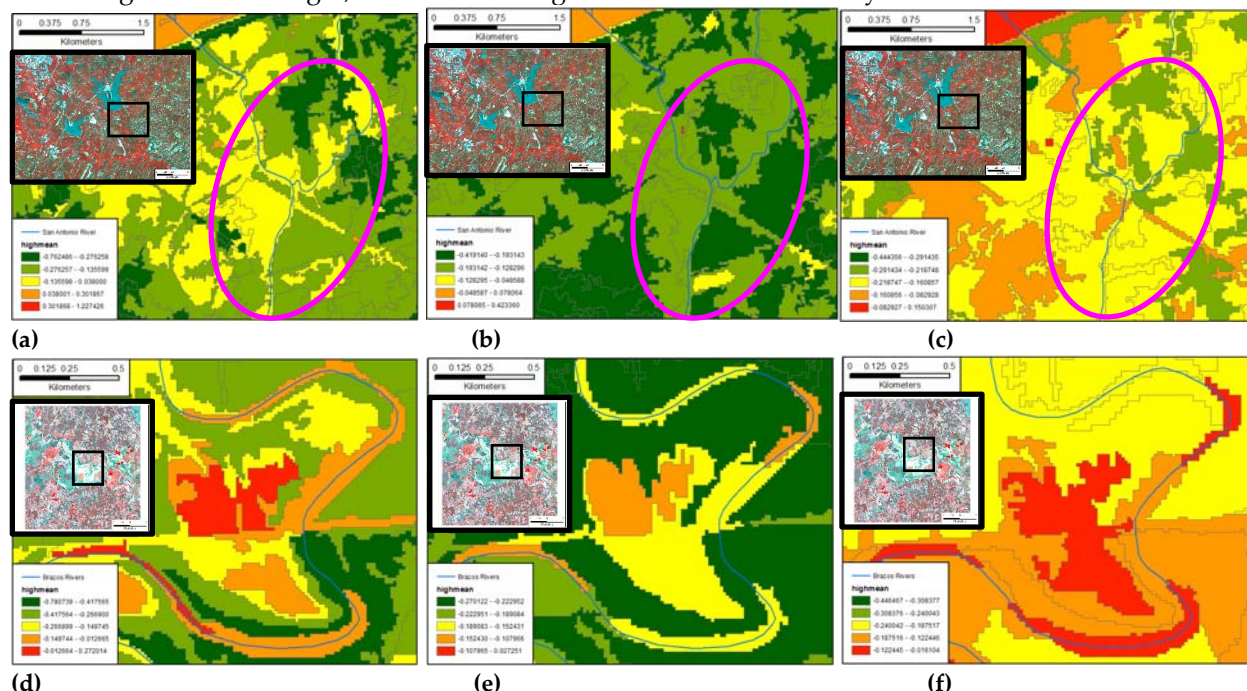


Figure 2 the difficult cases of segmenting river and water bodies (1) the Suburban of San Antonio (a) using MEI (b) using MNWI (c) using NDWI and (2) a Meandering of the Brazos River (d) using MEI (e) using MNWI (f) using NDWI. Note that the segmentation is based on multiresolution segmentation in

eCognition using the same segment parameters, and the color levels indicate the spectrum separations, based on the natural break classification scheme on the mean values of each segmentation

5.3. Integration of Vector Data on MEI

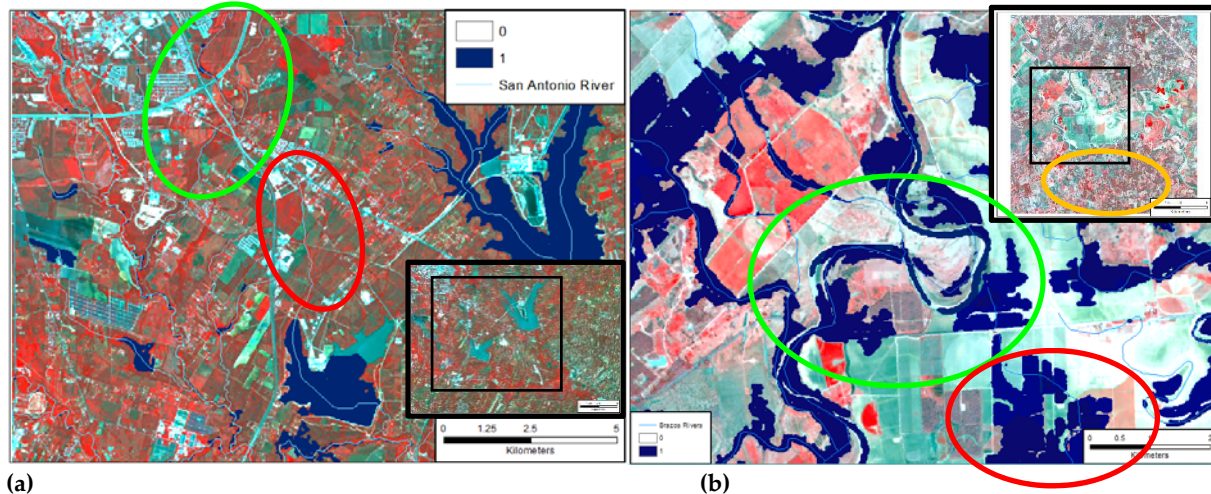


Figure 3 the performances of integrating vector data for water detections: (a) the Suburban of San Antonio, (b) a Meandering of the Brazos River. Note: (1) the results are the combinations of multiple temporal features; (2) the areas, 0 and 1, indicate two separated segmentations.

This study used an existing river shapefile to serve as known river locations. The morphological snake algorithm [7] was applied to MEI layers over 2015 to 2016(Figure 3). In comparison, segmentations based on MEI imagery were able to delineate small rivers which segmentations on other images could not elicit. Only segmentations on MEI imagery were able to detect Jackson Creek, Doe Run and other unnamed small creeks along the meandering of the Brazos River (Figure 4 (b) the orange circle). Likewise, Salado Creek, Rosillo Creek and other unnamed small creeks are only identified by MEI segmentations (Figure 4 (a) the green circle). However, MEI segmentations still overlooked some small rivers in the Suburban of San Antonio (Figure 4 (a) the red circle) but wrongfully detected linear features as rivers in the meandering of the Brazos River (Figure 4 (b) the red circle). The results present that the morphological snake algorithm is useful to detect the water bodies, even if the rivers in the shapefile is not aligned well to the image (Figure 4 (b) the green circle).

5.4. Integration of persistent Features on MEI

The extracted features were useful to correct the missing features of applying existing shapefiles to segmentation. Figure 4 (a) and (b) both show the ability to detect the oxbow lake (the green circles), which is missing in the existing river shapefile. Nevertheless, the best performance is still achieved by applying the images, taken by the same sensor (Figure 4 (a)), and using extracted features from the SAR image is still underdeveloped (Figure 4 (b)), because the gaussian filter seems insufficient to remove noises in this case.

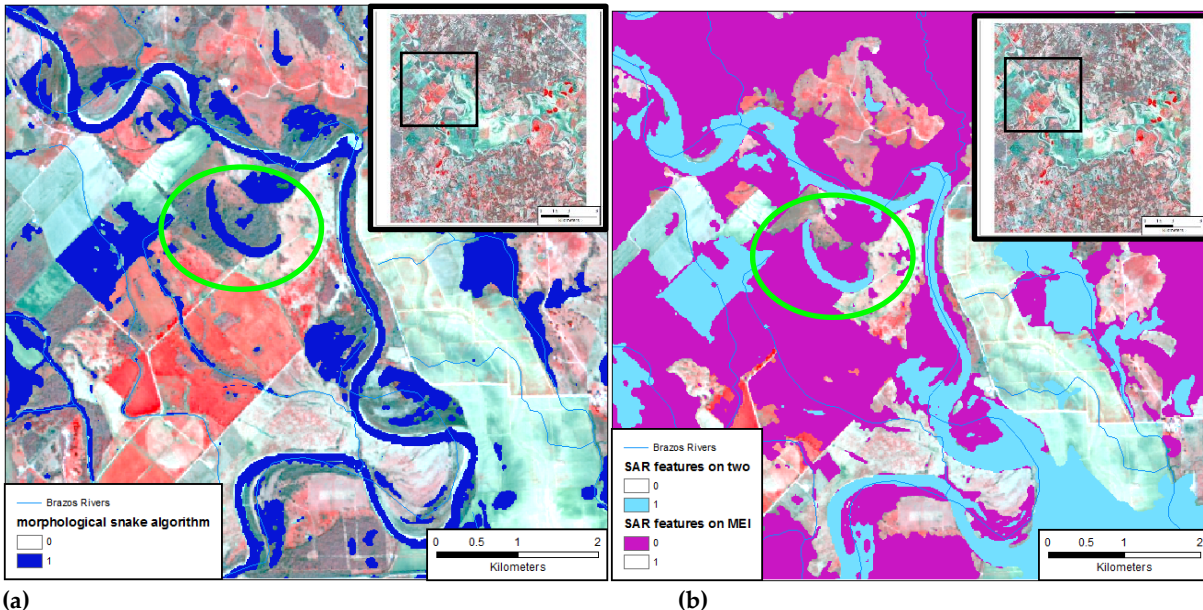


Figure 4 the visual results of using extracted features for segmentation: (a) using extracted features from Landsat 8 (the markers and the segmentation are derived from the same Landsat 8 image in 05/01/2016), (b) using the extracted features from SAR images on MEI (Purple) and the combination of NDWI and MNDWI (blue) (SAR image in 05/13/2015 is used as the markers and the segmentations are based on MEI in 05/01/2016) Note that the areas, 0 and 1, indicate two separated segmentations.

6. Conclusions and Further Study

This study demonstrates the initial results of applying persistent river features detected from Landsat 8 imagery, SAR imagery and existing river shapefiles, to river segmentation. The main contributions include the development of the moisture enhancement index and multiple data integration over time. The moisture enhancement index handles water weak differences of any two bands by combining three elements to increase the probability of detecting water, whereas the robust features are tested in river segmentation on the same image and on the images across different time and sources. Visually, the framework has achieved the goals of detecting existing big rivers and lakes as well as some of small rivers, which are almost invisible in Landsat 8 and SAR images. The proposed method inherits several limitations, which also lead to opportunities for future improvements:

1. Eliminate urban reflections: the third element of the current moisture index still has the issues of over- and under-estimations of rivers, and the exploration of other band differences and index combinations should be helpful for future practical use.
2. Implement cloud detection elements: the current version of the moisture enhancement index is only tested in the cloud-free Landsat 8 images. While NASA uses the Fmask algorithm [18-19] to mask clouds on an official layer of Landsat 8 image outputs, the masks may also block the treasured water information. In many cases, the flooding extents are still visible in the haze situation, but the cloud mask just blocks all regions.
3. Develop an implementation of handling robust features over time and across different data sources: the current algorithm is limited to provide consistent segmentations across different time and data sources, and the overlap and revision mechanism may help to improve the consistency.

7. References

1. Sun D, Zhang R, Li S, Yu Y. 2010. GOES-R Advanced Baseline Imager (ABI) Algorithm Theoretical Basis Document For Flood/Standing Water. NOAA NESDIS Center for Satellite Applications and Research.
2. Kuenzer C, Klein I, Ullmann T, Georgiou EF, Baumhauer R, Dech S. 2015. Remote Sensing of River Delta Inundation: Exploiting the Potential of Coarse Spatial Resolution, Temporally-Dense MODIS Time Series Remote Sensing, 7: 8516-8542.
3. Bates PD, Wilson MD, Horritt MS, Mason DC, Holden N, Currie A. 2006. Reach scale floodplain inundation dynamics observed using airborne synthetic aperture radar imagery: Data analysis and modelling. *Journal of Hydrology*, 328: 306-318.
4. Pulvirenti L, Chini M, Pierdicca N, Guerriero L, Ferrazzoli P. 2011. Flood monitoring using multi-temporal COSMO-SkyMed data: Image segmentation and signature interpretation. *Remote Sensing of Environment*, 115: 990-1002.
5. Gstaiger V, Huth J, Gebhardt S, Wehrmann T, German CK. 2012. Multi-sensoral and automated derivation of inundated areas using TerraSAR-X and ENVISAT ASAR data. *International Journal of Remote Sensing*, 33(22): 7291-7304.
6. Zhang Y, Mishra RK. 2012. A review and comparison of commercially available pan-sharpening techniques for high resolution satellite image fusion. In: 2012 IEEE International Geoscience and Remote Sensing Symposium, IEEE.
7. Marquez-Neila P, Baumela L, Alvarez L. 2013. A morphological approach to curvature-based evolution of curves and surfaces. *IEEE Transactions on Pattern Analysis and Machine Intelligence*, 36(1): 2-1
8. Vivone G, Alparone L, Chanussot J, Mura MD, Garzelli A, Licciardi GA, Restaino R, Wald L. 2015. A Critical Comparison Among Pansharpening Algorithms. *IEEE Transactions on Geoscience and Remote Sensing*, 53(5): 2565-2586.
9. Huang C, Wylie B, Yang L, Homer C, Zylstra G. 2002. Derivation of a tasseled cap transformation based on Landsat 7 at-satellite reflectance. *International Journal of Remote Sensing* 23(8): 1741-1748.
10. Jensen JR. 2007. *Remote Sensing of the Environment: A Earth Resource Perspective*. Pearson Prentice Hall.
11. Lobser SE, Cohen WB. 2007. MODIS tasseled cap: land cover characteristics expressed through transformed MODIS data. *International Journal of Remote Sensing*, 28(22): 5079-5101.
12. Varhola A, Coops NC. 2013. Estimation of watershed-level distributed forest structure metrics relevant to hydrologic modeling using LiDAR and Landsat. *Journal of Hydrology*, 487: 70-86.
13. Li P, Jiang L, Feng Z. 2014. Cross-Comparison of Vegetation Indices Derived from Landsat-7 Enhanced Thematic Mapper Plus (ETM+) and Landsat-8 Operational Land Imager (OLI) Sensors *Remote Sensing*, 6: 310-329.
14. Rokni K, Ahmad A, Selamat A, Hazini S. 2014. Water Feature Extraction and Change Detection Using Multitemporal Landsat Imagery. *Remote Sensing*, 6: 4173-4189.
15. Handisyde N, Lacalle DS, Arranz S, Ross LG. 2014. Modelling the flood cycle, aquaculture development potential and risk using MODIS data: A case study for the floodplain of the Rio Paraná, Argentina. *Aquaculture*, 422-423: 18-24.
16. Yang Y, Liu Y, Zhou M, Zhang S, Zhan W, Sun C, Duan Y. 2015. Landsat 8 OLI image based terrestrial water extraction from heterogeneous backgrounds using a reflectance homogenization approach. *Remote Sensing of Environment*, 171: 14-32.
17. Morphological snakes for image segmentation and tracking/ <https://github.com/pmneila/morphsnakes> (access at 7/5/2016)
18. Zhu Z, Woodcock CE. 2012. Object-based cloud and cloud shadow detection in Landsat imagery. *Remote Sensing of Environment*, 118: 83-94.
19. Zhu Z, Wang S, Woodcock CE. 2015. Improvement and expansion of the Fmask algorithm: Cloud, cloud shadow, and snow detection for Landsats 4-7, 8, and Sentinel 2 images. *Remote Sensing of Environment*, 159: 269-277.

Data Science Driven Hydrological Applications

Krishna Karthik Gadiraju ¹

¹North Carolina State University; kgadira@ncsu.edu

Academic Advisor: Ranga Raju Vatsavai, North Carolina State University, rrvatsav@ncsu.edu

Summer Institute Theme Advisor: David Maidment, University of Texas at Austin, maidment@utexas.edu

Abstract: Data intensive scientific discovery is touted as the 4th paradigm. Big data is influencing many new real-world applications including food, energy, water, and climate. Geospatial data sciences, which is at the intersection of data management, data analytics (including data mining and machine learning), and high-performance computing provides a unified framework for analyzing data arising out of in-situ and remote sensors that are spatially distributed. Analysis and management of big data has been the cornerstone of computer science research for the past decade, with large strides being made in terms of techniques, technology, and tools required to perform the analysis and management tasks. Given the spatio-temporal nature of hydrological data, and the fact that the analysis is now being conducted at continental scale (e.g., the National Water Model), a collaboration between data science and hydrological sciences would benefit both fields and facilitate the development of computationally efficient solutions. In this report, a data science perspective is given to the projects developed at the 2016 National Water Center Summer Institute, by identifying the unifying concepts and computational challenges across the broad spectrum of applications, and describing how data and computational sciences can help advance them. In addition, we describe the flood inundation mapping using remote sensing imagery and supervised machine learning techniques. What follows is a description of some of the challenges associated with using satellite imagery, followed by a demonstration of how pixel-based supervised machine learning approaches can help map inundated areas through the use of very little training data. We then build an ensemble of the pixel-based machine learning techniques to combine the strengths of different classifiers.

1. Motivation

Improved sensing equipment over the past decade has resulted in the availability of high resolution, and very high resolution (VHR) satellite imagery such as LANDSAT-8 (<http://earthexplorer.usgs.gov/>) and DigitalGlobe (<https://www.digitalglobe.com/>). This high spatial resolution, combined with improved temporal resolution, means that peta-byte scale spatio-temporal data repositories are now available for research, and are constantly being updated. Additionally, a variety of spatio-temporal data (geotagged images, text, and video) is also available from the web in the form of various social-media sources such as Twitter, Flickr, Instagram and Facebook. Google alone generates close to 25 petabytes of data per day in various forms such as images and video. In this realm of densified measurement networks, having a large variety of data collected from a variety of in-situ sensors (such as the USGS gauges, Sommer GmbH RQ-30 radar), in addition to the remote sensing data has become common place in today's advanced hydrological analyses. Storing and analyzing this spatio-temporal big data presents several unique challenges to the field of computer science, such as of computational complexity (both from the size, scale and speed at which data is collected as well as its spatio-temporal characteristics [1]), scalability and efficiency. Management and analysis of such spatio-temporal big data is a very active area of research [1-7]. Given the new emphasis on continent scale hydrology such as the National Water Model [8], the field of computer science has much to offer to some of the more technical and computational challenges associated with such analyses.

2. Objectives and Scope

The primary motivation of this work is to demonstrate how research being conducted in the data science field can help solve some of the computational challenges associated with research being conducted in the field of hydrology. In order to demonstrate this, we performed the following tasks:

- 1) Computational challenges associated with some of the projects performed at the NWC Summer Institute 2016 are identified, and a brief description of how these problems can be solved is provided.
- 2) A generic summary of the challenges associated with analysis and storage of spatiotemporal big data and satellite imagery is provided.
- 3) Finally, a case study for flood inundation mapping on LANDSAT-8 data using several popular supervised machine learning techniques was performed.

3. Methodology

3.1. Computer Science Solutions to Challenges associated with NWC SI Projects

3.1.1. Emergency Response Systems

Flood emergency response was one of the major themes focused upon in the Summer Institute. From a computational standpoint, the major requirements for an emergency response software system is that it should be able to gather data from a variety of sources (Henson et al.), should be able to scale to any number of actors, and should be fault-tolerant (high-availability). These requirements can be satisfied by conducting research towards building scalable, fault-tolerant database management systems that are capable of storing spatiotemporal data gathered from distributed, and heterogeneous datasets. In addition to collection and management of data, research being performed in the data science field in the areas of real-time data analytics, and Internet of Things [9, 10] could provide timely and reliable information to emergency first responders. In addition, research into crowd sourcing data [11], from various sources can also aid in providing additional information for emergency response. Ushahaidi [12] is one such platform, where crowd-sourced information has helped in disaster/crisis management. Many factors need to be taken into account when using crowd sourced data, from population skew and unrepresentative sample sizes to factual content, but its use fills a gap that traditional datasets cannot.

3.1.2. Nays2D Flood – Computation Time for high resolution data

Siddique et al. mention that the Nays2D Flood solver, which is part of an International River Interface Cooperative (iRIC) software, takes close to 2 months to compute when the grid size is 1m by 1m. Research can be conducted into first verifying the feasibility, and then identifying optimal parallel computing solutions such as, distributed memory processing (e.g., MPI - Message Passing Interface [13]), shared memory processing (e.g. pThreads and OpenMP [14]), distributed computing (e.g. Hadoop [15] and Spark [16]), GPU based computing (CUDA [17], OpenCL [18]) or a combination of one or more to implement the Nays2D Flood solver on, in order to reduce computation time. Parallelism can be achieved at two levels. The first level this can be performed is at the data level, where in same computation is performed on different sections of the data in parallel, and the second level is at the task level, wherein multiple tasks are performed on same data in parallel. [19] describes various approaches to building scalable machine learning solutions using the aforementioned parallel and distributed computing solutions. Research can be conducted to identify which type of parallelism works best for the Nays2D Flood solver, and then implemented using the most suitable parallel computing solution.

3.1.3. Cloud Computing and Distributed Database Management Systems

HAND method is one of the popular techniques that come across several applications at the Summer Institute. Owing to its computational demands, [20] is implemented on the ROGER computer at the CyberGIS Facility located at the University of Illinois, Urbana Champaign [21]. Given that the HAND method requires data from a variety of sources, all of which arrive in various formats and sizes, one challenge is to identify a single optimal data store that can store all these disparate formats of data into a common data format which the HAND method can use as an input, thereby reducing time spent on reading and writing data. This involves research into distributed data management systems (that would ideally be placed in a cloud computing platform) that are capable of storing large scale spatiotemporal data, and support fast retrieval and compatibility with data sources of various formats. Research should be conducted into methods to make such systems flexible enough to accommodate new standards of data formats that might appear in the future.

3.1.4. 3D Modeling

3D hydrological modeling is an important area that has not been well explored. As demonstrated by Coll et al., with the availability of modern RQ-30 radar, more information is now available to make it suitable to perform 3D modeling with little field collection time. Research being conducted in the field of Computer Graphics, particularly in regards to 3D modeling which, when combined with research being conducted on parallel computing systems, can help in building optimized 3D models.

3.2. Satellite Image Analysis – Challenges

One of the primary challenges of using satellite imagery to perform analysis tasks such as inundation mapping includes: availability of data during flooding, or at a date close to a flooding event. Even once this image is obtained, the second challenge is that, for optical satellites, such images are often covered with a large percentage of clouds that render the data obtained from such optical sensors unusable. Also, as the size of image under consideration increases, the amount of time required to perform analyses also increases. Lack of ground truth data, and the possibility of confusion between water pixels and pixels of other classes such as urban, roads and vegetation are the other challenges. In this report, we generate around 402 sample points, of which around 242 (around 60%) is used for training the supervised classification models, and 160 (~40%) is used to evaluate the accuracy of the classifiers. Feature generation and selection is performed in order to distinguish between water and other classes such as urban and roads.

3.3. Flood Inundation Mapping – A Case Study



Figure 1. LANDSAT-8 image for the Blanco River, NW Texas: **(a)** without flooding, March 25, 2016. **(b)** With flooding, May 28, 2016. Region of interest has been highlighted by yellow oval.

In this section, a case study was performed on identifying flood inundation on the Blanco River in South Western Texas, USA. The information for this flooding was obtained from [22]. Multi-spectral LANDSAT-8 OLI and TIRS (Operational Land Imager, Thermal Infrared Sensor) images were collected during the flood (Figure 1(b) - May 28, 2016), as well as before flooding (Figure 1(a) - March 25, 2015). The image was preprocessed, and a composite image using the bands 1-7 and band 9 was prepared using ESRI's ArcGIS Desktop. The spatial resolution of the bands is 30 m. Training data was built using the point sampling toolbox in QGIS on the flooded image. In total, the training dataset consisted of 242 training samples including 6 different labels – Clouds, Roads, Shadow, Urban, Vegetation and Water.

3.3.1 Supervised Classification – individual classifiers, Feature Generation and Feature Selection

Given the limited amount of training data, and the possibility of confusion between water and other classes such as urban and roads, we generate additional features to overcome this issue. Generating additional texture features in order to better identify urban areas has been described in [7]. Based on [7], we generated 18 different texture features, known as the Haralick features [23]. These features include energy, entropy, correlation, inverse difference moment, inertia, cluster shade, cluster prominence, haralick correlation, mean, variance, sum average, sum variance, sum entropy, difference of entropies, difference of variances and information measures of correlation 1 and 2 [24]. These bands, together with the 8 LANDSAT-8 bands, make a total of 25 bands of information. However, given this high dimensionality, in order to avoid the Hughes phenomenon, and reduce computational complexity, we identify the most important features/bands (i.e., feature selection) using a method known as Learning Vector Quantization (LVQ) [25]. LVQ is a supervised learning method that ranks features by their importance with respect to classification. LVQ is used to generate the top 10 features. A series of pixel based supervised classification models (Naive Bayes (NB), Decision Tree (DT), Random Forests (RF), Multi-Layer Perceptron (MLP) and K-Nearest Neighbors (KNN)) [26-29] were trained using these features, and the accuracy is evaluated on the test samples. In addition, labels were predicted for each pixel on the flooded image. For the K-Nearest Neighbor algorithm, a pixel was classified based on the classes of its 10 nearest neighbors (i.e., K=10).

3.3.2 Supervised Classification – ensemble classifier

The rationale behind using an ensemble classifier, which is a group of individual classifiers, is that single classifiers might be able to classify certain labels accurately, while they might be limited in classifying other labels. Combining the outcomes of all individual classifiers helps to normalize various classifiers strengths and weaknesses. The ensemble classifier used in this work is a linear combination of the outcomes of the 5 classifiers described above. In the ensemble classifier, a pixel is classified as water if at least two classifiers have classified it as water, and it is classified as a generic ‘other’ type otherwise. This is done because, in this study, failing to detect water is a bigger error when compared to failing to detect other types. In the next section, we show the outcomes of the supervised classification methods. This study used Weka and Java to perform the NB, DT, RF, MLP and KNN classifications, R for feature selection and ensemble classification and generating the visual maps and Orfeo Toolbox for Feature Generation.

4. Results

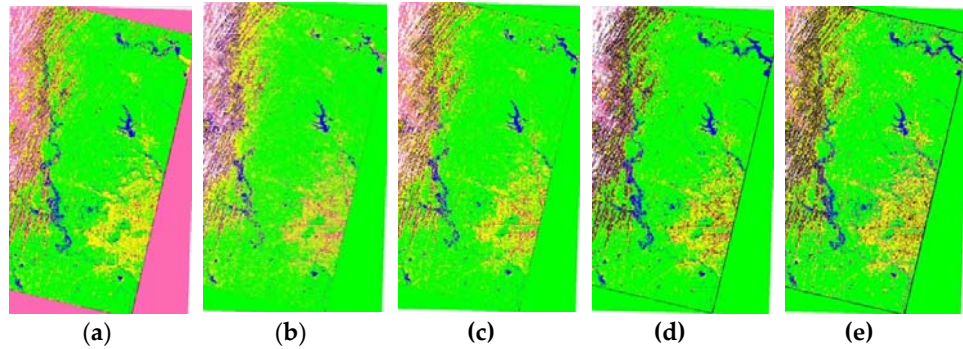


Figure 2. Classified images, with classes and their representative colors specified in Table 1 for classifier: (a) NB (b) DT (c) RF (d) MLP (e) KNN

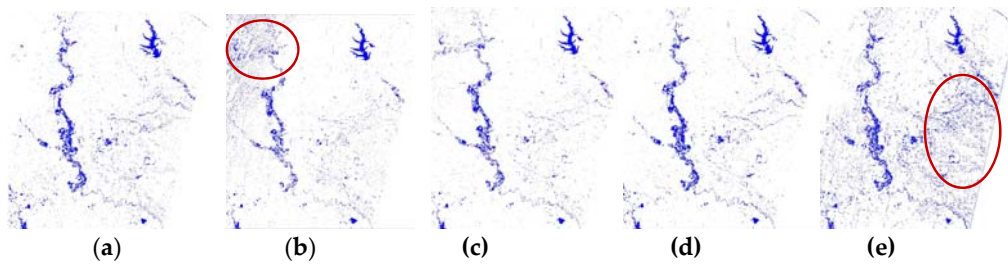


Figure 3. Classified images, with water specified by blue color, all other classes by white for the classifiers: (a) NB (b) DT (c) RF (d) MLP (e) KNN

Initially, bands 4(R), 3(G), 2(B) and 5 (NIR) of LANDSAT-8 were used to perform classification. It was observed that the classifiers were unable to distinguish between water, urban and road classes accurately. In order to incorporate more variation between water and other classes, as explained in the previous section, Haralick texture features were generated, and the LVQ was performed to identify the top 10 important features. Of all the 25 features, LVQ identified bands 4(R), 3(G), 2(B), 1 (aerosol), SWIR1, SWIR2 from the LANDSAT-8 bands, and energy, inverse difference moment, difference of entropies and inertia as the top 10 features in terms of importance. Upon training the aforementioned supervised learning models and performing classification on the test dataset of 160 points, it was observed that MLP had the highest overall accuracy (96.28%), while DT had the least (86.88%). In terms of accuracy for classifying water for the test set, RF and MLP had 100% accuracy, while NB and DT had least accuracy (92.86%). The ensemble method described above also achieved 100% accuracy for classifying water.

We then performed classification on the entire image. Table 1 provides a mapping of the color to corresponding class label for each pixel in all images. Given that our primary focus is towards identifying water, we re-visualize the images as shown in Figure 3, with water being visualized by blue, and everything else visualized as white. From Figure 3, we can observe that the KNN classifier performed poorly, with several urban points identified as water, as highlighted in regions 3(e). DT also performed poorly in comparison with other methods, with some regions over the Blanco River not identified as shown in Figure 3(b). However, the MLP performed the best, with it even able to identify all the water bodies as shown in Figure 3(d).

Table 1. List of labels and their corresponding colors.

Label	clouds	roads	shadow	urban	vegetation	Water
Color	white	yellow	black	pink	green	Blue

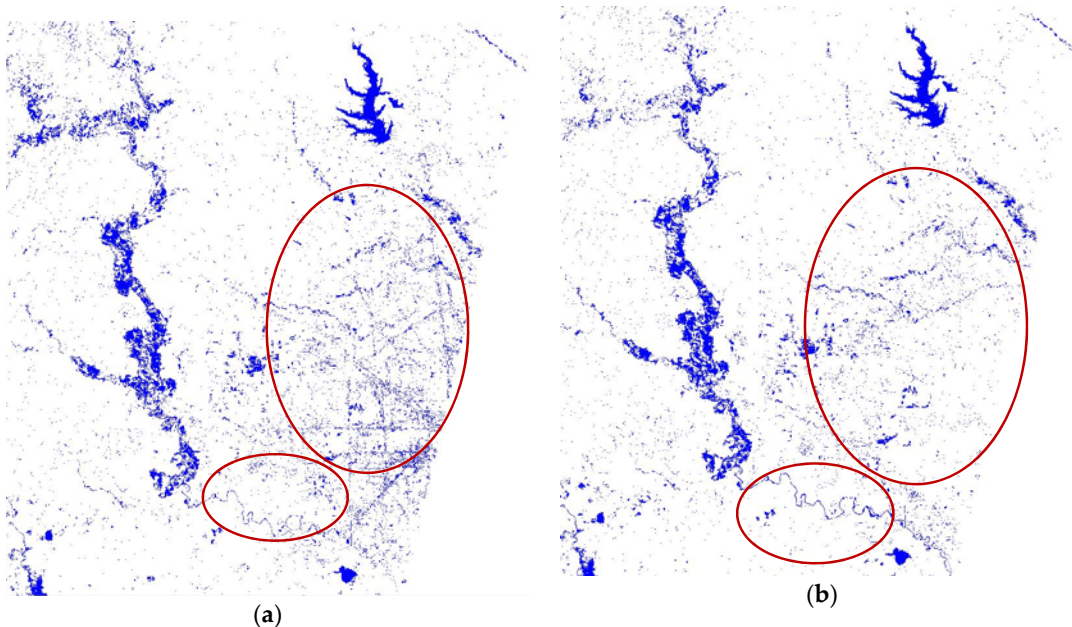


Figure 4. Classified images, with water specified by blue color, all other classes by black: (a) Outcome of Ensemble classifier without Texture Features and feature selection (b) Outcome of Ensemble classifier with Texture Features and using Feature Selection

As explained earlier, the Ensemble method was run using the condition that a pixel would be classified as water if at least two classifiers identified it as water. The outcome of the Ensemble method is displayed in Figure 4. Figure 4(a) represents the outcome of the ensemble classifier when the R, G, B and NIR bands were used for classification. Figure 4(b) represents the outcome of the ensemble classifier with the top 10 features generated using feature selection on 8 LANDSAT bands and 18 Texture Features. As shown in the highlighted regions in Figure 4(a) and (b), the second image has a lower noisy clutter generated due to confusion between urban, roads and water.

5. Conclusions and Future Work

In this study, an effort has been made to describe how research being conducted in the field of computer science can assist the hydrological research community. Areas of improvement in terms of computational complexity, ease of use were identified, and possible directions of collaborative research were identified. Five pixel-based classification methods were used to perform supervised classification to identify flood inundation over the Blanco River in TX, USA. In addition, an ensemble classification method using the outcomes from the five pixel based classifiers has been described to combine the strengths of different classifiers. Calculation of accuracy for the entire image is not possible, due to the lack of ground truth. In the future, given the presence of labelled data for the entire image, the ensemble method can be modified such that the label of each pixel is a weighted combination of the outcomes of the individual classifiers. These weights can then be learnt using another supervised learning method such as a neural network. This weighted ensemble method would be able to better classify flood inundation

Finally, a mode filter can be applied, which scans through the entire image, by searching through a 5×5 neighborhood of each pixel, identifying the most commonly occurring class, within this neighborhood and then replacing the current pixel class with this new class. This method will help in removing the wrongly classified individual water points that appear in the image as a side effect

of the pixel based classification procedure as well as filling in gaps in water detection at the pixel level because of cloud cover.

6. Acknowledgements

I would like to thank Jim Coll, Adnan Rajib, Hossein Hosseiny, Christopher Zarzar and Peirong Lin from the Summer Institute for their valuable feedback regarding the computational challenges associated with their work, and Bharathkumar Ramachandra from NC State University for his valuable suggestions regarding the classification methods.

References

1. Vatsavai, R. R., A. Ganguly, V. Chandola, A.. Stefanidis, S. Klasky, and S. Shekhar. "Spatiotemporal data mining in the era of big spatial data: algorithms and applications." Proceedings of the 1st ACM SIGSPATIAL international workshop on analytics for big geospatial data, pp. 1-10. ACM, 2012.
2. Sethi, M., Y. Yan, A. Rangarajan, R.R. Vatsavai, and S.Ranka. "Scalable machine learning approaches for neighborhood classification using very high resolution remote sensing imagery." Proceedings of the 21th ACM SIGKDD International Conference on Knowledge Discovery and Data Mining, pp. 2069-2078. ACM, 2015.
3. Chandola, Varun, and Ranga Raju Vatsavai. "A scalable gaussian process analysis algorithm for biomass monitoring." *Statistical Analysis and Data Mining* 4, no. 4 (2011): 430-445.
4. Shashidharan, Ashwin, Derek B. van Berkel, Ranga Raju Vatsavai, and Ross K. Meentemeyer. "pFUTURES: A Parallel Framework for Cellular Automaton Based Urban Growth Models." In *International Conference on Geographic Information Science*, pp. 163-177. Springer International Publishing, 2016.
5. Datta, Abhirup, Sudipto Banerjee, Andrew O. Finley, Nicholas AS Hamm, and Martijn Schaap. "Non-separable Dynamic Nearest-Neighbor Gaussian Process Models for Large spatio-temporal Data With an Application to Particulate Matter Analysis." arXiv preprint arXiv: 1510.07130 (2015).
6. Cavallaro, Gabriele, Morris Riedel, Matthias Richerzhagen, Jón Atli Benediktsson, and Antonio Plaza. "On understanding big data impacts in remotely sensed image classification using support vector machine methods." *IEEE journal of selected topics in applied earth observations and remote sensing* 8, 10 (2015): 4634-4646.
7. Vatsavai, Ranga Raju. "High-resolution urban image classification using extended features." In *2011 IEEE 11th International Conference on Data Mining Workshops*, pp. 869-876. IEEE, 2011.
8. National Water Model: <http://water.noaa.gov/about/nwm>
9. Yang, Lili, Shuang-Hua Yang, and L. Plotnick. "How the internet of things technology enhances emergency response operations." *Technological Forecasting and Social Change* 80, no. 9 (2013): 1854-1867.
10. Asimakopoulou, Eleana, and Nik Bessis. "Buildings and crowds: Forming smart cities for more effective disaster management." In *Innovative Mobile and Internet Services in Ubiquitous Computing (IMIS), 2011 Fifth International Conference on*, pp. 229-234. IEEE, 2011.
11. Narock, T., and P. Hitzler. "Crowdsourcing Semantics for Big Data in Geoscience Applications." (2013).
12. Okolloh, Ory. "Ushahidi, or 'testimony': Web 2.0 tools for crowdsourcing crisis information." *Participatory learning and action* 59, no. 1 (2009): 65-70.
13. Gropp, William, Ewing Lusk, Nathan Doss, and Anthony Skjellum. "A high-performance, portable implementation of the MPI message passing interface standard." *Parallel computing* 22, 6 (1996): 789-828.
14. Dagum, Leonardo, and Ramesh Menon. "OpenMP: an industry standard API for shared-memory programming." *IEEE computational science and engineering* 5, no. 1 (1998): 46-55.
15. Hadoop, Apache. "Hadoop." 2009-03-06]. <http://hadoop.apache.org> (2009).
16. Spark, Apache. "Apache Spark™-Lightning-Fast Cluster Computing." (2014).
17. Nvidia, C. U. D. A. "Compute unified device architecture programming guide." (2007).
18. Stone, John E., David Gohara, and Guochun Shi. "OpenCL: A parallel programming standard for heterogeneous computing systems." *Computing in science & engineering* 12, no. 1-3 (2010): 66-73.
19. Bekkerman, Ron, Mikhail Bilenko, and John Langford, eds. *Scaling up machine learning: Parallel and distributed approaches*. Cambridge University Press, 2011.
20. Nobre, A. D., L. A. Cuartas, M. Hodnett, C. D. Rennó, G. Rodrigues, A. Silveira, M. Waterloo, and Scott Saleska. "Height above the nearest drainage—a hydrologically relevant new terrain model." *Journal of Hydrology* 404, no. 1 (2011): 13-29.
21. Liu, Yan, David R. Maidment, David G. Tarboton, Xing Zheng, Ahmet Yildirim, Nazmus S. Sazib and Shaowen Wang. "A CyberGIS Approach to Generating High-resolution Height Above Nearest Drainage

- (HAND) Raster for National Flood Mapping", CyberGIS 16, The Third International Conference on CyberGIS and Geospatial Data Science, Urbana, Illinois, 2016.
- 22. NASA Earth Observatory Images: Blanco River Flood before and after images and corresponding information, <http://earthobservatory.nasa.gov/IOTD/view.php?id=88129>
 - 23. Haralick, Robert M., and Karthikeyan Shanmugam. "Textural features for image classification." *IEEE Transactions on systems, man, and cybernetics* 6 (1973): 610-621.
 - 24. Orfeo Toolbox Cookbook: <https://www.orfeo-toolbox.org/packages/OTBCookBook.pdf>
 - 25. Kohonen, Teuvo. "Learning vector quantization." In *Self-Organizing Maps*, pp. 175-189. Springer Berlin Heidelberg, 1995.
 - 26. Friedl, Mark A., and Carla E. Brodley. "Decision tree classification of land cover from remotely sensed data." *Remote sensing of environment* 61, no. 3 (1997): 399-409.
 - 27. Ham, Jisoo, Yangchi Chen, Melba M. Crawford, and Joydeep Ghosh. "Investigation of the random forest framework for classification of hyperspectral data." *IEEE Transactions on Geoscience and Remote Sensing* 43, no. 3 (2005): 492-501.
 - 28. Haykin, Simon, and Neural Network. "A comprehensive foundation." *Neural Networks* 2, no. 2004 (2004).
 - 29. Venkatesh, Y. V., and S. Kumar Raja. "On the classification of multispectral satellite images using the multilayer perceptron." *Pattern Recognition* 36, no. 9 (2003): 2161-2175.

Chapter 3

Forecast Errors

Quantifying uncertainty in flood inundation mapping using streamflow ensembles and hydraulic modeling techniques

Christopher Zarzar¹, Ridwan Siddique², Hossein Hosseiny³, Michael Gomez⁴

¹ Department of Geosciences, Mississippi State University, Mississippi State, Mississippi; cmz39@msstate.edu

² Department of Civil and Environmental Engineering, Pennsylvania State University, University Park, Pennsylvania; rxs490@psu.edu

³ Department of Civil and Environmental Engineering, Villanova University, Pennsylvania; shossein@villanova.edu

⁴ Department of Civil and Environmental Engineering, Pennsylvania State University, University Park, Pennsylvania; mvg5545@psu.edu

Academic Advisors: Jamie Dyer, Mississippi State University; Alfonso Mejia, Pennsylvania State University; Virginia Smith, Villanova University.

Summer Institute Theme Advisors: Alfonso Mejia, Department of Civil and Environmental Engineering, Pennsylvania State University, University Park, Pennsylvania, amejia@engr.psu.edu; Ibrahim Demir, Department of Electrical and computer Engineering, Iowa City, Iowa, ibrahim-demir@uiowa.edu.

Abstract: The National Water Model (NWM) provides a platform needed to operationalize nationwide flood inundation forecasting and mapping. The ability to model flood inundation on a national scale puts invaluable information into the hands of decision makers and local emergency officials. Often, forecast products use deterministic model output to provide a visual representation of a single inundation scenario, which is subject to uncertainty from various sources such as observation error or assumptions in model physics. While a single deterministic simulation provides a straightforward representation of potential inundation, the inherent uncertainty associated with the model output also needs to be conveyed for improved decision support. To this end, the goal of this study is to produce ensembles of future flood inundation conditions (i.e. extent, depth, and velocity) to quantify and visualize model uncertainty associated with simulated flood inundation maps. The study area is a highly urbanized watershed along the Darby Creek in Philadelphia, Pennsylvania. Time-lagged output from the NWM short-range forecasts were used as varying initial conditions for a 2D HEC-RAS model, which allowed for the generation of ensemble simulations of water extent, depth, and flow velocity. The ensemble output was then used to quantify model uncertainty through a calculation of statistical spread among the ensemble members. For visualization, a series of flood maps that display flood water extent, water depth, and flow velocity along with the underlying uncertainty associated with each of those forecasted variables were produced. The results from this study demonstrate the potential to incorporate and visualize model uncertainty in simulated flood inundation maps, enhancing the applicability of the NWM output for communication of flood risk.

1. Introduction

Floods are one of the most costly natural disasters in the United States [1]. Each year floods are responsible for numerous weather related fatalities alongside billions of dollars in damages to properties [2]. Effective and efficient flood preparation efforts depend heavily on the accuracy of the forecasted flood extent, depth of flood waters, and speed at which the water is moving. Beyond the accuracy of the forecast, the way in which the forecasted flood event is communicated can benefit or hinder the distribution of resources. Forecasted flood inundation maps are typically based on deterministic model output generated using a hydraulic model forced with a single discharge output from a hydrologic model [e.g. 3, 4]. However, these deterministic flood inundation maps can be

subject to uncertainty from many different sources, including numerical imprecision in the hydrologic input and/or assumptions in model physics within the hydraulic models [3].

Merwade et al. [3] provide an extensive review about the meteorological, geographic, hydrologic, hydraulic, and analysis factors that contribute to uncertainty in flood inundation mapping. The factors contributing to uncertainty have been echoed in greater detail with findings that the channel roughness parameter is one of the most influential sources of uncertainty in flood inundation mapping [5, 6, 7]. Among others, topographic data and hydraulic modeling techniques are also mentioned as substantial contributors of uncertainty in flood inundation mapping [8, 9]. Pappenberger et al. [10] mentioned that flow input data is one of the major sources of uncertainty since the stage-discharge curve is used to obtain the observed flow data to produce flood inundation maps. Pappenberger et al. [11] demonstrate how uncertainties can begin from the initial simulation time step in the short to medium range meteorological forcings used to generate the flood inundation maps.

Another important consideration beyond model uncertainty is the ability to communicate these uncertainties in disseminated flood forecast products. To this end, the objective of this paper is to quantify and visualize uncertainty in flood inundation for a flood event in a highly urbanized watershed. This study will address forecast uncertainty using time lagged ensembles by quantifying spread among the various ensemble members. The generation of probabilistic flood inundation maps based on these uncertainty metrics provides a method for communicating predicted flood risk, which will provide critical information to help decision makers better prepare for potential flood events.

2. Methodology

2.1 Study Area and DEM data

The river selected for this project is a segment of Darby Creek, located in urban Philadelphia, PA, and stretches from the Mt. Moriah Cemetery to its confluence to the Delaware River (Figure 1). The mean slope of Darby Creek is 0.001 m/m and average width of 50 meters. The length of the reach is approximately 15 kilometers.

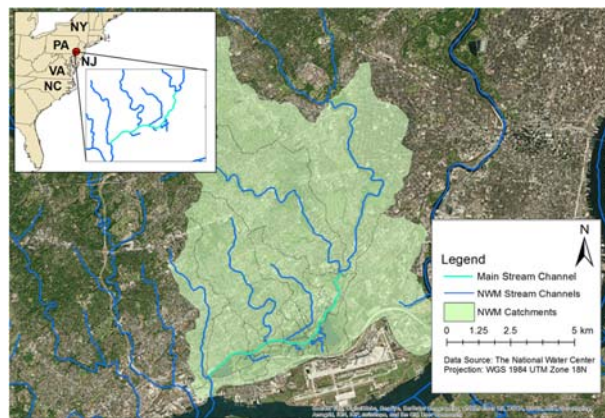


Figure 1. Study area.

The floodplains of Darby Creek are highly developed, and they have been highly developed for some time (Figure 2a & 2b). A simple analysis found that the variation in the National Land Cover Database (NLCD) developed areas for the region increased less than 0.1% of the total area from years 2001 to 2011.

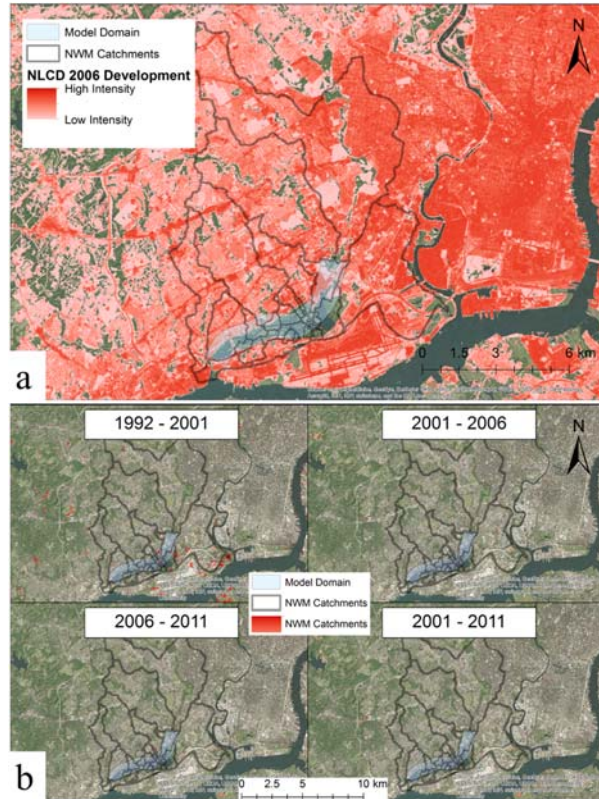


Figure 2. a) 2006 NLCD impervious land cover classification; b) NLCD land cover classification change to developed.

Due to the highly urbanized floodplains in the study area, it was necessary to use high resolution elevation data to correctly represent the terrain. A high resolution (1 meter) LiDAR derived digital elevation model (DEM) obtained from the Pennsylvania Spatial Data Access (PASDA) was used in combination with a bathymetry dataset collected by NOAA. Manual corrections were applied to the river terrain model in zones where bathymetry data was missing.

2.2 Selected flood event and flow observations

At the time of this study, NWM archives contained only a few months (June-July, 2016) of historical forecast data. This period of record did not include any major flood events, including the April 30 to May 1 of 2014 flood event selected for this study. Therefore, the USGS Cobb Creek gage at Mt. Moriah Cemetery (USGS 01475548) located at the upstream end of our model was used to get the initial streamflow data. This event marked the second highest streamflow ever recorded at the gage reaching near 100 cms on April 30 at 19:00 EDT (Figure 3).

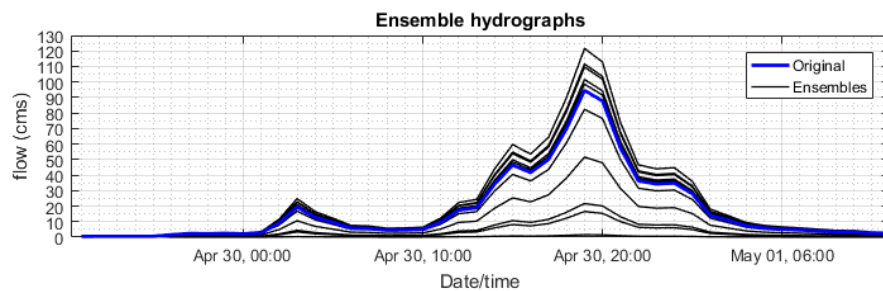


Figure 3. Ensemble hydrographs for the April 30, 2014 flood event.

2.3 Methods Time lagged ensembles from NWM short-range forecasts:

Time lagged ensembles were used as an alternative to forecast ensembles to account for uncertainty in NWM short-range streamflow forecasts. All available NWM historical forecast data was used in a time series (AR1) model to generate multiple realizations of streamflow discharges for the selected flood event. The statistical model can be described as below:

$$Z_{0,k+1} = (1 - b_{k+1})Z_{0,k} + b_{k+1}Z_{f,k+1} + E_{k+1} \quad (1)$$

where $Z_{0,k+1}$ and $Z_{0,k}$ denote the normal quantile transformed (NQT) observed flow at time steps $k+1$ and k , respectively, b_{k+1} denotes the regression coefficient at time step $k+1$, $Z_{f,k+1}$ denotes the NQT forecast flow valid at time step $k+1$, and E_{k+1} denotes the residual error at time step $k+1$. At time step $k+1$, $Z_{0,k}$ corresponds to the actual observed streamflow at time step k , whereas time step $k+2$ onwards $Z_{0,k}$ is the estimated observed value at the preceding time step, i.e., $Z_{0,k+1}$, using Eq. (1).

Regonda et al. [12] at the National Weather Service (NWS) used the above model to generate ensembles from short-range deterministic forecasts. For this study, we used USGS gage observations as observed flow and NWM model simulations as the exogenous variable.

2.4 Hydraulic modeling with HEC-RAS

The Hydrologic Engineering Center – River Analysis System Version (HEC-RAS) 5.0.0 is an unsteady 2D hydraulic model developed by U.S. Army Corps of Engineers that solves the 2-dimensional Shallow Water Equations (SWE) using an implicit finite volume algorithm over an unstructured computational mesh; this allows the user to add more detail where needed like in dikes, roads, buildings, etc.

The model mesh was composed of 82349 irregular shaped cells (3 to 8 sides), with an average cell size of 385 m², the Manning's n value for the main channel was 0.5 m^{-1/3} s, the spatial variability of the roughness parameter in the floodplains was determined by using the NLCD of 2011, it varies from 0.04 to 0.15 m^{-1/3} s. For the calibration of the model, the discharges recorded by the stream gage at the upstream end of the domain were used.

The upstream boundary condition was modeled as a hydrograph with 1 hour time steps, the input hydrograph was from April 29 at 0:00 am to May 1 12:00 pm. The downstream boundary was considered to be a normal flow condition because the slope of the Darby Creek at the downstream part of the reach is very mild. As an initial condition the domain is considered to be dry, but to account for the fact that the reach is not dry at the moment of the flooding event, the hydrograph was extended 24 hours before the event to create a more realistic condition. After running the HEC-RAS model, three inundation maps were generated for each ensemble in the form of raster files; the first for water surface elevation, the second for water depth and the last one for flow velocity.

2.5 Hydraulic model outputs post-processing

Outputs from HEC-RAS 2D were post-processed to convert the output to a common 5 meter by 5 meter gridded raster format. During this conversion processes, numerous threat metrics were extracted from the data (Table 1).

Table 1. Four primary flood threats with listed metrics extracted from the model output.

Flood Extent	Water Depth	Flow Velocity	Critical Conditions
	> 0.5 ft	> 1 mph	> 0.5 ft water flowing at > 4 mph
	> 1 ft	> 2 mph	> 1 ft water flowing at > 4 mph
	> 2 ft	> 4 mph	> 2 ft water flowing at > 4 mph
	> 3 ft	> 6 mph	> 0.5 ft water flowing at > 6 mph

> 4 ft	> 8 mph	> 1 ft water flowing at > 6 mph
> 5 ft		> 2 ft water flowing at > 6 mph
> 6 ft		> 3 ft water flowing at > 2 mph
		> 4 ft water flowing at > 2 mph
		> 5 ft water flowing at > 1 mph
		> 6 ft water flowing at > 1 mph

All output produced by HEC-RAS 2D were combined into threat-based composite rasters, where each grid value corresponds to the percent ensemble agreement that a certain threat metric would be exceeded. Those threat-based metrics were created with flood preparation efforts in mind. For example, a threat-based metric extracted from the data tested whether conditions in each grid exceeded a depth of 1 foot of water flowing at a rate faster than 4 miles per hour. These conditions are hazardous conditions to try to stand in, much less walk [13]. The final product portrays the model output agreement for certain hazardous conditions in each forecast grid cell. In other words, the final product uses the ensemble spread (i.e. uncertainty) as a measure of risk, where high risk corresponds to grids with greater ensemble agreement.

It is important to note that besides the 2D HEC-RAS model, attempts were made to simulate the flood event with the International River Interface cooperative (iRIC), but technical problems with modeling and post processing limited the use of iRIC in this paper. Nevertheless, iRIC will be incorporated in future work to quantify uncertainty of both forecasted streamflow and hydraulic models in the flood inundation maps.

3. Results

The value of this study is best demonstrated through a comparison between the flood extent generated by a deterministic HEC-RAS 2D model output using the maximum observed discharge, and the flood extent generated by the ensemble HEC-RAS 2D composited raster associated with a range of possible discharge scenarios (Figure 4).

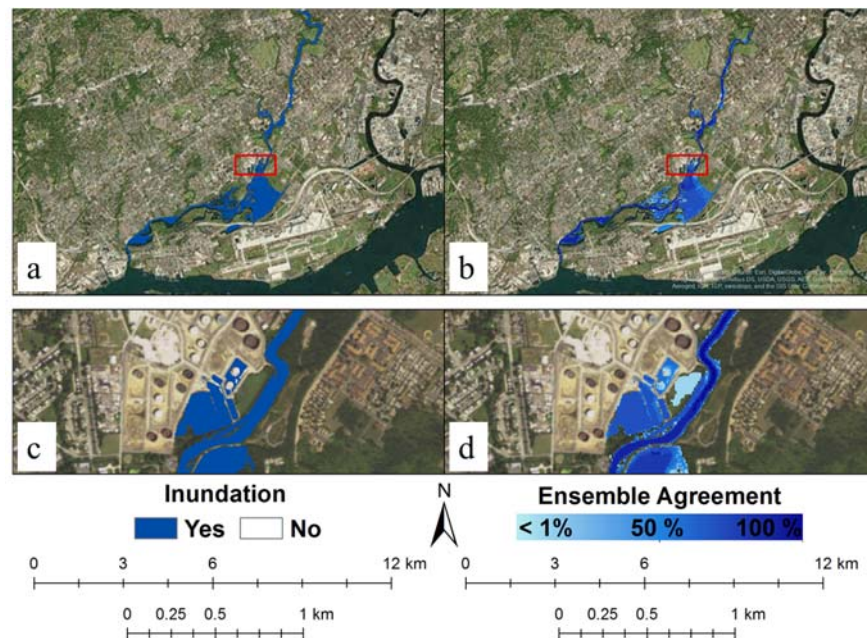


Figure 4. Side by side comparison of HEC-RAS 2D deterministic model output (left) and composited HEC-RAS 2D model output (right)

The flood extents in figure 4 look similar, but the advantages of this proposed ensemble method can be seen when zoomed into the Sunoco Logistics crude oil storage tank farm. Where it appears imminent that a couple of these oil tanks are at threat of flooding based on the deterministic output, the actual risk of flooding to these takes is not so certain. The probabilistic output shows that only about 5 out of 10 (50%) of the outputs agree this area will be inundated. To a decision maker, this may indicate that this is an area to keep a close eye on, but maybe not an area where resources will be needed immediately.

In addition to the flood extent, it was mentioned earlier that other flood threat metrics (Table 1) were also extracted from the data that could be useful towards flood preparation efforts. It would be challenging to sift through the great amount of flood threat metric information provided from the output in a typical GIS platform, especially if these products are used in emergency situations. In response to this, the flood metric information was compiled into a BYU web application platform called Tethys to disseminate the information contained in the final deliverables in a highly accessible way. Continuing with the previous example about the potential flooding at the Sunoco Logistics crude oil storage tank farm, what if there is a limit to the depth of water that these tanks can be subjected to? Beyond that, maybe the tanks can withstand a certain water flow velocity, or maybe a combination of both. The great advantage of integrating the output from this study into the Tethys platform is that all of these metrics can be easily and quickly viewed to assess the risk and severity of the situation (Figure 5).

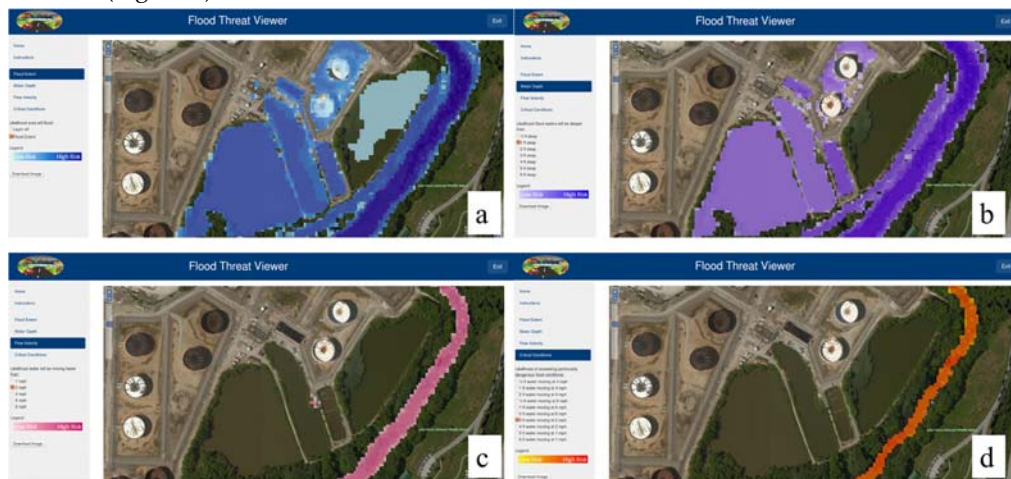


Figure 5. Tethys interface. Zoomed to Sunoco Logistics crude oil storage tank farm. Panels correspond to the Table 1 threat metrics of (a) flood extent, (b) water depth, (c) flow velocity, and (d) critical conditions.

While created as a decision support tool, the Tethys platform allows for the integration of the composited raster output into a publicly accessible user-friendly framework that can be used for many more applications outside of the emergency response community.

4. Conclusion

This study aimed to quantify and visualize model uncertainty in simulated flood inundation maps for a highly urbanized watershed. Uncertainty in streamflow forecasts were quantified by generating time-lagged initial conditions from the NWM short-range forecasts. The streamflow values were used to initialize a 2D hydraulic model to generate a range of estimates of flood extent, depth, and velocity. Compositing these estimates resulted in a probabilistic product that used the statistical spread among the ensemble members as a means to communicate predicted flood risk. The results from this study demonstrate the potential to incorporate and visualize model uncertainty in flood inundation maps to identify locations at higher risk of hazardous flood conditions.

The methods and results from this study have tremendous potential to help in flood preparation and mitigation on a local scale; however, the computationally intensive nature of the hydraulic models limits the spatial applicability of these methods. For example, the current study planned to use the two-dimensional unsteady state Nays 2D Flood solver and the steady state FaSTMECH solver available in the iRIC hydraulic modeling software. This would have allowed for the quantification of uncertainty related to initial streamflow values from the NWM and the various hydraulic models. However, running the Nays 2D Flood solver at a 1 meter grid resolution would have taken 3600 hours (1-2 months). Even a 50 meter grid resolution would have taken 12-15 hours to run for our study area using the available resources. While ongoing calibrations will permit the use of these models in future local-scale analyses, there is a need for alternative approaches to these intensive hydraulic models for flood inundation mapping. This would allow for the application of this methodology beyond the local scale.

Acknowledgments

This work was conducted during the 2016 National Flood Interoperability Experiment (NFIE) Summer Institute supported by the Consortium of Universities for the Advancement of Hydrologic Science, Inc. (CUAHSI) and the Office of Water Prediction (OWP). The authors would like to thank all those involved in the coordination and execution of the very successful 2016 NFIE Summer Institute. The authors would also like to thank Dr. Jamie Dyer, Dr. Virginia Smith, and Dr. Alfonso Mejia for their extremely helpful comments and suggestions on the manuscript.

References

1. R.A. Pielke, M.W. Downton, Precipitation and Damaging Floods: Trends in the United States, 1932–97. *Journal of Climate* 13 (2000) 3625-3637.
2. Team, N. I. S. (2015). Hydrologic Information Center - Flood Loss Data. Retrieved from <http://www.nws.noaa.gov/hic/>?
3. V. Merwade, F. Olivera, M. Arabi, S. Edleman, Uncertainty in Flood Inundation Mapping: Current Issues and Future Directions. *Journal of Hydrologic Engineering* 13 (2008) 608-620.
4. S. Grimaldi, A. Petroselli, E. Arcangeletti, F. Nardi, Flood mapping in ungauged basins using fully continuous hydrologic-hydraulic modeling. *J. Hydrol.* 487 (2013) 39–47.
5. M.S. Horritt, Parameterisation, validation and uncertainty analysis of CFD models of fluvial and flood hydraulics in the natural environment. Computational fluid dynamics: applications in environmental hydraulics (2005) 193-213.
6. N.M. Hunter, P.D. Bates, M.S. Horritt, A.P.J. De Roo, M.G.F. Werner, Utility of different data types for calibrating flood inundation models within a GLUE framework. *Hydrol. Earth Syst. Sc.* 9 (2005) 412-430.
7. A.P. Nicholas, Roughness parameterization in CFD modelling of gravel-bed rivers, John Wiley and Sons: Chichester, 2005.
8. K. Marks, P. Bates, Integration of high-resolution topographic data with floodplain flow models. *Hydrological Processes* 14 (2000) 2109-2122.
9. M.G.F. Werner, Impact of grid size in GIS based flood extent mapping using a 1D flow model. Physics and Chemistry of the Earth, Part B: Hydrology, *Oceans and Atmosphere* 26 (2001) 517-522.
10. F. Pappenberger, P. Matgen, K.J. Beven, J.-B. Henry, L. Pfister, P. Fraipont, Influence of uncertain boundary conditions and model structure on flood inundation predictions. *Adv. Water Resour.* 29 (2006) 1430-1449.
11. F. Pappenberger, et al., Cascading model uncertainty from medium range weather forecasts (10 days) through a rainfall-runoff model to flood inundation predictions within the European Flood Forecasting System (EFFS). *Hydrol. Earth Syst. Sc.* 9 (2005) 381-393.
12. S.K. Regonda, D.-J. Seo, B. Lawrence, J.D. Brown, J. Demargne, Short-term ensemble streamflow forecasting using operationally-produced single-valued streamflow forecasts – A Hydrologic Model Output Statistics (HMOS) approach. *Journal of Hydrology* 497 (2013) 80-96.
13. S.N. Jonkman, E. Penning-Rowsell, Human Instability in Flood Flows. *J. Am. Water Resour. Assoc.*, 44 (2008) 1208–1218.

Assimilation of water level observations in river models to update flood inundation maps

Amir Javaheri ¹ and Mohammad Nabatian ²

¹ Oregon State University; javaheam@oregonstate.edu

² The University of Texas at Arlington; mohammad.nabatian@mavs.uta.edu

Academic Advisors: Meghna Babbar-Sebens, Oregon State University, meghna@oregonstate.edu;

Dong-Jun Seo, The University of Texas at Arlington, djseo@uta.edu

Summer Institute Theme Advisors: Ibrahim Demir, University of Iowa, ibrahim-demir@uiowa.edu

Abstract: This study proposes a framework that (i) uses data assimilation methods as a post processing technique to update water depth in order to generate more accurate flood inundation maps, and (ii) updates the flows generated by National Water Model (NWM). Predicted flows by NWM for each stream were converted to the water depth using the Height Above the Nearest Drainage (HAND) method. Then, the water level measurements provided by Iowa Flood Inundation System (IFIS) were converted to water depths and then they were assimilated into the model in order to update the water depths. After assimilation of water depth measurements, the updated depths were converted to the river flows using rating curves generated by HAND model. These updated flows can be used as new initial condition for running National Water Model. Ensemble Kalman Filter (EnKF) was used as assimilation technique. This method is easy to implement and computational requirements are affordable. Results showed that after assimilation of water depth for a flood event during 2015, normalized root mean square error was reduced by 0.50 m for training tributaries. Comparing the updated results with observations of testing locations showed that proposed methodology is also effective on the tributaries with no observation. The overall error was reduce from 0.89 to 0.44 m for testing tributaries.

1. Motivation

Flooding is one of the most destructive natural disasters in the United States. Flood inundation maps can be used to provide reliable information to the public about the flood-risk. Assimilation of water depth measurements, as a post-processing technique, can help to reduce the error between model predictions and observations in order to generate more reliable flood inundation maps. Moreover, the improved water depths can be converted to the corresponding flows using rating curves generated by hand in order to update the initial conditions of National Water Model (NWM).

2. Objectives and Scope

The main objectives of this study include:

- Assimilate water depth measurements to update the model predictions in order to create more accurate flood inundation maps.
- Use updated water depth to improve the flows predicted by NWM and run the NWM using updated initial conditions. However, due to computational limits, this part is not done in this study.

3. Previous Studies

Sequential data assimilation techniques can be used for updating of model's state variables when new observations become available [1]. A data assimilation process is also able to reduce the uncertainty in prediction by integrating real-time observations from a variety of monitoring technologies [2]. Kalman filter [3] is a commonly used data assimilation technique that was initially developed to update the state variables of linear systems [4]. However, this method has been used for nonlinear problems as well [5]. Ensemble Kalman filter (EnKF) is another data assimilation technique that was introduced by Evensen [6] (<http://www.sciencedirect.com/science/article/pii/S0309170816300768>). In case of non-linear models that assumption of linearity cannot be used, EnKF can be used as an effective technique. Multiple studies have also used this method in the past to update hydraulic, hydrologic and hydrodynamic models [7, 8].

4. Methodology

4.1. Study area

Squaw Creek watershed located in the middle of Iowa State was selected as study area (Figure 1). There are 85 tributaries and 20 bridge sensors that measure the water levels. Since the cross sections were not available for all of these sensor locations, measurements of only 10 sensors were assimilated into the model. Six sensors were randomly selected for training and the other four sensors were selected for testing to make sure that this approach is also suitable for tributaries with no observation. NWM predicts the flow at the outlet of each sub-basin, however, bridge sensors are located upstream of outlets. Assuming the equal soil type and land use for each sub-basin, flow at the outlet was linearly distributed along the river.

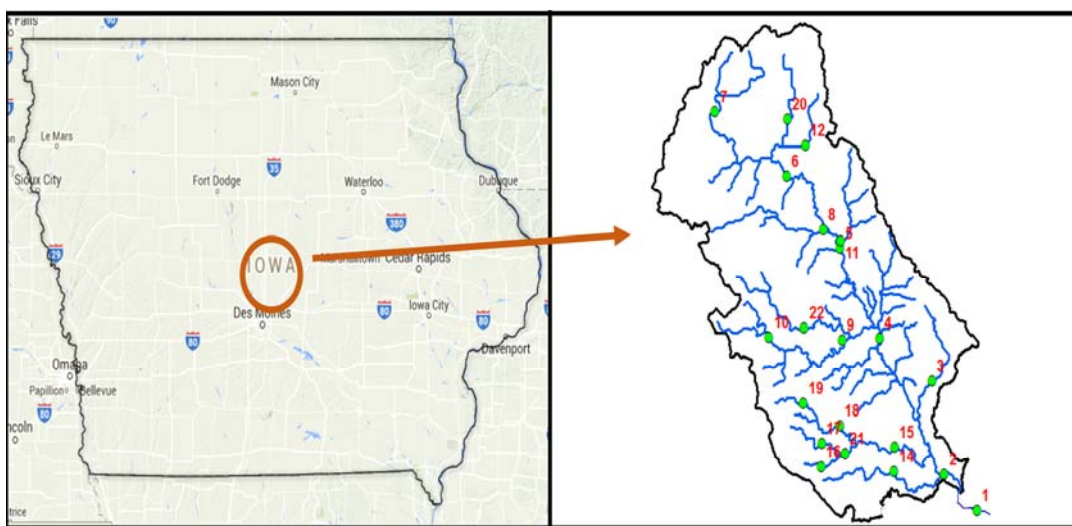


Figure 1. Squaw Creek watershed. Blue lines show tributaries and green dots show locations of bridge sensors.

4.2. Proposed approach

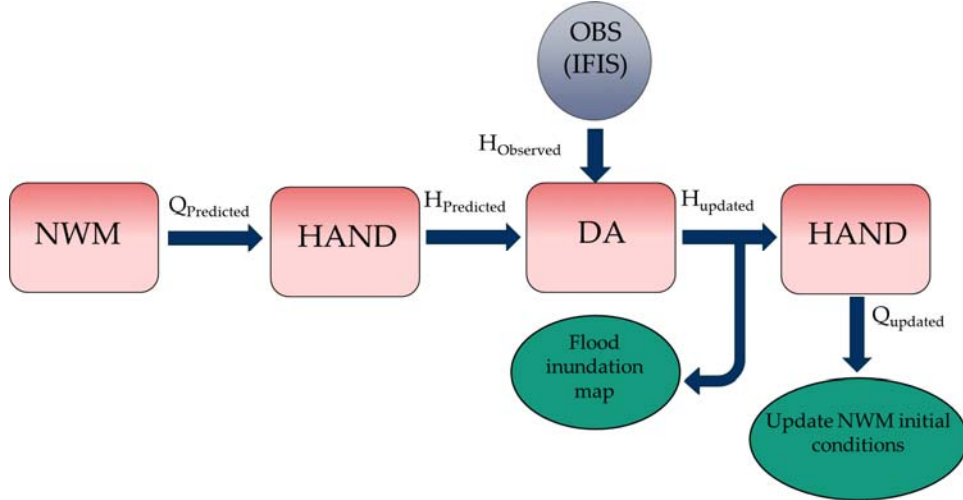


Figure 2. Schematic methodology.

Figure 2 illustrates the proposed methodology. Flow for each tributary was estimated by NWM. HAND [9] method was used to predict the water depth. Water level observations from Iowa Flood Information System (IFIS) were converted to water depth and then they were assimilated into the model. Updated water depth can be used to create the flood inundation maps. Also rating curves generated by HAND can be used to estimate the flow and updated flows can be used as new initials conditions to run the National Water Model.

4.3. Ensemble Kalman Filter

The ensemble Kalman filter algorithm was used in the proposed methodology to assimilate water depth observations into the model. In the ensemble Kalman Filter, the prediction model is represented using:

$$h_k = F(Q) + w_k \quad (1)$$

where h denotes the vector of state variables (water depth), Q is the flows from National Water Model, w_k is stationary zero-mean white noises, F represents the prediction model (HAND model), and the subscript “ k ” denotes the time step. If an ensemble of n predicted state variables is available, h^f can be written as

$$h^f = (h^{f1}, \dots, h^{fn}) \quad (2)$$

where superscript “ f ” represent the i^{th} forecast ensemble member. In order to create the ensembles, different flows at different times before the selected events were selected and then converted to water depth using rating curves generated by HAND. For this study, 10 ensembles were created to estimate the error matrix in the model.

The average of ensemble is defined by

$$\hat{h}^f = (1/n) \sum h^{fi} \quad (3)$$

Since true states are not known, we estimate them using the average of realizations in the ensemble. Then the error matrix can be estimated by

$$P^f = 1/(n-1) \{ (h^f - \hat{h}^f)(h^f - \hat{h}^f)^T \} \quad (4)$$

The error matrix is then used to calculate the Kalman gain matrix by

$$K_k = P_k^f H_k^T (H_k P_k^f H_k^T - R_k)^{-1} \quad (5)$$

where H is the linear transformation which relates the state variables to observations. The updated state vector (h^a) is taken to be a linear combination of the forecast and the observations. The observations should be treated as random variables to get consistent error propagation in the ensemble Kalman filter [10]. Hence, the actual measurements were used as reference and random noise with zero mean and covariance R was added to measurements. The updating equation is given by:

$$h^{a*} = h_k^f + K_k(h_k^* - H_k h_k^f) \quad (6)$$

5. Results

Figure 3 shows the water depth at training locations a) before data assimilation and b) after data assimilation comparing with observations from IFIS. We found that by assimilating water depth, the overall error was reduced from 98 cm to 48 cm. We also calculated the error for the testing locations to make sure that Kalman Filter can improve the model predictions for the sites that there is no observations. It was found that the overall error was reduced for testing locations as well (from 89 to 44 cm). Table 1 compares the water depths before and after data assimilation with observations from IFIS for training and testing tributaries. Results show that overall error was reduced by 48 cm.

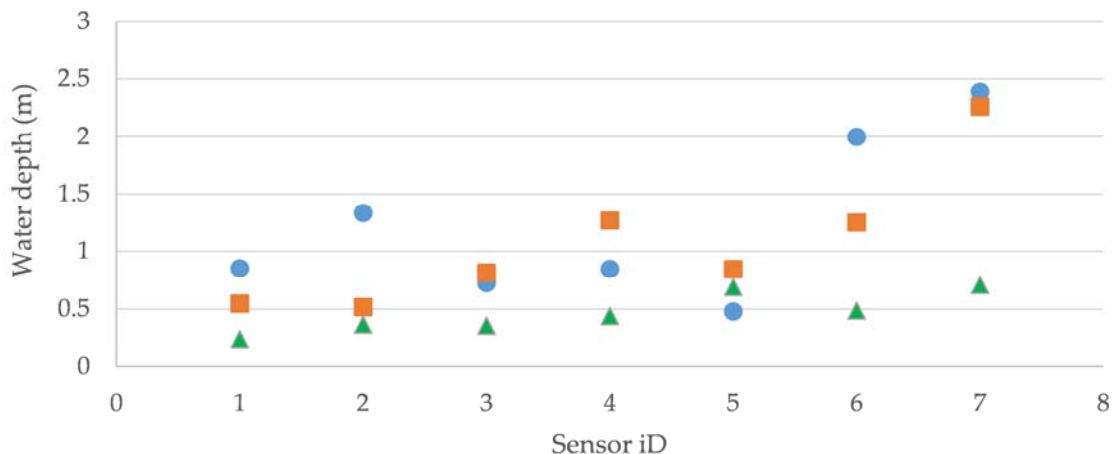


Figure 3. Water depth at each sensor location. Green triangles are model predictions from HAND before data assimilation, red squares are updated water depths after data assimilation, and blue dots are water depth observations from IFIS.

Table 1. Water depth before and after data assimilation comparing with water depth measurement from ISIF for training and testing tributaries

	Water depth (m)		
	Observation	Before Data assimilation	After Data Assimilation
Training tributaries	0.85	0.24	0.55
	1.34	0.37	0.52
	0.72	0.36	0.81
	0.85	0.44	1.27
	0.48	0.69	0.84

	2.00	0.49	1.25
	2.39	0.71	2.26
Testing tributaries	1.30	2.01	1.67
	0.32	1.01	0.71
	1.50	0.30	0.81
	1.86	1.01	1.99
Overall error (m)		0.95	0.47

Figure 4 illustrates the time series of flow predicted by NWM versus flow observation at USGS station at Squaw Creek at Ames. After updating water depth, rating curve from USGS station was used to estimate the corresponding flow. Because of time limitation, only for different time during June 24, 2016 were selected to assimilate the water depth and then update the flow (green dots in Figure 4). It was found that overall error between USGS measurements and updated flows from NWM was reduced by about 35% for selected times. It is recommended to assimilate all the available observation when they are collected, then update the water depth and create more accurate flood inundation maps. Afterward, use updated water depth to also update the flow from NWM and use corrected flows as new initial conditions for running NWM.

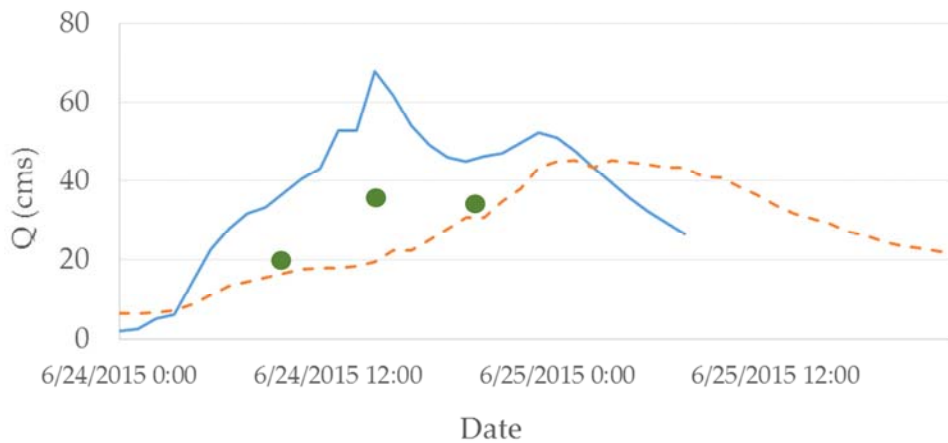


Figure 4. River flow at USGS station at Squaw Creek at Ames. Solid blue line shows the NWM predictions, dashed-red line shows the observations at USGS station, and green dots show the updated flows.

6. Conclusion

National Water Model prepares water depth for 85 tributaries in the study area, as all models have uncertainty, it seems reasonable to implement data assimilation model in order to reduce the uncertainty. After assimilation of water depth measurements, the root mean square errors of the estimated depth reduced by 50 cm. It was found that the proposed methodology is also effective for the tributaries without observation. The error was reduced by 45 cm for tributaries that their observations were not assimilated in to the model. In the next step, the updated water depths can be used to calculate the flows using rating curves and then use them in National Water Model which would be a future study.

More accurate observations are required in order to minimize the error. It is recommended to collect cross sections at the locations that bridge sensors are placed. It helps to convert water level to water depth more accurately.

References

1. Evensen, G. *Data Assimilation*. Springer, New York, USA, 2007, p. 279.
2. Moradkhani, H. Hydrologic remote sensing and land surface data assimilation. *Sensors*, 2008, 8 (5), 2986–3004.
3. Kalman, R. New approach to linear filtering and prediction problems. *Trans. AMSE J. Basin Eng.*, 1960, 82D, 35–45.
4. Maybeck, P.S. *Stochastic models, estimation, and control*; Academic Press, New York, USA, 1982, volume 3.
5. Krener, A.J.; Duarte, A. A Hybrid Computational Approach to Nonlinear Estimation. *Proceedings of Conference on Decision and Control*, Kobe, Japan, 2004, pp. 1815–1819.
6. Evensen, G. Sequential data assimilation with a nonlinear quasi-geostrophic model using Monte Carlo methods to forecast error statistics. *J. Geophys. Res. Oceans.*, 1994, 99 (C5), 10143–10162.
7. Crow, W.T.; Wood, E.F. The assimilation of remotely sensed soil brightness temperature imagery into a land surface model using ensemble Kalman filtering: A case study based on ESTAR measurements during SGP97. *Adv. Water Resourc.*, 2003, 26 (2) , 137–149.
8. Miller, R.N.; Cane M.A. A Kalman filter analysis of sea level height in the tropical Pacific. *J. Phys. Oceanography*, 1989, 19, 773–790.
9. Liu, Y. Y.; Maidment, D. R.; Tarboton, D. G.; Zheng, X.; Yildirim, A.; Sazib, N. S.; Wang, S. A CyberGIS approach to generate high-resolution Height Above Nearest Drainage (HAND) raster for national flood mapping. *CyberGIS Center Technical Report*, 2016.
10. Burgers, G.; Jan van Leeuwen, P.; Evensen, G. Analysis scheme in the ensemble Kalman filter. *Mon. Weather Rev.*, 1998, 126 (6), 1719–1724.

Real Time Postprocessor towards Improving Flood Inundation Mapping

Sanjib Sharma¹ and Bingqing Lu²

¹ The Pennsylvania State University, University Park, PA 16802 ; sanjibsharma66@gmail.com

² The University of Alabama, Tuscaloosa, AL 35487; blu5@crimson.ua.edu

Academic Advisors: Alfonso Mejia, The Pennsylvania State University, amejia@engr.psu.edu; Yong Zhang, The University of Alabama, yzhang264@ua.edu

Summer Institute Theme Advisors: Alfonso Mejia, The Pennsylvania State University, amejia@engr.psu.edu; Ibrahim Demir, The University of Iowa, ibrahim-demir@uiowa.edu

Abstract: The objective of this study is to evaluate the potential for real time post-processing of flood inundation maps. In order to support and facilitate the effective communication of flood forecasts and flood risk, we implement a statistical model to produce unbiased, reliable and skillful flow-stage output from the National Water Model (NWM). For the statistical model, we evaluate a first-order auto regressive (AR1) model to encourage efficient processing times. Post-processed streamflow-stage outputs were verified against stage observations from USGS and bridge sensor operated by the Iowa Flood Center as a case study. For the case study, we select the main stream of the Shell Rock River at Iowa. We selected the Shell Rock River because it contains a densified network of stage-flow observations, and it has historical records for severe flooding. We compare three main results, each comprised by a characteristic flood inundation map generated by using Height Above Nearest Drainage (HAND) method. The first map displays NWM simulation result, while the second map displays the observations from bridge sensor. A third map shows the post-processed results. Overall, the post-processed map shows improved capabilities in matching the observed map.

1. Motivation

Accurate geospatial information about flood extent is essential for effective communication of flood forecast and to assess the risk related to floods [1]. For these reasons, flood maps have been widely used in practice to assess the potential risk of floods. However, the shortcomings associated with meteorological forcing variables, topographical representation, structural parameters of the hydrologic model, flow information and inundation mapping techniques lead to uncertainties in flood inundation maps [2]. It is essential to understand and account these uncertainties to produce reliable and accurate streamflow information, which facilitate to produce accurate flood maps.

With the recent development in quantifying the meteorological and hydrologic uncertainties, the greatest issue still is to develop an effective way of communicating the meaning and values of the hydrologic and hydraulic model output. In streamflow forecasting system, the general trend is to display the streamflow information in the form of hydrographs, which are sometimes very confusing and often add difficulties in interpreting the information. Study has rarely focused toward improving the ability to communicate what will happen during a flood event. In order to translate flood forecasts into an easy-to-use format, it is necessary to make a shift from the verification of hydrographs to flood inundation maps.

2. Objectives and Scope

In this study, our primary goal was to assess and verify the potential of real time post-processing of flood inundation maps. We employed a statistical model to produce unbiased, reliable and skillful

simulation product from the National Water Model (NWM). For the statistical model, we first evaluated a first-order auto regressive (AR1) model to enable efficient processing times. We used the observations from USGS gauge and bridge sensors for training the postprocessor and verifying the raw and post-processed NWM stage simulation. Finally, we used the Height Above Nearest Drainage (HAND) method to display a characteristic flood inundation map. The ultimate goal here was to encourage a shift from the verification of forecast hydrographs to flood maps, which are a more appealing display for purposes of general communication.

3. Previous Studies

Bias in meteorological forcing variables propagate through the hydrologic forecasting model and lead to uncertainties about streamflow forecast. In order to correct systematic forecast biases in forcing variables, several preprocessing techniques (e.g., extended logistic regression, heteroscedastic extended logistic regression, Bayesian model averaging, and quantile regression) are frequently applied. However, preprocessor cannot account the uncertainties arising from the model parameterizations together with the uncertainties in structure. Therefore, post-processing techniques (see e.g., general linear model [4], auto-regressive model [5], and Bayesian postprocessor [6]) are applied aimed at accounting these additional uncertainties.

The majority of studies has been focused on producing accurate and reliable streamflow forecast. But very few studies have been carried out to examine the best way of communicating the hydrologic model output. Especially in streamflow forecasting, there is a necessity to make a shift from the verification of forecast hydrograph to flood map with effective visualization technique. A promising work has been done in Iowa Flood Center (IFC) to develop a user friendly and interactive web platform, which provides flood conditions, flood forecasts, and data visualizations applications for over 1000 communities in Iowa. Similar example is from the Federal Emergency Management Agency's (FEMA) flood hazard mapping program, which provide flood hazard maps to guide policy makers and community to mitigation actions.

4. Methodology

For implementing the postprocessor, we used simulation output from NWM. Simulated stage was obtained by transforming discharge to stage, for the selected station, by using the rating curve. We applied the statistical post-processing technique to the transformed stage, aimed at correcting the bias in stage simulation result. The quality of the post-processed stage was then verified against the corresponding observation from bridge sensor and USGS gauges. Finally, three different flood inundation maps were compared to display the raw, post-processed and observed flood extent. The schematic of the overall process is shown in Figure 1.

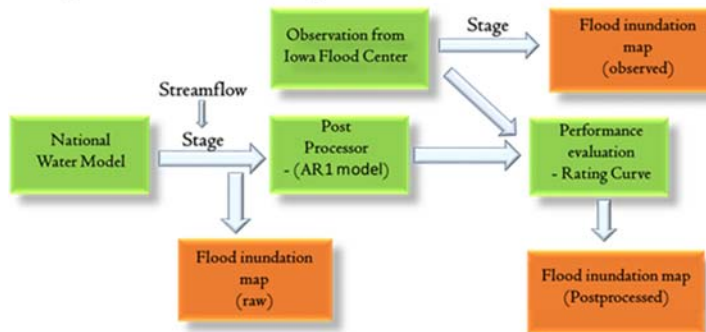


Figure 1. Framework for verification of flood inundation maps.

4.1. Study area

We used the Shell Rock River at Iowa as a case study. The geographic location and main stream of the Shell Rock River is illustrated in Figure 2. We selected the Shell Rock River because i) it contains a densified network of stage-flow observations, and ii) it has historical records for severe flooding. This study focus in the downstream reaches of the Shell Rock River, which contains 2 USGS gauge stations (Stations 1 and 5) and 3 bridge sensors (Stations 2, 3 and 4) (Figure 2). NWM assign a unique identifier, or COMID, for each reach catchment and the flowline corresponding to these observation stations. The area of the reach catchment, for the selected 5 stations, varies from 1.5 sq. miles to 3 sq. miles. The NWM computes the flow in all these reaches, considering the flow within that catchment.

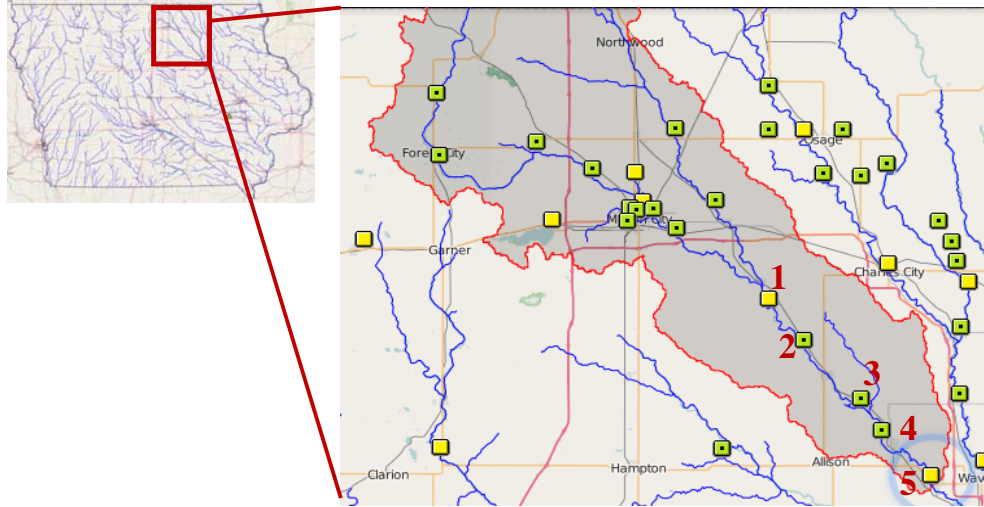


Figure 2. Case study area: Shell Rock River, Iowa.

4.2. Data

In order to evaluate the potential of postprocessor, we used retrospective and real-time NWM hourly test simulations output for year 2015. National Water Center (NWC) is the lead organization that in charge of developing the NWM in collaboration with the National Centers for Environmental Predictions (NCEP) and the National Center for Atmospheric Research (NCAR). Raw and post-processed stage was verified using the observations from USGS gauges and IFC bridge sensors. USGS gauges provides continuous record of stage. IFC operates the densified network of bridge sensors, which make river stage measurements every 15 minutes. These measurements are available to the general public in real-time via the IFC flood information system (IFIS).

4.3. Post-processing technique

In order to produce a reliable and accurate NWM streamflow simulation, we applied the first order autoregressive model (AR1) [5] with prior observation and NWM simulation stage output as predictors. The selection of the AR1 model was motivated by the i) effectiveness of the parsimonious model, ii) limited amount of historical data, and iii) efficient processing time. In order to remove bias in the model output, the sum of regression coefficient was constrained to one. Further, computation was facilitated through the Markovian assumption, implying that the stage at one step ahead in the normal space is dependent on the stage at current time step and independent of stage at the preceding time steps. This can be represented as

$$Y_{0,t+1} = (1 - a_{t+1}) Y_{0,t} + a_{t+1} Y_{s,t+1} + E_{t+1}, \quad (1)$$

where $Y_{0,t+1}, Y_{0,t}$ denote the Normal Quantile Transformed (NQT) observation at time step $t+1$ and t , respectively; a denotes the regression coefficient; $Y_{s,t+1}$ denotes the NQT stage simulation at time step $t+1$; E_{t+1} is the residual error term given by

$$E_{t+1} = \frac{\sigma_{E_{t+1}}}{\sigma_{E_t}} \rho(E_{t+1}, E_t) E_t + W_{t+1}; \quad (2)$$

$\sigma_{E_{t+1}}$ and σ_{E_t} denotes the standard deviation of the error terms; $\rho(E_{t+1}, E_t)$ denotes the serial

correlation between the error terms; and W_{t+1} denotes the white noise defined as

$$\sigma^2 W_{t+1} = (1 - \rho^2(E_{t+1}, E_t)) \sigma^2 E_{t+1}. \quad (3)$$

Using the NQT-transformed observation and NWM simulation stage output, we estimated b_{t+1} following the parameter estimation procedure proposed in [3].

iv) HAND method

We used the Height Above the Nearest Drainage (HAND) [7], a digital elevation model (DEM) normalized using the nearest drainage for mapping reach scale flood inundation and for determining reach scale hydraulic properties. Along with the DEM, the national hydrography datasets plus (NHDPlus) streams provide the information needed to generate the height of each grid cell above the nearest drainage. Selection of the HAND method was motivated by its efficient reach scale computation time.

5. Results

5.1. Rating Curve

To investigate the potential of the postprocessor in improving the flood maps, this study focused on the particular flood event of 2015-06-23 for 24-hour duration, which has the highest flow record (6000 cfs, USGS 05460400 Shell Rock River near Rockford) in year 2015. Figure 3 shows the stage versus time plot for raw stage from NWM simulation (COMID- 6561261), observed stage from bridge sensor (Station Id-SHLRK02) and post processed stage. The difference in stage provided by the bridge sensor and NWM is ~ 3 ft. With the implementation of postprocessor, this difference limits to less than 0.5 ft. Further, the post-processed stage follows the trend of the observation and matches well for the high flows.

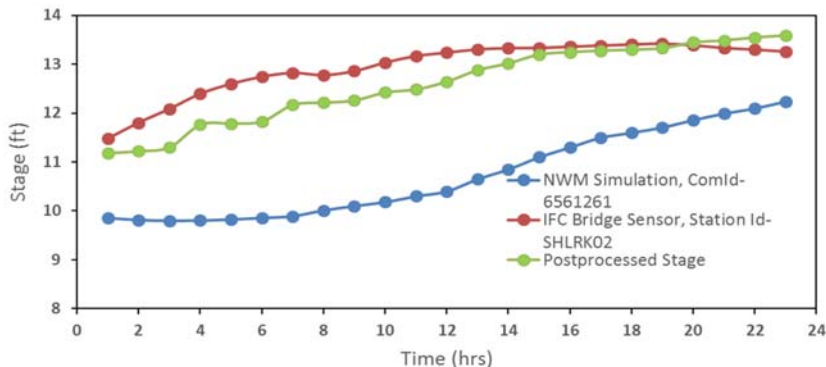


Figure 3. Stage from NWM simulation, post processed stage and observation from bridge sensor for a flood event of June 23, 2015.

In Figure 4, we have compared the raw rating curve for NWM simulation with the rating curve from USGS data. Rating curve from USGS is for the location: USGS 05462000 Shell Rock River at Shell Rock, Iowa, and corresponding COMID from NWM is 6561217. We have noticed that the raw rating

curve is significantly different than the rating curve provided by the USGS. It is necessary to have an accurate rating curve to produce an accurate flood maps. In order to produce an accurate rating curve, we applied the postprocessor to the NWM discharge simulation output. Post-processed stage and discharge are plotted in Figure 4, and called as post-processed rating curve. Overall, the post-processed rating curve match well with the USGS rating curve, and further fits well for the high flows.

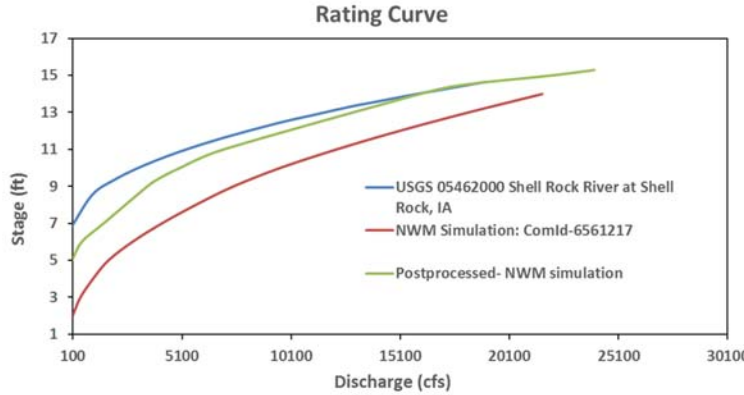


Figure 4. Raw and post-processed rating curve comparison for Shell Rock River at Shell Rock, IA.

5.2. Postprocessor performance evaluation

We used the correlation coefficient and root mean square error (RMSE) as the measure of raw and post processed stage quality. We have compared in Figure 1, for five stations being considered, the correlation coefficient (Figure 4a) and RMSE (Figure 4b) for both raw and post-processed flood stage. The stage result is then compared with the corresponding observed data from IFC operated bridge sensor. The overall trend in Figure 1 is for the correlation coefficient to increase and RMSE to decrease with the application of postprocessor to the NWM simulated stage output.

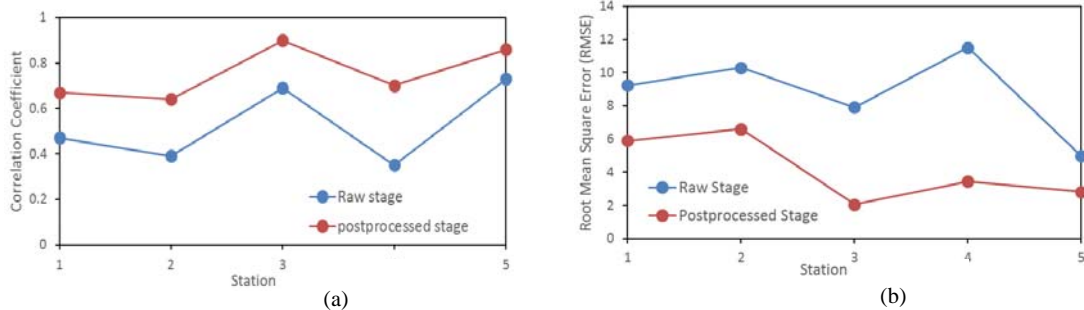


Figure 5. (a) Correlation coefficient and (b) RMSE for the raw and post-processed stage corresponding to the observation from bridge sensor and USGS station.

5.3. Inundation maps

The inundation maps developed using the HAND method is shown in Figure 6 for a reach catchment with COMID- 6561261. Figure 5a-c display the flood extent at 2015-06-23 12:00, respectively, for NWM simulation stage, bridge sensor stage observation, and post-processed stage. Figure 6d-f display the similar information at 2015-06-23 18:00. We have developed the similar plots for different reach catchment for different time. On considering all the five reach catchment, it is noticeable that the raw inundation maps vary up-to 19% in underestimating the inundation area as compared to the observed map. Overall, the post-processed maps show improved capabilities in matching the observed map.

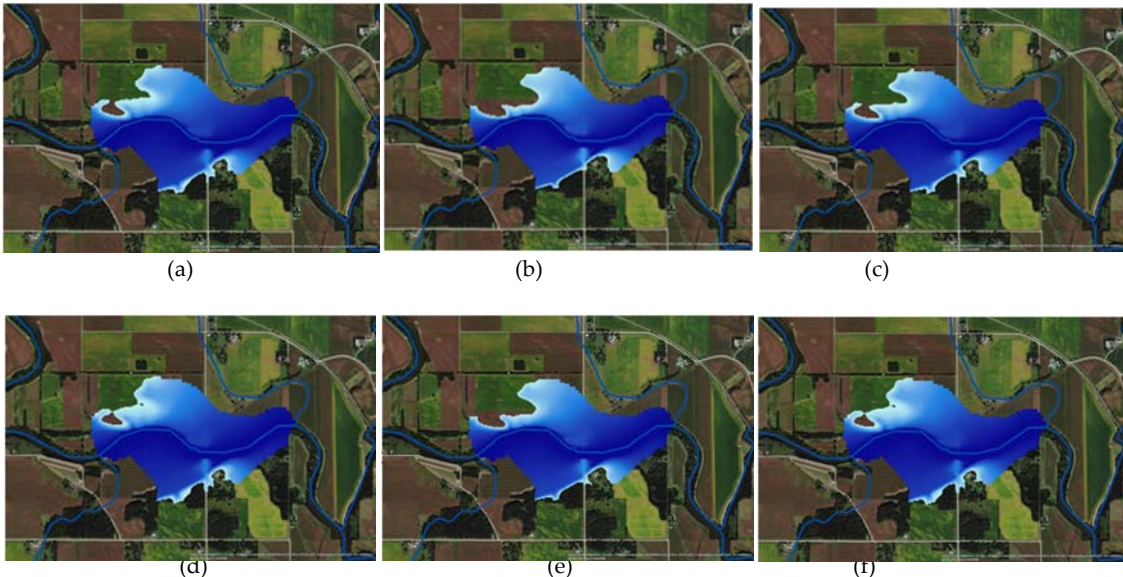


Figure 6. Raw, observed and post-processed map for a reach catchment (ComId- 6561261) for a flood event of 2015-06-12.

6. Conclusion

The ultimate goal of this study was to encourage a shift from the verification of forecast hydrographs to flood maps, which are more workable for purposes of general communication. We implement a statistical model to produce unbiased, reliable and skillful stage output from the NWM. In summary, based on our analysis and comparison, post-processed flood stage shows higher correlation coefficient and lower root mean square error as compared to raw stage. Overall, post-processed map shows improved capabilities in matching observed map. Also, post-processed rating curve matches well with that of USGS.

Accurate streamflow information is the pre-requisite to produce improved flood hazard and risk map. Further assessment of rating curve is fundamental in making effective flood management decision. The benefit of using the post-processed streamflow and post-processed rating curve is that the accurate streamflow transformed to stage using the accurate rating curve will lead to an accurate flood map. Further study should be done considering a larger study area. However, this may come at a considerable computational cost, particularly when considering a range of lead times and multiyear simulation or forecast datasets.

References

1. Jung, Y., et al. (2014). Simplified flood inundation mapping based on flood elevation-discharge rating curves using satellite images in gauged watersheds. *Water*, 6(5), 1280-1299.
2. Merwade, V., Olivera, F., Arabi, M., & Edleman, S. (2008). Uncertainty in flood inundation mapping: current issues and future directions. *Journal of Hydrologic Engineering*, 13(7), 608-620.
3. Zhao L, Duan Q, Schaake J, Ye A, Xia J. 2011. A hydrologic post-processor for ensemble streamflow predictions. *Advances in Geosciences*, 29: 51-59.
4. Regonda, S. K., Seo, D. J., Lawrence, B., Brown, J. D., & Demargne, J. (2013). Short-term ensemble streamflow forecasting using operationally-produced single-valued streamflow forecasts—A Hydrologic Model Output Statistics (HMOS) approach. *Journal of Hydrology*, 497, 80-96.
5. Reggiani P, Renner M, Weerts A, Van Gelder P. (2009). Uncertainty assessment via Bayesian revision of ensemble streamflow predictions in the operational river Rhine forecasting system. *Water Resour. Res.*, 45.
6. Liu, Y., D.R. Maidment, D.G. Tarboton, X. Zheng, A. Yildirim, N.S. Sazib, S. Wang (2016). A CyberGIS Approach to Generating High-resolution Height Above Nearest Drainage (HAND) Raster for National Flood Mapping. CyberGIS Center Technical Report. CYBERGIS-TR-2016-005-i.

Chapter 4

Emergency Response

HAND Flood Mapping through the Tethys Platform

Savannah Keane ¹, Christian Kesler ² and Xing Zheng ³

¹ Brigham Young University; savk22@gmail.com

² Brigham Young University; cpkesler@byu.edu

³ University of Texas at Austin; zhengxing@utexas.edu

Academic Advisors: Jim Nelson, Brigham Young University, jimn@byu.edu; David Maidment, University of Texas at Austin, maidment@utexas.edu

Summer Institute Theme Advisor: David Maidment, University of Texas at Austin, maidment@utexas.edu

Abstract: The Height Above Nearest Drainage (HAND) model is a method for generating flood inundation maps. Currently, HAND is calculated with a 10 meter digital elevation model (DEM) in ArcMap. The purpose of the project is to create an online application to easily view the flood maps generated from HAND. The online application is run through Tethys, which is a platform created by Brigham Young University (BYU). The online app uses streamflow forecasts generated by the National Water Model (NWM) to predict potential flooding.

1. Motivation

The flood maps are important tools for emergency preparedness and first responders. Being able to properly show where a flood could occur has the potential to keep people safe from hazards. By creating an online flood mapping application, anyone could go on and see the potential harm that their home could be under. It would be as simple as checking the weather forecast in an area. A flood map program could help better inform the public such that necessary precautions could be taken. It would supply better understanding and knowledge to first responders and the citizens in danger.

2. Objectives and Scope

The HAND model takes a DEM and a user defined height to generate a flood map. There are three parts to this project:

- 1) Create preprocessing tools to generate inundation maps from the HAND raster.
- 2) Create an online Tethys application that shows possible flood areas with potential homes threatened and use the NWM streamflow forecast to predict floods.
- 3) Create an online Tethys application that focuses on specified areas to create flood maps for each stream reach in the NHDPlus stream network based on real-time NWM data predictions

3. Previous Studies

Recently, several models have been developed and implemented for high-resolution, large-scale, real-time inundation mapping, including the two-dimensional physical model (LISFLOOD-FP) [1], the one-dimensional physical model (AutoRoute) [2], and the GIS-based non-physical model (NHD-HAND) [3, 4]. However, no convenient inundation user interface has been developed for a large area and provided to the emergency response community to guide their preplanning and response activities before and during flood events. In this study, the NHD-HAND method is chosen among several methods mentioned above because of its simplicity and effectiveness. Xing et. al. (in preparation for publication) have performed a real-time inundation mapping case study for Travis County, Texas during the Memorial Flood in May, 2015. From this study, a framework has been

designed for inundation mapping with the NHD-HAND method. Following that framework, two web applications will be designed using the Tethys platform.

Tethys is a platform that can be used to develop and host water resources web applications or web apps. It includes a suite of free and open source software (FOSS) that has been carefully selected to address the unique development needs of water resources web apps. Tethys web apps are developed using a Python software development kit (SDK), which includes programmatic links to each software component. The Django Python web framework powers the Tethys Platform. This gives it a solid web foundation with excellent security and performance.

4. Methodology

4.1 Preprocessing Tools Workflow

In order to increase the real-time responding speed of the Tethys web apps, two geoprocessing tools have been developed during this project to provide preprocessed inundation results hosted on the Tethys server. This first tool is designed to create an inundation library for each NHDPlus reach in the study area. Given a minimum stage height, a maximum stage height and an increment, a water depth raster is generated from the HAND raster for each incremental stage height within the predefined water level range. All the water depth rasters for the same reach make up a floodplain library named by the COMID of that reach. The second tool is designed to transform the National Water Model short-term and medium-term forecast discharge into real-time inundation maps for each NHDPlus reach at each time step. A rating curve has been generated for each reach in the study area from the NHD-HAND-SPRNT method. By looking up the discharge-stage height pairs in the rating curve, the National Water Model forecast discharges could be transformed into forecast stage heights. Inundation maps corresponding to these stage heights are selected for different reaches, and put in the folder for the same time-step.

4.2 Tethys HAND Flood Map Applications Workflow

Two separate apps were created for visualizing flooding. The first area is centered on Tuscaloosa, AL with the second app focusing on the recent floods that killed 23 people in West Virginia. Below in Figure 1, the workflow of the app is shown.

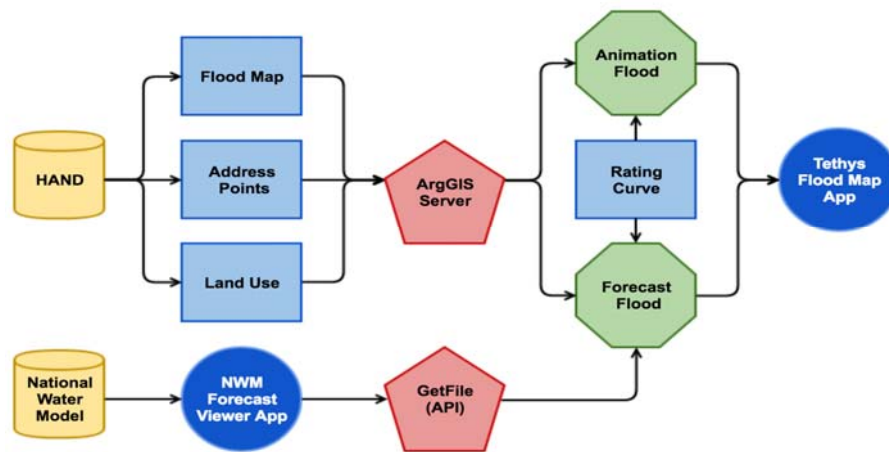


Figure 1. Tethys app workflow for generating flood maps in Tuscaloosa, AL and West Virginia.

Both the Tuscaloosa and West Virginia Tethys flood apps feature the following:

- View a flood by depth as it would potentially grow in the area
- Use the NWM data to predict flooding in the area based on a main stream reach in the area

The West Virginia app additionally has the ability to use historical NWM forecast data from the time around June 24, 2016 when the deadly floods struck this area. This shows the predicted flooding that the app would have predicted through the NWM and is an example of how the app can be used in the future.

4.3 Tethys App for Flood Mapping at Each COMID Stream Reach

This application was intended to focus on each COMID and populate a flood map for each of these reaches. A study area of Tuscaloosa was chosen to use as an example to set up the main structure of the application, which can be seen below in Figure 2.

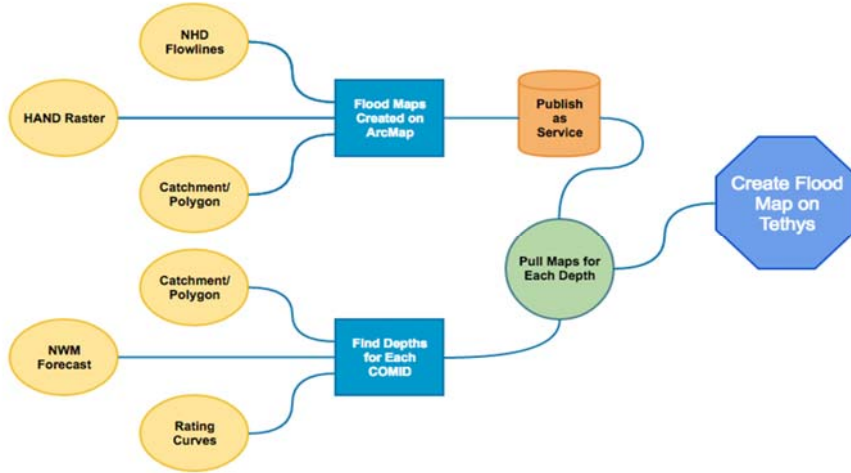


Figure 2. Workflow of creating a dynamic flood map for an area in Tuscaloosa.

In ArcMap, a library of flood maps was populated for a HUC12 watershed in Tuscaloosa. An ArcMap tool, as seen in Figure 4, was written to generate these maps at each stream reach in the selected area. This app takes requested data from the NWM and uses SPRNT rating curves to interpolate the streamflow data into depths. The app then takes those depth values and parses through the inundation library to find the correlating flood maps. Then it displays the flood maps on the app for each time step of the NWM forecast. The user can move a slider bar to step through the different time steps of the forecasted flood maps.

5. Results

5.1. ArcMap Preprocessing and Python Scripting

An ArcGIS toolbox has been developed for the Tethys-HAND project, shown below in Figure 3.

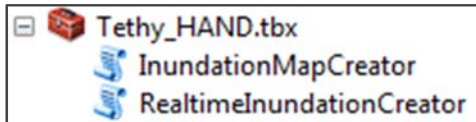


Figure 3. ArcGIS toolbox for creating a Tethys-HAND project.

For the first tool, once the inputs are set, as below in Figure 4, an inundation map library will be generated for each reach in the study area. The model allows the user to choose the desired area, the beginning depth and ending depth, and the increment steps of the flood maps.

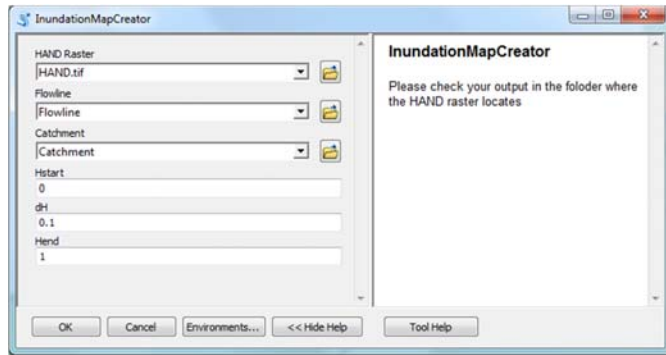


Figure 4. Inputs for the ArcGIS toolbox for creating a Tethys-HAND project.

The second tool takes a National Water Model output netCDF file from another Tethys web application named National Water Model Filesystem Explorer, in Figure 5 (https://apps.hydroshare.org/apps/nwm-data-explorer/files_explorer/).

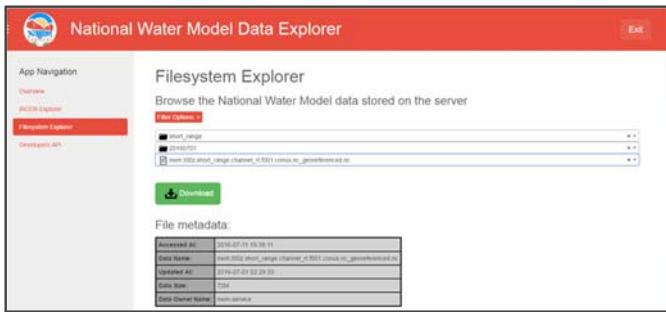


Figure 5. National Water Model Data Explorer App for retrieving netCDF files.

The real time inundation tool script has specific inputs as seen in Figure 6.

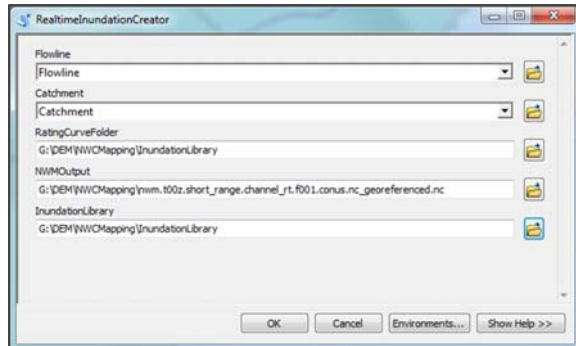


Figure 6. Inputs for real time inundation creator.

After the tool is completed, a csv table named as the forecast time-step is created with the COMID, discharge and stage height for each reach stored inside, as shown in Table 1.

Also, an inundation map folder for that time-step is created with the separate inundation map for each reach stored inside.

Table 1. Outputs of the csv file for the forecasted time step.

COMID	Discharge	StageHeight
18228791	6.24	0.31
18228803	0.92	0.21
18228847	0.92	0.23

5.2. Tethys HAND Flood Map Applications

The two Tethys apps that were created are available to view online at appsdev.hydroshare.org. The Hand Flood Map apps provide visualization of the potential flooding in the areas of Tuscaloosa County, AL and Greenbrier County, WV. Below in Figure 7 are shown the different parts of the app interface. The user interface is divided in five parts:

- 1) Toggle the layers to display the flood map, developed areas, and address points (address points only for Tuscaloosa County)
- 2) Click the “View Flood Animation” button to manually view a flood as it progresses with depth
- 3) Choose a forecast range, date, and time, then click “View Flood Forecast” to view the flood prediction by referencing the NWM
- 4) Slide the “Forecast Slider” bar to change time or depth
- 5) View the flood map

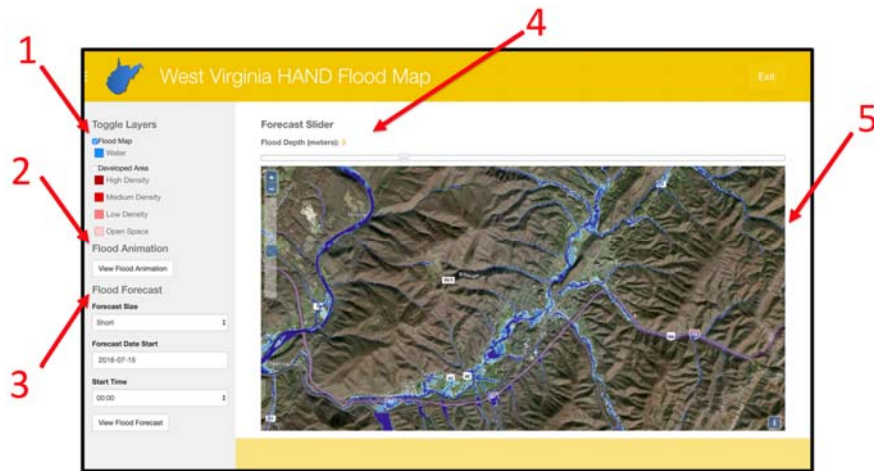


Figure 7. Components of the Tethys West Virginia HAND Flood Map.

5.3. App Development

This app is available to view online at appsdev.hydroshare.org. It provides visualization of potential flooding that is predicted by the NWM. The web app interface is shown in Figure 8. It has been successfully completed for a HUC12 watershed study area in Tuscaloosa. The watershed contains 48 COMIDs. The Inundation Map Creator tool, found in Figure 4, was successfully used on the watershed to populate a flood map library. For the study area, flood maps were created from 0-14.7 meters high of flooding in 0.3 meter increments. These flood maps were archived inside the app for the code to parse through when data is called.

Layers were pulled in to show the study area. On the left navigation bar, a user can turn these layers on and off. For later production, these layers can be used for a user to select a watershed that they would like to analyze. The navigation bar is also where the user can select what forecast they would like to analyze. A slider bar appears above the map and the user can move through the time steps of the forecast.

This app allows a user to view a dynamic map of a potential flood that is predicted by the NWM. It analyzes by each COMID, so the maps can have improved accuracy. The app was set up using this study area but everything was coded in a way that it can easily have usability for other areas as well. The preprocessing to input a new study area involves populating a flood inundation library and generating rating curves by the SPRNT method. Further production of the app will include

setting up other pages for an admin user to upload new data for different areas. A selection tool can be added so that the user could select a watershed area or draw a polygon around the desired area.

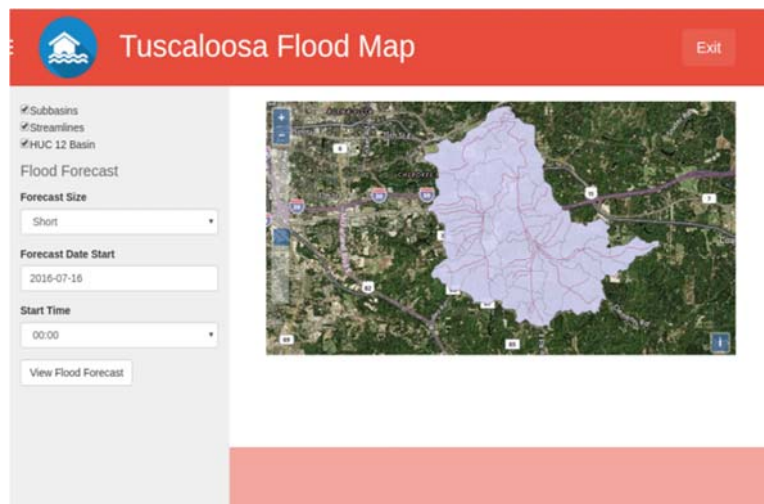


Figure 8. Tuscaloosa Study Area Web App Interface.

6. Conclusion

With the framework we established and validated in this project, we have successfully realized the transformation from the National Water Model real-time forecast discharge to real-time forecast stage height, and eventually real-time forecast inundation maps. Emergency responders get an easy access to the water information provided by the National Weather Services without any requirement for engineering and GIS backgrounds. The workflow we implement and the tools we develop during our project are applicable and portable for the same application for a larger scale.

The Tethys app structure allows easy visualization of possible floods and flood forecasts. The app is a good source for emergency preparedness personnel to prepare the first responders for flood events. Currently, there is a process to create a flood map app for a given area. In the future, a flood map app similar to this can be created to give live updates for floods anywhere in the world.

References

1. Marks, Kate, and Paul Bates. "Integration of high-resolution topographic data with floodplain flow models." *Hydrological Processes* 14.11-12 (2000): 2109-2122.
2. Follum, Michael L. *AutoRoute Rapid Flood Inundation Model*, 2013. Available online at: <http://acwc.sdp.sirsi.net/client/search/asset/1024883>
3. Nobre, A. D., et al. "Height Above the Nearest Drainage—a hydrologically relevant new terrain model." *Journal of Hydrology* 404.1 (2011): 13-29.
4. Nobre, Antonio Donato, et al. "HAND contour: a new proxy predictor of inundation extent." *Hydrological Processes* (2015).
5. Paiva, Rodrigo CD, Walter Collischonn, and Carlos EM Tucci. "Large scale hydrologic and hydrodynamic modeling using limited data and a GIS based approach." *Journal of Hydrology* 406.3 (2011): 170-181.
6. Schumann, GJ-P., et al. "A first large-scale flood inundation forecasting model." *Water Resources Research* 49.10 (2013): 6248-6257.
7. Tavakoly, Ahmad. "Hyper-Resolution Large Scale Flood Inundation Modeling: Development of AutoRAPID Model." 2015 AGU Fall Meeting. Agu, 2015.
8. Swain, Nathan R., "Tethys Platform: A Development and Hosting Platform for Water Resources Web Apps" (2015). All Theses and Dissertations. Paper 5832.
9. Christensen, Scott D., "A Comprehensive Python Toolkit for Harnessing Cloud-Based High-Throughput Computing to Support Hydrologic Modeling Workflows" (2016). All Theses and Dissertations. Paper 5667.

OPERA – Operational Platform for Emergency Response and Awareness: Reimagining Disaster Alerts

Mike Johnson ¹, Paul Ruess ² and Jim Coll ³

¹ University of California, Santa Barbara; mike.johnson@geog.ucsb.edu

² University of Texas, Austin; pjruess@utexas.edu

³ University of Kansas; jcoll@ku.edu

Academic Advisors: Keith Clarke, University of California, Santa Barbara, kcclarke@ucsb.edu; David Maidment, University of Texas at Austin, maidment@utexas.edu; Xingong Li, University of Kansas, lixi@ku.edu

Summer Institute Theme Advisors: David Maidment, University of Texas at Austin, maidment@utexas.edu

Abstract: Present-day disaster alert systems are underdeveloped in relation to modern forecasting capabilities, geospatial technologies, and telecommunications. Consequently, alerts are often spatially vague, temporally imprecise, and fail to provide actionable information, resulting in confusing warnings that are easily ignored. This research describes the integration of predictive models into an Operational Platform for Emergency Response Awareness (OPERA), colloquially known as the “Disaster Zoo”. The Disaster Zoo operates across the initial phases of a disaster event, including preparedness, warning, and response, by capitalizing on social media to promote awareness, leveraging Geographic Information System (GIS) techniques to improve spatiotemporal accuracy, and cellular Global Position Systems (GPS) technology to deliver individualized actionable alerts. Currently, the Disaster Zoo showcases alerts for floods, wildfires, and chemical spills; other disaster types may be considered in the future. This research is not intended to be a new approach to emergency response *per se*, but rather to reimagine emergency alert systems, demonstrate their improvements, and argue for their viability, and indeed, necessity.

1. Motivation

Despite dramatic improvements in numerical weather prediction, flood modeling, global interconnectedness, and flood related deaths have remained constant over the last eight decades [1]. In the United States., flooding accounts for 44% of deaths caused by natural disasters, the most of any natural hazard [2]. In 2014, NOAA reported 66% of flood related drowning when a vehicle is driven into hazardous flood water, while walking into or near flood waters accounts for 7%. In 2013, these statistics were 53% and 14%, respectively [3].

All of these indicate that the current alert systems are not effective in preventing the loss of life despite the advent of cell phones (1973), the world wide web (1990), the modern conceptions of GIS (1992) and GPS (1995) [4, 5, 6, 7]. The lack of effectiveness is a particularly large concern in the US, which has the highest number of natural disasters in the world [8].

Central to providing meaningful alerts for all hazards is to understand where the danger is/will be, where people are, and the relationship between the two. In 2000, the National Science and Technology Council’s Effective Disaster Warnings Report noted that “people at risk from disasters, whether natural or human in origin, can take actions that save lives, reduce losses, speed responses, and reduce human suffering when they receive accurate warnings in a timely manner” [9]. This implies that individual action is a valuable and underutilized means for disaster mitigation. However, the focus of emergency response over the last decade has

been on utilizing numerical models to forecast flood extents [10], ignoring methods for delivering forecast information to individuals and thus failing to enlist the public in mitigating losses and saving lives.

Today, the National Oceanic and Atmospheric Administration (NOAA) [11], the National Weather Service (NWS) [12], and the Office of Water Prediction (OWP) [13] are integrating advanced weather forecasting tools with hydrologic models to generate real-time dynamic flood inundation mapping for each of the 2.67 million river reaches within the contiguous US [14, 15, 16]. Other organizations including the US Department of Agriculture (USDA) National Forest Service [17] and NCAR [18] are working to develop wildfire forecast models to model fire behavior [19]. These advances offer the potential for more clear, relevant, and possibly life-saving alerts than ever before. Despite these breakthroughs, attempts at sharing flood-related information with the public and emergency response communities have not evolved. Described below is a contemporary disaster alert system utilizing modern geospatial and telecommunications technologies, focused initially on floods, which we also show could be developed into a multi-hazard disaster response platform.

2. Objectives and Scope

The vague geographic scope and broad dissemination of current alerts limits their effectiveness and desensitizes users due to their frequency and applicability [20]. In this way, disaster alerts are mirroring a decade-old problem facing meteorology that has led to an inherent distrust of predictions amongst the general public [21].

In an effort to combat this problem, a prototype system is offered: the Operational Platform for Emergency Response and Awareness (OPERA). OPERA aims to provide awareness, alerts, and interactive functionalities through the marriage of predictive models, geospatial technologies, and social media. The need for this system is reinforced by the requests for simplified, accurate and timely information from groups such as the California Department of Transportation [22]; Travis County, Texas [23, 24]; and Tuscaloosa County, Alabama [25]. Further, predictive flood mapping is being supported by funding organizations [26, 27] across the country.

OPERA focuses on three key elements of emergency response: (i) pre- and ongoing disaster awareness, (ii) real-time, hyper-local alerts, and (iii) interactive, actionable intelligence. These stages are demonstrated in three OPERA services. These services are neither exhaustive nor complete, but serve to demonstrate the potential of a centralized system that can be customized to a given disaster. Further, to encourage individuals to remember and engage with the OPERA system, each service has been assigned a character. With these characters, the OPERA system colloquially becomes the Disaster Zoo housing the FloodHippo, FireBadger, and ChemicalSpillPenguin services (Figure 1).



Figure 1. The three prototypes within the DisasterZoo: FloodHippo, FireBadger, and ChemicalSpillPenguin.

Prior to the development of OPERA, five needs were identified for achieving improved disaster warnings:

- 1) **Actionable:** Alerts and information must be interactive, relevant at the personal level, and intuitively understood, providing users with safe options that meet their needs.
- 2) **Real-time, hyper-local:** Alerts must be easily disseminated through a variety of outlets using consistent, well-documented terminology. The information provided must also be spatially and temporally accurate and come from an authoritative source.

- 3) **Consistent:** All functionality should use a simple Graphical User Interface that mirrors or integrates with well-established platforms. Alerts should be consistent across all software systems, and translatable across demographic and economic subgroups.
- 4) **Social:** Alerts should integrate with social networks, allowing users to share, recognize, and heed disasters promptly.
- 5) **Impartial:** The OPERA system should be able to ingest predictions from any source in order to remain up to date with the leading advances in science.

3. The OPERA System

In alignment with the key stages of emergency response and the goals defined above, each OPERA service has three components: an interactive awareness and education portal, a hyperlink-based alert system, and a server-based GIS response application.

- A. **Awareness:** an online hub with a variety of applications useful for educating individuals about what disasters they are susceptible to, what current conditions are, and where disasters are taking place around the country. These apps are interactive and pull data from Twitter and online real estate information to allow users to focus on both broad and local spatial scales.
- B. **Alert:** Currently Twitter-based, with the goal of integrating with the FEMA wireless emergency alerts (WEA) (28). OPERA alerts provide general information alongside a hyperlink to a server-based GIS application.
- C. **Response:** Merges current event forecasts, GIS functionalities, and a user's location to provide guidance based on location and the dynamic event extents.

Further, all DisasterZoo services use an online interface to facilitate easy access, collaboration, data integration, and use, without requiring an application to be downloaded or updated by a user.

A. Interactive Awareness and Education Portal: Exposure to memorable information before an event is critical for influencing how people respond during an emergency (21). Formal education has been shown to increase disaster preparedness and reduce vulnerability. While incorporating disaster education into formal education is ideal, other routes must be utilized to create a disaster ready nation (29, 30, 31, 32, 33).

To initialize this learning momentum, the OPERA main page uses the online real estate company Trulia (34). This allows users to enter a location of interest and see a map of what natural hazard risks exist in their area. With this information, users can elect to follow and explore the OPERA services that are most relevant to them. Once relevant risks are identified, each services page offers two modes of interacting with disaster information to visually and dynamically interact with disasters, fostering a better understanding of their magnitude.

A.1 Social Media Data: The first means of interacting with information focuses on mobilizing the power of social media sharing. In this section two methods are created using the Twitter and ESRI application programming interfaces (API). In both applications Tweets from around the country that include disaster specific words within the text string or hashtags are aggregated.

The first map (Figure 2.a) is built to quickly highlight where disasters are occurring. ESRI's API selects Tweets based on specific words in the text string, thus tweets returned by this filter primarily come from county governments, news organizations, or businesses. The current weakness of this method is the reliance on geo-tagged (geo-referenced) tweets. Currently, only 3% of tweets are actively geo-tagged, and approximately two-thirds of those come from 1% of users (35). However, one study shows that up to 1 in 5 Tweets inadvertently provide geo-location data (36), while another shows that geocoding can infer location for more than one third of all tweets (35). Additionally, advances in de-anonymization have shown geo-locations may be able to be inferred not from the user but from the user's friends (37). With a more robust understanding of Twitter, geo-information could become more available, advancing the ways in which OPERA can provide real-time disaster information.

The second method (Figure 2.b) focuses on tweets with hashtags relating to disasters using Twitter's API. This allows images, news hyperlinks, and more subjective content to be displayed in a 'news feed' style that users might see on Facebook or Twitter. This offers a more visual and personal representation of the geo-referenced map. In addition to predefined methods for aggregating Tweets, however as this prototype grows, a number of methods can be explored for customizing and controlling what Tweets are shown and how they are displayed.



Figure 2. (a) Live geo-referenced Twitter map, (b) '#Flooding' live feed.

While there are inherent flaws with crowd-sourced data, the intent is to view disasters from the eyes of others around the country. This method will hopefully impart a better understanding of the severity and frequency of specific disasters in a way that will, if needed, positively impact reactions to alerts.

A.2 Static and Dynamic GIS: The second web application (Figure 3) is built with ArcGIS Online and allows individuals to search for an area of interest such as their homes, the address of a friend, or even a state that is in the news. In this map both static and dynamic GIS layers can be displayed allowing users to explore real-time, historic, and probabilistic shapefiles. For example, FloodHippo displays hourly NOAA SPC Storm Reports (38) along a static map of the 100-year flood extent for the United States. The end goal of this application is to integrate with real-time flood inundation maps. However, at this point the application shows that emergency response related GIS data can be shared in an educational way through existing platforms.

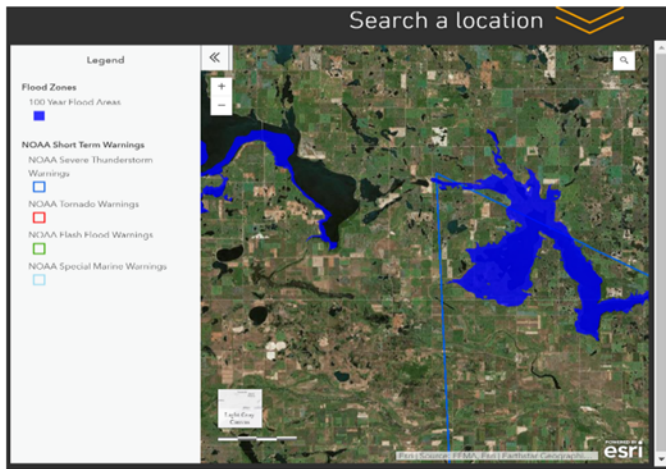


Figure 3. Dynamic hourly NOAA warnings paired with static shapefile.

B. Hyperlink-based Alert System: Pre-event, OPERA aims to show the potential of a centralized disaster awareness and preparedness platform. The combination of web-based maps and crowd-sourced data aims to make disaster awareness easier, more interesting, and personally relevant. During an event, however, individuals need actionable and accurate information. Currently, wireless emergency alerts (WEA) are the main method of alert provision. WEA's can be sent out by pre-authorized national, state, and local government authorities, and alerts from authenticated public safety officials are sent through FEMA's integrated Public Alert

and Warning System (IPAWS) to participating wireless carriers; these carriers then push the alerts to mobile devices in the affected areas (28).

An OPERA alert will add a hyperlink to the existing alert structure. This hyperlink is the crux of the OPERA system and will house real-time, actionable intelligence that can be used on any internet capable device. OPERA alerts are currently delivered via Twitter, with a goal being to merge with WEA. An example of an existing WEA alert system compared with the proposed OPERA emergency alert system can be seen in Figure 4.



Figure 4. Current WEA alert (left) vs. proposed OPERA FloodHippo alert (right).

Twitter was selected as a dissemination platform because it provides a powerful, low-cost, and already existing solution. Twitter is used by 20% of American adults (39), but its integration with SMS, email, Facebook, and other forms of communications could enable users to customize their experience and see alerts even if they are not an active Twitter user. 83% of Twitter users also utilize mobile devices, which is critical to maximizing the effectiveness of the DisasterZoo (40). The ability for citizens to tweet and re-tweet information further adds value in the form of understanding, validation, and cognition.

C. GIS Response Application: While OPERA is designed to be a holistic platform for all disasters, with a focus on people's relations to forecasted events, ideal behaviors do vary by disaster type. The response application for each service looks to these behaviors as a framework for what actionable information should be provided. Currently OPERA focuses on integrating buffer, navigate, and network paths with an individual's location, with the goal of adding more functionalities as additional first-responders are consulted about what features would be useful while not overwhelming users. Within the Disaster Zoo, FloodHippo focuses on navigating citizens to predefined shelters or locations of choice; FireBadger showcases the ability to buffer existing extents to provide immediate feedback, such as evacuation probabilities; and ChemicalSpillPenguin demonstrates how networks can be used to track hazard paths and the communities impacted by them. Each service within OPERA uses the same common operating framework so that functionalities can be used and combined for unique disasters.

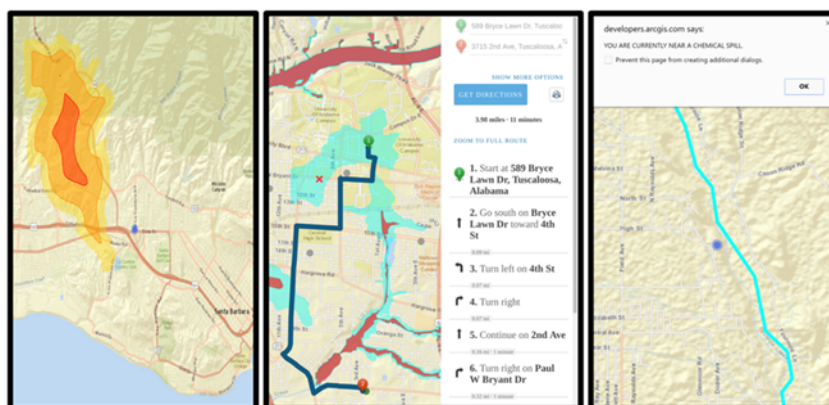


Figure 5. FireBadger (left), FloodHippo (center), and ChemicalSpillPenguin (right).

4. Flood Response Case Study

In the case of a flood like those in West Virginia (41) or Louisiana (42), citizens received warnings with no direction of how to best act. An explanation of how FloodHippo would operate follows, with the improvements it offers to standard WEA alerts. In the prototype demonstrated online, a modeled flood for the Black Warrior River in Tuscaloosa, Alabama was generated by the OWP. The red polygon represents real-time flood extents (red) and the blue polygon represents a three-hour forecasted flood extent, mirroring the projected outputs of the National Water Model.

In this case, citizens of Northport and Tuscaloosa would receive an alert via FloodHippo similar to the one seen in Figure 4. Initially this warning would be received by those who proactively subscribed to FloodHippo, however these alerts could be quickly disseminated across the social network by local personalities, organizations, friends, and businesses. We imagine that by engaging the social sharing nature of Twitter, citizens will share the information of the incoming flood via Twitter, Facebook, email, text message, and phone calls to encourage and direct others to the DisasterZoo home page in a time of crisis. Whether accessed from the warning or through another channel (SMS, email, Facebook), users would ultimately end up at the FloodHippo alerts page through the hyperlink.

Within the hyperlink, a user will be informed of whether or not their location will experience flooding over the life of the predicted event. This is the key to making this product hyper-local. If a user will be impacted, they are presented with two options: evacuate or navigate. The “evacuate” option routes users from their current location to the nearest shelter around current flood extents. Active shelter locations would be controlled by the Red Cross or other local NGO through an online spreadsheet, and FloodHippo will preventatively deactivate any shelters that are in a forecasted flood extent.

Acting similarly, “navigate” allows users to select a destination to route to. This application is intended for users who have somewhere specific to go, such as a school to pick up children. Both the “navigate” and “evacuate” applications were constructed using ESRI’s API for JavaScript, relying on ESRI routing services (43). In both applications, careful attention was paid to mobile device compatibility and color, in an attempt to develop the most intuitive flood alert system possible.

This case study is the most tangible example of the potential union between government emergency planning systems and a system like OPERA, largely due to the initial motivation and the aid received and offered by the OWP. All around, these apps work to unify and centralize the information that citizens, NGOs, and first responders have, making efforts more complimentary and synchronized.

5. Conclusion

By combining awareness, alerts, and response, the OPERA system meets our stated goals. The limitations withholding this prototype from national application are ESRI’s size limitation on polygon extents, and a provider of real-time disaster polygons. The first of these issues can be solved by running the GIS services on a localized server rather than ESRI’s ArcGIS online server, while the second issue depends solely on when this data becomes available (14, 23, 26, 27). The intent of OPERA was to establish the foundations, so that a communications platform already exists when these issues are resolved.

As a new form of alert system, OPERA is more than the sum of its parts: it offers a way to graphically interact at a personal level throughout an emergency event’s life history. The strength of this system is demonstrated by its ability to coordinate citizens, first responders, and NGOs, allowing each entity to focus on their responsibilities with new tools that help them do their job to the best of their ability. OPERA not only offers an improved means of intelligently reacting to an emergency, it also demonstrates how complicated science can be presented in a straightforward manner that is accessible to everyone. Further, while the goal is that relevant warning agencies adopt this form of alert system, social media – and particularly Twitter – has proven itself to be a supplemental platform for education and warning dissemination.

In conclusion, a summary of the needs previously identified for reimaging a new alert system is offered, and how OPERA, with a focus on FloodHippo, meets each:

1. **Actionable:** Through this system, individuals receive actionable intelligence describing how to navigate around a disaster regardless of where they need/want to go.
2. **Real-time, hyper-local:** A future partnership between OWP and the OPERA system will provide accurate information at the street scale, and the proposed partnership with ESRI allows for alerts to be delivered in real-time using their navigation services. Disaster Zoo “brands” are easy to remember during emergencies, allowing individuals to seek out the services even in the absence of an alert.
3. **Consistent:** OPERA’s services all mimic existing applications that people are familiar with: the routing services mirror similar applications such as Google Maps, and the use of web applications allows for consistent use across all mobile and desktop devices. The intent of this cross-platform integration is to provide a sense of familiarity and clarity for users which, in times of emergency, are critical for impacting behavior.
4. **Social:** The ability to share a hyperlink across social networks, government push notifications, and web pages maximizes the audience an alert will reach.
5. **Impartial:** By only requiring a polygon as input, OPERA remains open to integration with any organization: in terms of viability, it doesn’t matter if flood polygons come from private research groups, academic labs, or governmental agencies, OPERA will maintain relevance.

OPERA offers a hyper-local, event-specific, community-based response system that improves on existing disaster alerts by integrating the power of existing, yet underutilized, technologies, thus tapping into a robust social network of communications. The OPERA system was designed to be usable across all disasters including chemical spills, wildfires, nuclear accidents, infrastructure failures, and man-made disasters. The system has the ability to scale up from the community to the national level, and has potential to be integrated in current navigation systems as well as existing emergency response infrastructure. The building blocks to dramatically improve the way warnings are generated do exist, and OPERA is one method of combining alerts in an improved platform. OPERA is not argued as the final solution, it is solely intended to expose the need and potential for something better. To see the prototype in action please see the OPERA webpage at <http://disasterzoo.wixsite.com/main>.

References

1. Office of Climate, Water and Weather Services, National Weather Service. Natural Hazards Statistics. 2016. <http://www.nws.noaa.gov/om/hazstats.shtml>
2. International Federation of Red Cross and Red Crescent Societies. World Disasters Report. (2013).
3. National Weather Service. Flood Safety Awareness. <http://www.srh.noaa.gov/bro/?n=floodsafety>
4. Seward, Z. M. The First Mobile Phone Call was Made 40 Years ago Today. The Atlantic (2013). <http://www.theatlantic.com/technology/archive/2013/04/the-first-mobile-phone-call-was-made-40-years-ago-today/274611/>
5. Andrews, E. Who Invented the Internet? AskHistory. (2013). <http://www.history.com/news/ask-history/who-invented-the-internet>
6. Goodchild, M. Geographic Information Science. *Int. J. Geogr. Inf. Syst.* 6 (1): 31-45. (1992)
7. National Research Council (U.S.). Committee on the Future of the Global Positioning System; National Academy of Public Administration). The global positioning system: a shared national asset: recommendations for technical improvements and enhancements. National Academies Press. (1995).
8. Centre for Research of the Epidemiology of Disasters. The human cost of weather-related disasters 1995-2015. (2015). <http://www.preventionweb.net/publications/view/46796>
9. Working Group on Natural Disaster Information Systems Subcommittee on Natural Disaster Reduction. (2000). Effective Disaster Warnings. http://www.sdr.gov/docs/NDIS_rev_Oct27.pdf (2000).
10. Bauer, Thorpe, Brunet. The Quiet Revolution of Numerical Weather Prediction. *Nature* 525, 47-55. doi:10.1038/nature14956 (2015).
11. National Oceanic and Atmospheric Administration. United States Department of Commerce. <http://www.noaa.gov>

National Water Center Innovators Program Summer Institute 2016

12. National Weather Service. NOAA. <http://www.weather.gov>
13. Office of Water Prediction. NOAA. <http://water.noaa.gov>
14. NOAA. NOAA launches America's First National Water Model. <http://www.noaa.gov/media-release/noaa-launches-america-s-first-national-water-forecast-model> (2016)
15. Maidment, D. R. (2015). A Conceptual Framework for the National Flood Interoperability Experiment. Retrieved from https://www.cuahsi.org/Files/Pages/documents/13623/nfieconceptualframework_revised_feb_9.pdf
16. National Water Center. (2015). Overview: National Water Center (NWC). Retrieved from <http://www.nws.noaa.gov/oh/nwc/>
17. US Forest Service. USDA. <http://www.fs.fed.us>
18. National Center for Atmospheric Research. National Science Foundation. <https://ncar.ucar.edu>
19. Hosansky, D. NCAR to Develop Wildland Fire Prediction System for Colorado. <http://www2.ucar.edu/atmosnews/news/18317/ncar-develop-wildland-fire-prediction-system-for-colorado> (2015)
20. National Weather Service. (2016). Watches, Warnings & Advisories. Retrieved from <http://forecast.weather.gov/wwamap/wwatxtget.php?cwa=usa&wwa=Flood%20Advisory>
21. Miletic, D. S. & Sorensen, J. H. (2015). A Guide to Public Alerts and Warnings for Dam and Levee Emergencies. Retrieved from http://silverjackets.nfrmp.us/Portals/0/doc/WarningGuidebook_USACE.pdf?ver=2015-08-10-213008-520
22. Lissade, H. (2012). Flood Warning Alert Systems. http://www.dot.ca.gov/newtech/researchreports/preliminary_investigations/docs/flood_warning_systems_pi_12-5-12.pdf (2012)
23. Buchele, M. Texas Researchers Unveil New Real-Time Flood Forecasting System. Kut.org. (2015)
24. Easter, M. The University of Austin at Texas. Saving Lives Through Real-Time Flood Forcasting. (2016)
25. Staff. Tuscaloosa EMA. <http://tuscaloosacountyema.org/new-flood-predication-and-response-tools/> (2016)
26. Staff. WIAT Birmingham News. UA Professor Receives Grant to Develop Flood Prediciton System. (2016)
27. CUASHI. National Flood Interoperability Experiment. <https://www.cuahsi.org/NFIE>. (2015)
28. Federal Communications Commission. Wireless Emergency Alerts (WEA). <https://www.fcc.gov/consumers/guides/wireless-emergency-alerts-wea>
29. Wisner, B. (2006). Let our children teach us! A review of the role of education and knowledge in disaster risk reduction. Retrieved from http://www.crin.org/en/docs/ISDR_let_teach.pdf
30. Campbell, J. & Yates, R. (2007). Lessons for life: Building a culture of safety and resilience to disasters through schools. Retrieved from <http://www.unisdr.org/2007/campaign/iddr/docs/UK-actionaid-report.pdf>
31. United Nations International Strategy for Disaster Reduction. (2007). 2006-2007 World Disaster Reduction Campaign: Disaster risk reduction begins at school. Received from <http://www.unisdr.org/2007/campaign/pdf/WDRC-2006-2007-English-fullversion.pdf>
32. Rego, L. et al. (2008). Impacts of Disasters on the Education Sector in Cambodia. Retrieved from http://www.adpc.net/v2007/IKM/ONLINE%20DOCUMENTS/downloads/2008/Mar/MDRDEducationCambodiaFinal_Mar08.pdf
33. Muttarak, R., and W. Pothisiri. 2013. The role of education on disaster preparedness: case study of 2012 Indian Ocean earthquakes on Thailand's Andaman Coast. Ecology and Society 18(4): 51. <http://dx.doi.org/10.5751/ES-06101-180451>
34. Buhler, K. Trulia Corporate Blog. Do You Live Near a Natural Disaster Zone? Our new Natural Hazards Map Will Tell You. <http://www.trulia.com/corp/2013/08/15/natural-hazard-maps-2/> (2013)
35. Leetaru, K.H et al. Mapping the Global Twitter Heartbeat: The Geography of Twitter. First Monday. 18:5. <http://firstmonday.org/ojs/index.php/fm/article/view/4366/3654> (2013).
36. Weildemann, C. Social Media Location Intelligence: The Next Privacy Battle - An ArcGIS add-in and Analysis of Geospatial Data Collected from Twitter.com. International Journal of Geoinformatics. (2013).
37. Compton R., Jurgens D., Allen D. Geotagging One Hundred Million Twitter Accounts with Total Variation Minimization. IEEE BigData. <10.1109/BigData.2014.7004256> (2014)
38. SPC Storm Reports. NOAA Storm Prediction Center. <http://www.spc.noaa.gov/climo/reports/>
39. Duggan, M. The Demographics of Social Media Users. Pew Research Center. <http://www.pewinternet.org/2015/08/19/the-demographics-of-social-media-users/>. (2015)
40. Twitter. (2016). Twitter Usage / Company Facts. Retrieved from <https://about.twitter.com/company>
41. Visser, S., Savidge, M. West Virginia Floods Devastate 1,200, Many Lives. CNN. <http://www.cnn.com/2016/06/28/us/west-virginia-flooding-weather/> (2016)
42. BBC News. Louisiana Floods: Photographs capture wreaked homes and lost memories. <http://www.bbc.com/news/world-us-canada-37207977> (2016).
43. Environmental Systems Research Institute. (2016). Esri Directions and Routing Services. Retrieved from <https://developers.arcgis.com/features/directions/>

Translator TTX – Bridging the Communication Gap between Researchers and Emergency Responders

Whitney Henson¹, Richard Garth² and Christopher Franklin³

¹ Jacksonville State University ; whenson@stu.jsu.edu

² University of Texas, Dallas ; rhg090020@utdallas.edu

³ University of Texas, Dallas ; cxf106020@utdallas.edu

Advisors: Tanveer Islam, Jacksonville State University, tislam@jsu.edu; Bryan Chastain, University of Texas Dallas, bjc062000@utdallas.edu

Summer Institute Theme Advisor: David Maidment, University of Texas Austin, maidment@mail.utexas.edu

Abstract: This study focuses specifically on what emergency management agencies at all hierarchical levels consider as a “gap” between the critical needs of first responders and the deliverables offered by advancing science. For this study, we posit that this gap is in fact not an engineering science problem but rather a communication problem. Social norms and human behavior hold the key to better understanding and reducing loss of life from flood events. The objective of this study is to develop a conceptual model to translate and interconnect the “science domain” (i.e., weather information sources) with the “social domain” (i.e. emergency managers, first responders and those affected by an event). To address communication problems between the science domain and the social domain, we adopt a “Rosetta Stone” metaphor as a model paradigm. We refer to this “translation” concept as the “Translator-TTX”. The study has the potential to make a contribution through maximizing the applied value of disaster science and management research and technology. Our investigation supports the notion that with simplification and efficient delivery of the knowledge contained in the science domain, using just-in-time techniques, and state-of-the-art algorithms, the needs of first responder practitioners met and exceeded. Finally the first responders engaged in this study were eager to close the communication gap between researchers and practitioners. The main findings suggest further research opportunities exist in implementing ESRI Story Maps for pre-planning tabletop exercises (TTX); reverse look-up inundation mapping updates through first responder windshield survey methods and spatial-temporal locational 3D object analytics provide emergency personnel at different hierarchical levels with enhanced visual perceptions and situational awareness. In conclusion, an expert decision support system utilizing an evolving knowledge warehouse repository of events, scenarios, standard operating procedures (SOPs), and best practices appears possible and meriting of further research. Also the feasibility of implementing such approaches in a serious game software platform is supported by the literature. Finally, helping connect the efforts of engineering science with the needs of first responders, serving the public safety interest, is the primary motivation behind this study.

1. Motivation

According to NOAA, in 2015, water related events alone affected 7 million citizens in 15 states across the country for an estimated cost exceeding \$1 billion. Many lives at risk were saved, but too many were unnecessarily lost. Persistent lack of knowledge and respect for the dangers associated with the physical forces of flooding by the general population likely contribute to the loss of life. First responders are also not immune to these risks. After-Action Reviews (AARs) from past incidents cite “lack of effective communication” as a primary issue in responding to incidents. This issue must be overcome in order to significantly reduce current loss of life due to flooding. In weather related events, any opportunity to strengthen the capabilities of the interface between the science domain

and the social domain is an opportunity to strengthen and enhance the efficiency and effectiveness of operations, further reducing loss of life and property.

The National Water Model can now be utilized to predict flood timing, heights, flow rates and other parameters, but the only way it can be useful in a flood event to first responders and the public is if this information is delivered in a timely and simplified manner. The specific weather hazard investigated in this study is inundation flooding (e.g. watershed downstream flooding, simplified dam and levee breach).

The translator is also distinguished from other efforts through the use of an expert system, a logic engine and a data repository with a robust maintenance module that will provide a knowledge warehouse capability that is scalable three-dimensionally. Additional models can be added to include an all hazards approach. As of now, the model can be used to execute pre-planning training, but eventually will be available for live situational awareness enhancement to emergency managers facing real events. It will also be developed as a post analysis tool collecting and storing standard operating procedures and modifications as well as best practices for individual jurisdictions. Finally, Translator-TTX can be tailored and delivered to address the different hierarchical training needs of various levels of emergency management.

2. Objectives and Scope

The purpose of the study is to explore the potential for new National Water Model scientific prediction capabilities and initiatives to be implemented as useful enhancements to first responder preparedness at all hierarchical levels of emergency response and management (i.e., EOCs; Police, Fire and Rescue Chiefs; actual on-scene crews).

Our goal is to save lives and property.

- Objective – Provide enhanced predictive anticipatory information and instruction to ensure whole community flood resiliency
 - Strategy #1 – Provide tabletop exercises as a service to meet the needs of first responders in protecting vulnerable population groups
 - Tactic #1 – Real-time pre-planning simulations (Translator-TTX, serious game software)
 - Strategy #2 – Create innovative utilizations of geospatial information and informatics to improve situational awareness, flood evacuation and rescue
 - Tactic #1 – Reverse look-up to improve first responders' situational awareness (using windshield survey methodologies)
 - Tactic #2 – Provide deliverable preventable actions, education, planning and training programs

Translator-TTX has specifically addressed each tactic through its knowledge warehouse and expert decision support system software platform (Figure 1). A website proof of concept is provided in supplementary materials to demonstrate the flow and logic of such a model.

Finally, an innovative three-dimensional object was incorporated into the model as a potential emergency management decision making tool called "Avatar" to allow visual semaphore object representation of the unfolding events for various emergency management roles.

3. Previous Studies

There is a strong movement to adopt serious game software approaches to meet the needs of first responders [1]. One of the most popular applications of a software "role playing" approach is in development referred to as RimSim [2]. A leading author of "Emergency Response and Training" has written extensively about the subject and has gained acceptance for his scholarship from the

Department of Homeland Security and USGS [3]. Further justifications and rationale for “Adapting Simulation Environments for Emergency Response Planning” can be found in good measure in this doctoral thesis [4]. The literature not only talks about the potential for weather hazard simulation but also the applicability to emergency processes like hospital evacuation [5]. Further possibilities for analytic solutions to the problems faced by first responders appear in the work associated with GIS network analyst using Capacity Aware Shortest Path Evacuation Routing (CASPER) algorithms [6]. Our study briefly features one potential adoption of an integration of mapping demographics and CASPER.

The architecture and conceptual structure of our Translator-TTX approach is supported in the literature discussing “...game architecture centered on a modeling and simulation infrastructure” [7]. The best of computerized intentions cannot ignore human cognitive visual limitations. This literature provides discussion of the analytics appropriate for human cognitive capacities [8]. Funding and interest for a “translator” approach to the communication problem presented in our study can be found in literature describing the Department of Homeland Security involvement with this initiative [9]. “Realistic evaluation” of an emergency management organization’s disaster preparedness is another role a computerized infrastructure may be able to provide in combination with a knowledge warehouse as discussed from an IT management perspective [10]. We explore the future of visualization and analytics with our suggestion for a three-way factor analysis, using our “Avatar” semaphore, 3D printed object or software model to visualize situational awareness. This literature supports such a discussion and development through “3D Crisis Mapping for Disaster Simulation training” from an information systems perspective [11, 12]. Finally, a report on simulation by the Department of Homeland Security and a case study from New Zealand with live call data provide guidance from previous studies.

4. Methodology

We utilized a mixed method of inquiry combining qualitative and exploratory research designs in a phenomenological approach. We conducted primary research in the form of face-to-face, open-ended interviews with scientists and first responders selected using a convenience-sampling frame. In support of the study, we conducted a thorough review of the literature in our secondary research within the emergency management science domain.

We conducted three informal, face-to-face interviews. The first was with Tuscaloosa County Fire and Rescue Deputy Chief Chris Williamson and staff, the second with Northport Fire and Rescue Chief Bart Marshall and staff, and the third with Tuscaloosa County EMA Director Rob Robertson. After conducting these interviews, it was clear that communication gaps existed between the science community and first responder community. This feedback was used to develop the Translator – TTX software platform. Due to time and resource constraints, we developed a small proof of concept to test the capabilities of Translator – TTX.

This proof of concept included a number of approaches:

- Provide first responders and emergency managers access to a user friendly website (powered by WIX) that is broken down by organization (NGO’s, Police, EMA, and Fire and Rescue) [see Supplementary Details for more information]
- Develop online tabletop exercise templates (powered by ESRI Story Maps) that can be tailored to a community’s needs.
- Develop a knowledge warehouse that categorizes information using an if-then logic system.
 - For example, IF a dam breaches, THEN certain actions must be taken. These actions are taken from best practices and lessons learned from After Action Reports (AARs)

5. Discussion

5.1. Description of Results - The investigation to date has identified two main results (1) what is needed and (2) by whom.

Result #1 – “**What is needed?**” More pre-planning opportunities for integrating the engineering/science advances exemplified by the National Water Model.

Result #2 – “**Who needs what?**” The hierarchical structure of emergency management organizations (from on-the-ground first responders to chiefs and directors) dictates the delivery of different pre-planning services for different roles within each organizational job function.

5.2. Interpretations

5.2.1. Interpretation of Result #1 “What is needed?”– Based on our investigations, we believe an intelligent transfer mechanism is needed to facilitate the “translation” of scientific data and derive results into usable information, knowledge and actionable understandings in the language of first responders. That language typically consists of “visual” maps such as flood inundation maps. In addition, since the National Water Model covers all of the contiguous United States, any first responder within that area utilizing the Translator-TTX Tabletop Exercises as a Service will be able to work with their local and familiar real data.

Our conceptual model (called Translator-TTX) has provided the theoretical framework to address the communications gap between researchers and practitioners. We believe such a mechanism could also be scaled to address all hazard scenarios across time and in formats to address the hierarchical needs of emergency management and first responders. Translator-TTX is conceptually like an integrated “switchboard”. Such a software platform would connect a robust knowledge warehouse to provide the training needs of first responders with data for realistic simulations in familiar geographic settings provided by the National Water Model (Figure 2).

In preparing for an event, emergency managers and responders participate in various exercises to clarify roles and responsibilities. Tabletop exercises (TTX), for instance, are meetings to discuss a simulated emergency situation. Members of the group review and discuss the actions they would take in a particular emergency, testing their emergency plan in an informal, low-stress environment [15]. Tabletop exercises have recently taken on a new, modern approach such as a software emulation called “RimSim”. This is a simulation-based software platform designed specifically for countries around the Pacific Rim and their emergency management organizations for pre-planning exercises associated with hazards that affect the area, such as earthquakes. Their approach, however, does not have the advantage of using real data and thus adopts fictitious place names, events and scenarios. We have developed a series of tabletop exercises (TTX) using ESRI’s ArcGIS Online Story Maps to describe flood scenarios based on a community’s needs (Figure 3). These tabletop exercises use real data and events in order to better prepare first responders.

Due to time and resource constraints, we have chosen to demonstrate our approach by delimiting it to a proof-of-concept visualization (through the use of an innovative web design cloud host called WIX.com). The WIX proof-of-concept site [see Supplementary Details for more information] offers a tour of the essential components envisaged in the Translator-TTX (Figure 4).

5.2.2. Interpretation of Result #2 “Who needs what?”– There is a need for a comprehensive “intelligent transfer” mechanism to take the detailed data, information and interpretations derived from the “science cloud” so as to filter that content into improved knowledge and meaningful understandings to the hierarchical structure of the first responder/emergency management community. Specifically, by improving the detail and awareness of the geocoded property at risk and its demographics, this platform can shorten lead times and ultimately save lives.

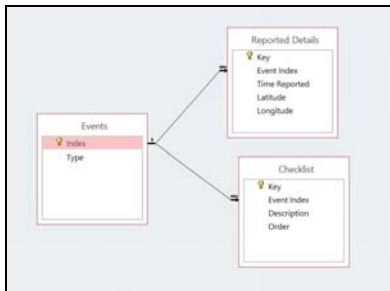


Figure 1. Knowledge Warehouse
Level 1 Entity Relationships

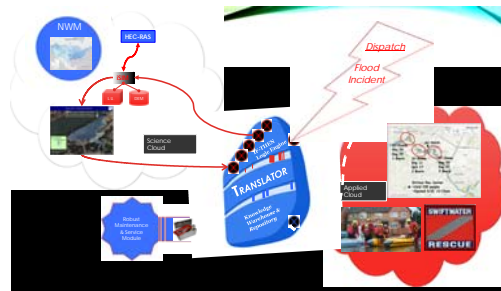


Figure 2. Sample of Translator – TTX

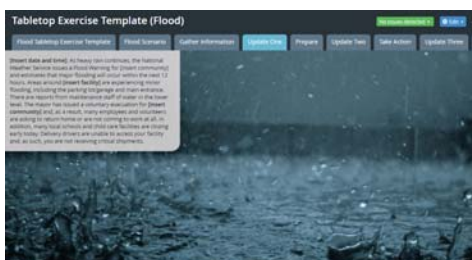


Figure 3. Sample of Tabletop Exercise Story



Figure 4. Translator – TTX Software Platform

6. Conclusion

The Summer Institute environment has allowed us the privilege and opportunity to explore, investigate and examine our intellectual curiosities using a rapid prototyping methodology on new topics and to tease out potential solutions that might offer innovative breakthroughs to tough unsolved-to-date problems. We have taken the opportunity to explore and experiment with a wide range of investigations, without fear.

This has in turn spawned new opportunities to address the “communication problem” discussed earlier. The communication problem refers to the translation of scientific information into knowledge that is useable and adaptable for first responders. These improvement opportunities are derivative of significant recent scientific developments. For example, the National Water Model dramatically strengthens the geographic coverage, predictability and advanced warning time intervals for flood inundation effects mitigation.

Other promising research directions for further investigation:

- **Reverse-Lookup** shows how flood conditions verified as ground truth by first responder crews (using standard Windshield Surveys) in real time could play an important role in recasting the geographic event scene and potentially uncovering upcoming weakness while identifying just-in-time opportunistic recover and rescue efforts as dynamic conditions unfold.
- **Distant Learning** implementations for classrooms could be applied to pre-planning tabletop exercises as a service.
- **Real Time** - With appropriate resources, the Translator-TTX platform need not be limited to flooding or pre-planning only and could effectively organize and manage simultaneous numbers of unexpected hazards either as a simulator or eventually through development of real-time and eventual post-event analyses
- **Avatar** – Space-time three-way factor analysis

- **iMDE** – Integrated Mapping Demography and Evacuation
- **iSIM** – Integrated Simplified Inundation Mapping
- **Costs** – Flood Damage Estimator
- **Site Locator** – A siting approach that looks not only at population density and drive time for siting new Rescue Service facilities, but also weights using GIS buffered layers for flood and other hazards

This information would be housed in a knowledge warehouse to accumulate as a repository of best practices and lessons learned. It would be envisaged as a three-dimensional conceptual platform horizontally scaling to all hazards; vertically addressing the various needs of the traditional hierarchical emergency management governmental structures over the third axis of time (pre-event, event and post-event).

Supplementary Materials: More information on Figures 3 and 4 are available online at <http://liamgesahc.wix.com/translator-ttx>; ESRI Story Maps Tabletop Exercises are available at <http://arcg.is/29sE921> and <http://arcg.is/29sFRAc>

Acknowledgement: The author is thankful to CUAHSI, NOAA's National Water Center, Northport Fire and Rescue Station #2, Tuscaloosa Fire and Rescue Station #2, and Tuscaloosa County Emergency Management Agency.

References

1. Alhadeff, E. (2010). SERIOUS GAMES MARKET. Retrieved July 14, 2016, from <http://seriousgamesmarket.blogspot.com/2010/11/rescuesim-serious-games-for-multi.html>
2. Barrett, R. (2003). Rim Sim: A Role-Play Simulation. Retrieved July 14, 2016, from <https://pubs.er.usgs.gov/publication/b2212>
3. Campbell, B. D. (2008). Emergency Response Planning and Training. [https://www.purdue.edu/discoverypark/vaccine/assets/pdfs/publications/pdf/Emergency Response Planning.pdf](https://www.purdue.edu/discoverypark/vaccine/assets/pdfs/publications/pdf/Emergency%20Response%20Planning.pdf)
4. Campbell, B. D. (2010). Adapting Simulation Environments for Emergency Response Planning and Training (Doctoral dissertation, University of Washington).
5. Campbell, Bruce, and Weaver. 2013. "RimSim Response Hospital Evacuation." International Journal of Information Systems for Crisis Response and Management.
6. Shahabi, K., & Wilson, J. P. (2014). CASPER: Intelligent capacity-aware evacuation routing. *Computers, Environment and Urban Systems*, 46, 12-24.
7. Garro, A., Longo, F., & Nicoletti, L. (2013). Disasters management: a serious game architecture centered on a modeling and simulation infrastructure. *SCS M&S Magazine*, 4(1).
8. Greitzer, F. L., Noonan, C. F., & Franklin, L. R. (2011). Cognitive foundations for visual analytics. Pacific Northwest National Laboratory (PNNL): Richland, WA.
9. Kielman, J. (2007). A Message from the Department of Homeland Security. VAC Views, 2.
10. Meesters, K. (2014). Towards using Serious Games for realistic evaluation of disaster management IT tools. In AIM SG (pp. 38-48).
11. Meier, Patrick P., 2008. "3D Crisis Mapping for Disaster Simulation Training" <https://irevolutions.org/2008/12/14/3d-disaster-simulation/> [<https://twitter.com/PatrickMeier>]
12. Silvera Victor A. B. and Murray E. Jennex, 2009. "International Journal of Information Systems for Crisis Response and Management (IJISCRAM)"
13. U.S. Dept. of Homeland Security, 2007. "RimSim: Technology Solutions for Pacific Rim Disasters" VAC Views – A publication of the visualization and Analytics Centers, pp 17-18
14. Vaidyanathan, A. (2010). A test-bed for emergency management simulations A case-study including live call data in New Zealand.
15. What is a tabletop exercise? - UWPD. (2012, May 9). Retrieved July 15, 2016, from http://uwpd.wisc.edu/content/uploads/2014/01/What_is_a_tabletop_exercise.pdf

Increasing Citizen Awareness of Floodwater Risks: An Effort at Reducing Flood-related Fatalities

Dawne Butler

University of Texas at San Antonio; dawne.butler@yahoo.com

Academic Advisor: Hatim Sharif, University of Texas at San Antonio, hatim.sharif@utsa.edu

Summer Institute Theme Advisors: David Maidment, University of Texas at Austin, maidment@utexas.edu; Harry Evans, University of Texas at Austin, harryevans@utexas.edu

Abstract: Flood-related fatalities are often avoidable, but the number of total annual deaths from flooding events has been resistant to governments' efforts at reduction (e.g., flood emergency alerts, "Turn around, don't drown" signage, website-based education, etc.). A more effective flood hazard reduction/education program needs to be developed. In order to better tailor and target education, flood fatality data from 1996 to 2015 was analyzed to determine the basic demographics of which people were dying and where they were dying. Also determined were average minimum floodwater depths at which fatality risks are significant. It was found that across the adult population, men made up ~63% of the fatalities, while women accounted for ~37%. It has also been reported that fatality risks are significant at floodwater depths as low as 7.9 inches for people in vehicles [1] and as low as 12 inches for people on foot [2]. A possible factor in the persistence of flood-related deaths is the relatively low perception of the risks of crossing floodwaters [3-7]. An improved education program would include thoroughly communicating flood risks to all ages, not just to the proactive adults who research websites and heed flood emergency alerts.

1. Motivation

Flooding is a significant cause of deaths due to weather hazards, and unlike other hazard-related deaths, there has not been a declining trend [3] (Figure 1). The top two locations of where these fatalities occur are in vehicles (e.g., driving into flooded areas of roads) and in water (e.g., trying to cross flooded areas on foot or by swimming) (Figure 2). Both of these risks are highly avoidable. It has been proposed in numerous studies that, among other factors, risk perception plays a significant role in whether people take these risks [3-7]. Therefore, various education methods, targeted to different audiences, have the potential to reduce flood-related fatalities.

2. Objectives and Scope

The development of targeted education materials is the objective of the author's Summer Institute project. Assessment of which groups of people were dying, and where it was occurring, was accomplished by analyzing the most recent 20 years of data obtained from the National Weather Service (NWS) [8]. Also determined were the average minimum floodwater depths at which fatality risks are significant [1, 2]. From these, Citizen Maps which include some flood hazard avoidance facts, will be generated.

3. Previous Studies

Although there has some research on flood fatalities [3-7], most of it is not recent (e.g., data only up to 2005 was analyzed). The author analyzed more recent, and a longer period of data; 1996-2015.

4. Methodology

Flood fatality data for the United States and its territories (U.S.) was obtained from the NWS website [8] for the period of 1996-2015. This data included a break-down of deaths by year, state, gender, 10-year age group, and location. Analyses conducted included: Total flood-related fatalities by year (1940-2015), totals and percentages by gender (ages 20 and higher; children 0-19 were excluded due to the author's assumption that they were passengers and not decision-making drivers), totals and percentages by age group and gender (ages 20 and higher; 0-19 ages were excluded, as previously noted), totals and percentages by location, totals and percentages by state (including average number of fatalities per year in which flood deaths occur), and totals and percentages by location and state. Data has not been normalized by population, yet. Research was also conducted to determine what the average minimum floodwater depths at which fatality risk becomes significant for both the vehicle [1] and the in water locations [2].

As part of communicating risk, a Citizen's Map was developed using Esri's ArcMap 10.3. The map uses a street basemap, a 10-meter by 10-meter resolution National Elevation Dataset [9] digital elevation model (DEM), and a house location. The symbology of the DEM was then adjusted to reflect elevation groupings; red ("don't go" zone) for elevations at and below the house level, orange ("slightly better" zone) for elevations up to 10 feet over the house elevation, yellow ("better" zone) for elevations of 10 to 30 feet over the house elevation, and green ("much better" zone) for elevations at least 30 feet over the house elevation. Two versions of the map were created; one for people evacuating on foot (1 to 4,000 scale, Figure 3) and one for people that may be able to evacuate by vehicle (1 to 10,000 scale, Figure 4). Also included with the map printout are some flood hazard avoidance facts.

5. Results

5.1. Fatality Research

5.1.1. Data Analysis

Basic demographics of the people who are dying and where are they dying in the U.S., from 1996 to 2015:

- 1) The total annual flood-related deaths were highly variable and there was no significant trend (Note that this data is for the period of 1940 to 2015, Figure 1).
- 2) Gender: Of the people aged 20 and higher, men were ~63% of fatalities, while women were ~37% of fatalities, which is a rate of ~1.73 to 1 (men to women) (Figure 5). Since males are only ~49.2% of the population [10], this may indicate that significant sociological factors are driving the higher mortality rate for men. Breaking this down by 10-year age group, men die at a rate of 1.5 to 2.1 times more often than women (this excludes the anomalous rate of 5 to 1 men to women in the 90+ age group) (Figure 6).
- 3) Location: Approximately 52% of deaths occurred in vehicles or towed trailers and ~25% of deaths occurred in water, making these, by far, the most common locations for flood-related fatalities (Figure 2).
- 4) Of the 52 states and territories with flood fatalities, 21 had deaths in at least 50% of the years analyzed. Those states, in descending order of percentage of years with flood deaths are: Texas (95%), Missouri (95%), Kentucky (90%), Ohio (90%), California (85%), Arizona (80%), Indiana (75%), Virginia (75%), Washington (75%), Illinois (70%), New York (70%), Arkansas (65%), Oklahoma (65%), Puerto Rico (60%), Tennessee (60%), West Virginia (60%), Mississippi (55%), Pennsylvania (55%), Kansas (50%), New Mexico (50%), and Utah (50%).
- 5) The highest average number of flood fatalities per year, in years with flood fatalities, varied by state. The top 12 averages by state: Texas = 14.16, Pennsylvania = 6.91, North Carolina = 5.67, Arkansas = 5.54, Missouri = 5.37, Tennessee = 5.25, Colorado = 4.80, Oklahoma = 4.46, Arizona = 4.38, Kentucky = 4.22, California = 4.12, American Samoa = 4.00.

- 6) In the top 4 states (by number of years with flood deaths) ~65% to ~89% of the deaths occurred in vehicles or in water (Figure 7). In the top 6 states (by number of deaths per year with flood deaths) ~54% to ~92% of the deaths occurred in vehicles or in water.

5.1.2. Flood Hazard Statistics

Dangers of driving into floodwaters: Vehicles can float when water depth reaches the car floor.

- 1) Sub-compact cars (weighing a little over 2,300 pounds) can become unstable and difficult to maneuver in water as shallow as 7.9 inches and moving as slowly as 2.25 miles per hour (mph) (average walking speed is approximately 3 miles per hour) [1].
- 2) Large trucks/SUVs (weighing approximately 5,500 pounds) can become unstable and difficult to maneuver in water as shallow as 17.7 inches and moving as slowly as 3 mph (average walking speed) [1].

Dangers of walking into floodwaters: Water that is as shallow as 3 feet deep and moving as slowly as 2.6 mph can knock down an adult male. The same can happen at a depth of 2 feet at 4 mph, and at 1-foot-deep at 6.7 mph [2]. It is presumed that the depths and speeds that are hazardous for women would be lower because, on average, women are shorter and weigh less.

5.2. Figures

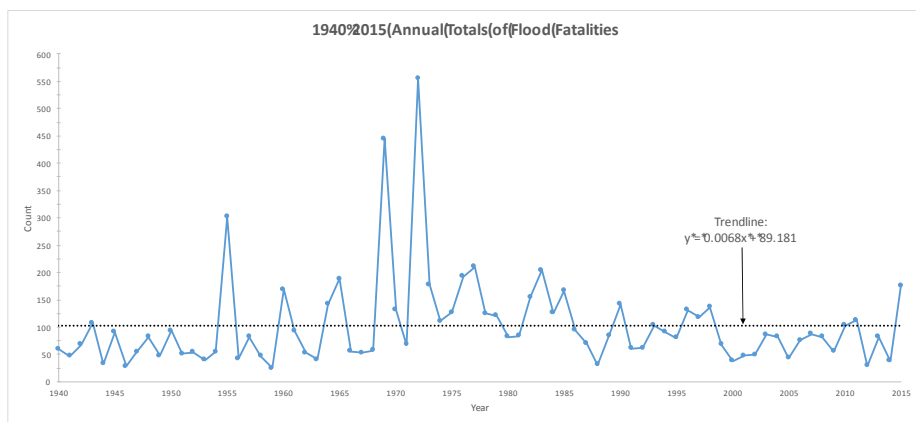


Figure 1. This graph depicts the total number of flood fatalities by year, for the period of 1940 to 2015. The Excel-computed trendline indicates that the number of deaths per year is neither declining nor increasing (the author believes that the 0.0068 positive slope value is not significant).

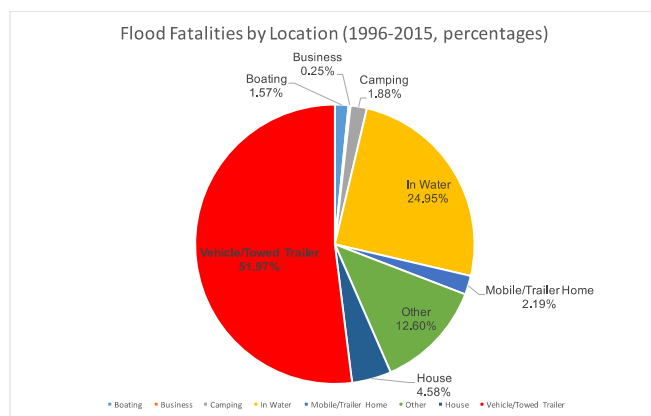


Figure 2. This chart shows the percentages of flood-related fatalities in the U.S., by location, for the period of 1996-2015.

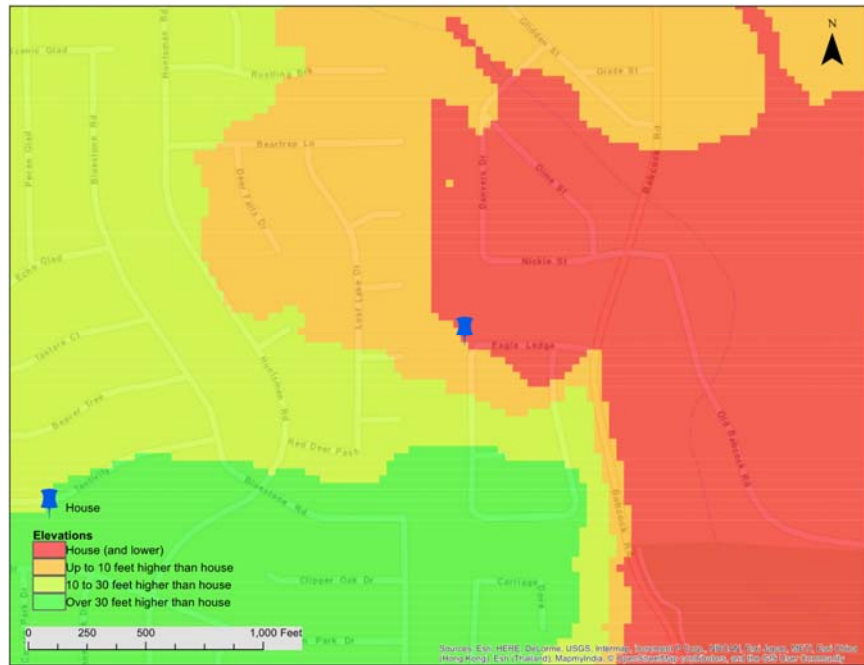


Figure 3. Elevation map showing roads and elevation ranges in relation to a house at 1 to 4,000 scale (in order to aid in on-foot evacuation).

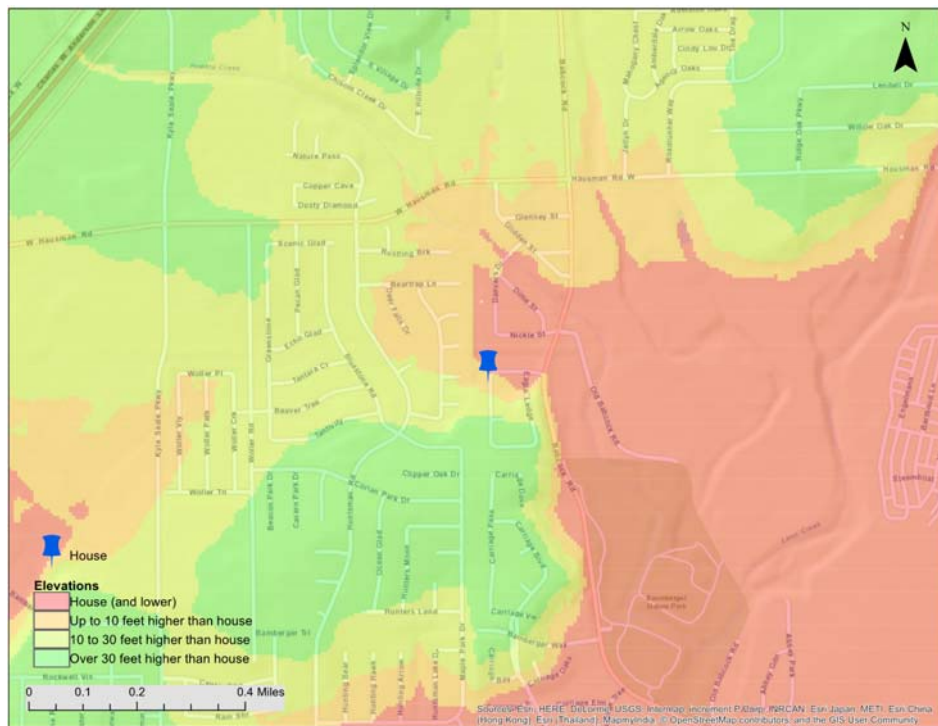


Figure 4. Elevation map showing roads and elevation ranges in relation to a house at 1 to 10,000 scale (in order to aid in in-vehicle evacuation, if possible).

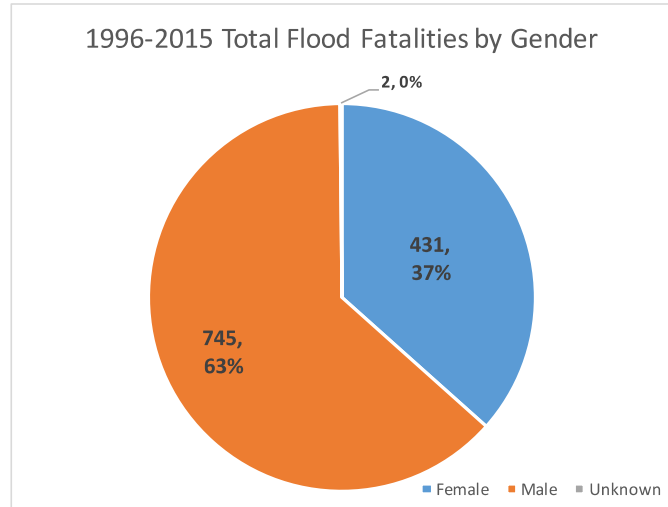


Figure 5. This chart depicts flood-related fatalities, by gender, of adults aged 20 and higher, in the U.S. from 1996-2015. Men were ~63% of fatalities, while women were ~36% of fatalities.

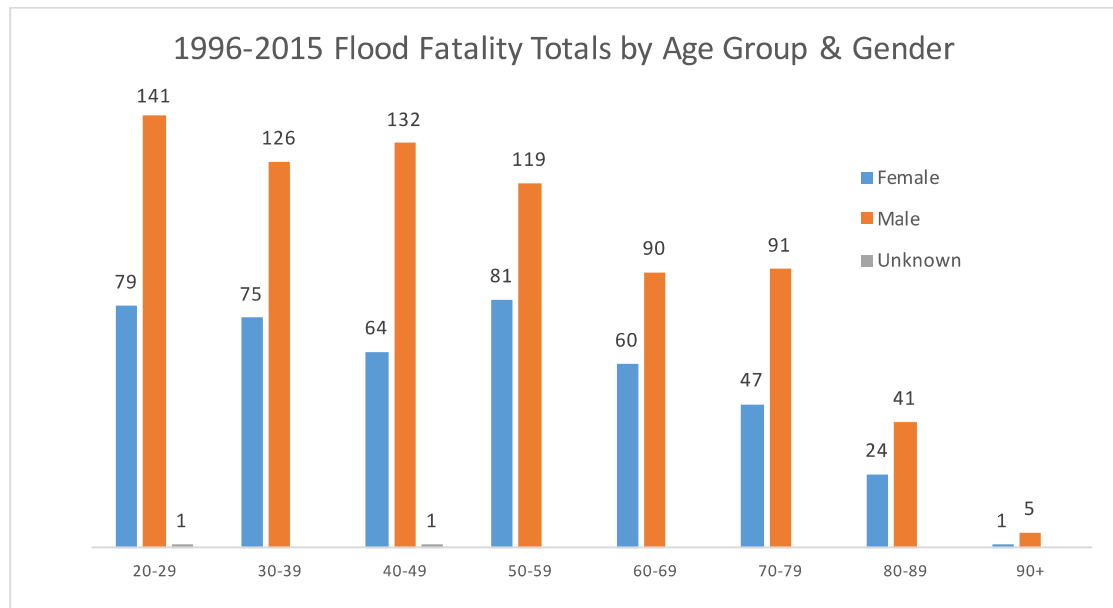


Figure 6. Chart depicting flood-related fatalities, by gender and age group, in the U.S. from 1996-2015. Men die at a rate of 1.5 to 2.1 times more often than women (this excludes the anomalous rate of 5 to 1 men to women in the 90+ age group).

6. Conclusion

Flood-related fatalities are a persistent problem with numbers that vary by year and is not exhibiting a declining trend as other weather-related hazards have [3]. A possible large factor in this persistence is a relatively low perception of the risk of driving or walking into flooded areas [3-7].

A common and often effective method of changing perceptions is through education. Flood hazard education should be conducted at all ages.

- For the school-aged children (i.e., pre-driving and newly-driving ages), "Safety Week" programs should include a unit on flood hazards. Included could be the slogans "If it's flowing, don't be going" (to avoid vehicle deaths) and "Don't drown, get to higher ground" (to avoid in water

deaths). Depending on the age group, the statistics would be explained at various levels of detail. Also included in the program would be a printout of the Citizen's Maps (laminated, if possible) for each child to give to their parents or guardians for keeping in the car and/or posting on the back of their house's front door. People in driver education programs should receive education along the same lines. Other methods of distribution for the maps might include churches, retail businesses, and social service agencies.

- For adults, the primary education methods could include public service announcements that include floating vehicle video with a voice-over of floodwater risks and the slogans "Turn around, don't drown" (to tie in the message with signage many drivers already see during their commutes), "If it's flowing, don't be going" (to avoid vehicle deaths) and "Don't drown, get to higher ground" (to avoid in water deaths).

References

1. Daniel, S; Fogarty, S. Car experiment shows extent of flood danger. *ABC News (Australian Broadcasting Corp.)* **2016**. Available online: <http://www.abc.net.au/news/2016-06-18/research-shows-cars-deadly-in-floodwaters/7522798>. (accessed 22 June 2016).
2. Oregon Department of Geology and Mineral Industries. Not-so-fun-fact-. *Cascadia* **2012 Winter**, 7. Available online: <http://www.oregongeology.org/pubs/cascadia/CascadiaWinter2012.pdf>. (accessed 7 July 2016).
3. Drobot, S.D.; Benight, C.; Gruntfest, E.C. Risk factors for driving into flooded roads. *Env Hazards* **2007**, 7, 227–234.
4. Ruin, I.; Gaillard, J.-C.; Lutoff, C. How to get there? Assessing motorists' flash flood risk perception on daily itineraries. *Env Hazards* **2007** 7, 235–244.
5. Shabanikiya, H.; Seyedin, H.; Haghani, H.; Ebrahimian, A. Behavior of crossing flood on foot, associated risk factors and estimating a predictive model. *Nat Hazards* **2014** 73, 1119–1126.
6. Ashley, S.T.; Ashley, W.S. Flood Fatalities in the United States. *Jrnl of Appl Meteorology & Climatology* **2008**, 47.3, 805-818.
7. Jonkman, S.N.; Kelman, I. An analysis of the causes and circumstances of flood disaster deaths. *Disasters* **2005**, 29(1), 75-97.
8. National Weather Service, Office of Climate, Water, and Weather Services. Natural Hazard Statistics. [Data available from: <http://www.nws.noaa.gov/om/hazstats.shtml#>] (accessed 18 June 2016).
9. United States Geological Survey, TNM Download (v1.0), Elevation Products (3DEP). USGS NED n30w099 1/3 arc-second 2013 1 x 1 degree IMG. [DEM available from: <http://viewer.nationalmap.gov/basic/>] (accessed 6 July 2016).
10. United States Census Bureau. Age and Sex Composition: 2010. *2010 Census Briefs* **2011**. Available online: <http://www.census.gov/prod/cen2010/briefs/c2010br-03.pdf> (accessed 10 July 2016).

Appendix

I. Summer Institute Technical Director



Dr. David Maidment
University of Texas at Austin

II. Summer Institute Theme Advisors



Dr. Sagy Cohen
University of Alabama



Dr. Sarah Praskievicz
University of Alabama



Dr. Alfonso Mejia
Pennsylvania State University



Dr. Ibrahim Demir
University of Iowa



Dr. Albert Van Dijk
Australian National University

III. National Water Center Advisor



Edward P. Clark
Director, Geo-intelligence
National Water Center – Office of Water Prediction
NOAA National Weather

IV. Summer Institute Student Coordinators



Adnan Rajib
Purdue University



Peirong Lin
University of Texas at Austin

V. Summer Institute Research Fellows



James Coll
University of Kansas



Mike Johnson
Univ. of California, Santa Barbara



Paul Ruess
University of Texas at Austin



Brenda Elisa Bazan
Univ. Texas Rio Grande Valley



Mark Hagemann
Univ. Massachusetts Amherst



Kyungmin Kim
University of Texas at Austin



Shahab Afshari
City University of New York



Ehsan Omranian
University Texas at San Antonio



Dongmei Feng
Northeastern University



Ryan P. McGehee
Auburn University



Lingcheng Li
University of Texas at Austin



Emily Poston
University of Texas at Austin



Yan-Ting Liau
University of Texas at Dallas



Krishna Karthik Gadiraju
North Carolina State University



Jiaqi Zhang
University of Texas at Arlington



Sanjib Sharma
Pennsylvania State University



Dinuke Munasinghe
University of Alabama



Yu-Fen Huang
University of Hawaii at Manoa



Bingqing Lu
University of Alabama



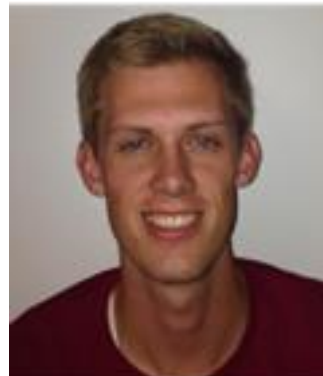
Amir Javaheri
Oregon State University



Mohammad Nabatian
University of Texas at Arlington



Savannah Keane
Brigham Young University
(Assistant Theme Coordinator)



Christian Kesler
Brigham Young University
(Assistant Theme Coordinator)



Xing Zheng
University of Texas at Austin
(Assistant Theme Coordinator)



Ridwan Siddique
Pennsylvania State University
(Assistant Theme Coordinator)



Christopher Zarzar
Mississippi State University



Hossein Hosseiny
Villanova University



Michael Gomez
Pennsylvania State University



Whitney Henson
Jacksonville State University



Christopher Franklin
University of Texas at Dallas
(Assistant Theme Coordinator)



Richard H. Garth
University of Texas at Dallas



Dawne Butler
University of Texas at San Antonio